Summer 2013

Protein Tyrosine Phosphatase Receptor Type Kappa Is A Glioma Tumor Suppressor That Predicts Survival And Response To Therapy

Supreet Agarwal
University of Iowa

PROTEIN TYROSINE PHOSPHATASE RECEPTOR TYPE KAPPA IS A GLIOMA TUMOR SUPPRESSOR THAT PREDICTS SURVIVAL AND RESPONSE TO THERAPY

by

Supreet Agarwal

A thesis submitted in partial fulfillment
of the requirements for the Doctor of
Philosophy degree in Pharmacy
in the Graduate College of
The University of Iowa

August 2013

Thesis Supervisor: Assistant Professor Mahfoud Assem

Graduate College
The University of Iowa
Iowa City, Iowa

CERTIFICATE OF APPROVAL

_____

PH.D. THESIS

_____

This is to certify that the Ph.D. thesis of

Supreet Agarwal

has been approved by the Examining Committee
for the thesis requirement for the Doctor of Philosophy
degree in Pharmacy at the August 2013 graduation.

Thesis Committee: _____
Mahfoud Assem, Thesis Supervisor

_____
Lawrence Fleckenstein

_____
Daryl Murry

_____
Gary Milavetz

_____
Dawn Quelle

To my parents

ACKNOWLEDGMENTS

I am extremely grateful to many people for their support, guidance and mentorship during my time as a graduate student. First, I express my sincere gratitude to my mentor Dr. Mahfoud Assem, for his relentless support, exemplary mentorship and friendship which has been the foundation of my success. He has always been there to advise and inspire, whenever needed. Thank you for believing in me during all these years. I also thank all the faculty members in the Clinical Pharmaceutical Sciences program, Dr. Daryl Murry, Dr. Lawrence Fleckenstein and Dr. Gary Milavetz for their valuable inputs during coursework and journal club discussions. Their critical insights have immensely helped in my scientific growth. I extend special thanks to Dr. Dawn Quelle and her lab member Jussara Hagen for helping me during my research work. They have been very kind and always welcomed me in their lab. My time at the University of Iowa has been fruitful as a researcher as well as in building friendships. I am very thankful to all my friends, especially those at the College of Pharmacy, for their companionship, hours of laughter and assistance. They have always made work enjoyable. Finally, I appreciate all the support from staff members at the College of Pharmacy. Specially, I would like to mention Lois Baker and Rita Schneider who were always there to provide help with any administrative issues. Thank you.

ABSTRACT

Poor prognosis and resistance to therapy in malignant gliomas is mainly due to highly dispersive nature of glioma cells. Aggressive infiltration in the brain parenchyma poses a serious challenge to complete tumor resection and effective treatment. Moreover, absence of valid biomarkers confounds definitive diagnosis and therapy response prediction. Identification of novel markers will require improved understanding of glioma genetics, particularly as it relates to key regulatory signals that control glioma cell migration. Since, these tumors are genetically heterogeneous, genomic explorations could improve understanding of molecular mechanisms underlying glioma migration and aid in discovery of molecular markers of clinical impact. Thus the central aim of our study is to identify novel genetic markers in patients with glioma for better prognosis, diagnosis and prediction of response to treatment.

In this study we screened for genome wide copy number alterations and loss of heterozygosity in a representative glioma population of sixty patients. Alterations were detected at multiple chromosomal loci with putative tumor suppressor genes and oncogenes. In relation to molecular determinants of glioma cell migration, alterations at the Protein Tyrosine Phosphatase Receptor type Kappa (PTPRK) locus were the most frequent in our glioma population. PTPRK alterations are relevant to glioma biology as PTPRK is a cell adhesion molecule that is highly expressed in brain. However, function of PTPRK has not been described previously in gliomas. This led to our central hypothesis that PTPRK is a novel biomarker that suppresses diffusive capacity of glioma cells and thereby may improve glioma therapeutic outcome.

Overexpression and knockdown experiments were performed to study PTPRK function using malignant glioma cell lines. We explored molecular mechanisms underlying PTPRK function and its effect on response to therapy. Moreover, we discovered novel PTPRK mutations by sequencing full length PTPRK transcripts in

numerous glioma biopsies. Effect of these mutations on PTPRK function and response to anti-glioma therapeutics were subsequently analyzed using *in vitro* cell based assays.

Our results suggest that PTPRK is an independent prognostic marker and a glioma tumor suppressor that is altered at both transcriptional and post-translational levels. Proteolytic processing of transmembrane PTPRK protein generates a series of fragments which are the only detectable PTPRK forms in glioblastoma. Short hairpin RNA (shRNA) mediated downregulation of PTPRK reduces glioblastoma cell migration suggesting that proteolysis of PTPRK contribute to migration of glioblastoma cells. Additionally, overexpression of wild-type PTPRK suppresses growth and migration of malignant glioma cells which correlates with inhibition of EGFR and β-catenin signaling, and improves effect of conventional therapies for glioma. However, PTPRK mutations abrogate tumor suppressive effects of wild-type PTPRK and alter sensitivity of glioma cells to chemotherapy.

These results indicate that the cell surface PTPRK protein is a tumor suppressor of prognostic and predictive value which is frequently inactivated in malignant gliomas.

TABLE OF CONTENTS

LIST OF TABLES

Table

LIST OF FIGURES

Figure

LIST OF ABBREVIATIONS

AAC	Anaplastic astrocytoma
ABCTs	ATP-binding cassette transporters
AC	Astrocytoma
ADAM	A disintegrin and metalloproteinase
AOA	Anaplastic oligoastrocytoma
AOD	Anaplastic oligodendroglioma
ARF	ADP-ribosylation factor
ATCC	American Type Culture Collection
BLNK	B-cell linker
CACNA2D2	Calcium channel, voltage-dependent, alpha 2/delta subunit 2
Cdc42	Cell division cycle 42
CDK4	Cyclin-dependent kinase 4
CDK6	Cyclin-dependent kinase 6
CDKN2B	Cyclin-dependent kinase inhibitor 2B
CDKN2C	Cyclin-dependent kinase inhibitor 2C
CNAs	Copy number alterations
DCN	Decorin
DMSO	Dimethyl sulfoxide
ECM	Extracellular matrix
EDTA	Ethylenediamine tetraacetic acid
EGFR	Epidermal growth factor receptor
EGTA	Ethylene glycol tetraacetic acid
ERL	Erlotinib
FLPTPRK	Full length PTPRK
GAPDH	Glyceraldehyde-3-phosphate dehydrogenase

GBM	Glioblastoma
GTB	Gefitinib
HDAC9	Histone deacetylase 9
HEPES	(4-(2-hydroxyethyl)-1-piperazineethanesulfonic acid)
HIF-α	Hypoxia inducible factor 1, alpha subunit
ICD	Intracellular domain
KCNH7	Potassium voltage-gated channel, subfamily H (eag-related), member 7
KPS	Karnofsky performance status
LOH	Loss of Heterozygosity
MAM	Meprin/A5-protein/PTPmu
MAP2	Microtubule-associated protein 2
MAPK	Mitogen-activated protein kinases
MDM2	Mouse double minute 2, human homolog of; p53-binding protein
MDM4	Mouse double minute 4, human homolog of; p53-binding protein
MEK	Mitogen-activated protein kinase kinase
MMP-1	Matrix metalloproteinase -1
mTOR	Mammalian target of rapamycin
MTT	3-(4,5-Dimethylthiazol-2-yl)-2,5-Diphenyltetrazolium Bromide
NCAM	Neural cell adhesion molecule
NF1	Neurofibromin 1
NRXN3	Neurexin 3
ODG	Oligodendroglioma
P4HA1	Prolyl 4-hydroxylase, alpha polypeptide I
PBS	Phosphate buffered saline
PDGFR	Platelet-derived growth factor receptor
PI3K	Phosphoinositide-3-kinase

PMSF	phenylmethylsulfonyl fluoride
PNLIPRP3	Pancreatic lipase-related protein 3
pNPP	p-Nitrophenyl Phosphate
PTEN	Phosphatase and tensin homolog
PTPRK	Protein tyrosine phosphatase receptor type kappa
PTPRK –wt	Wild-type PTPRK
PTPRM	Receptor-type tyrosine-protein phosphatase mu
PTPRZ1	Receptor-type tyrosine-protein phosphatase zeta
PΔE	P-subunit of PTPRK without most of the extracellular region
Q-PCR	Quantitative - polymerase chain reaction
Rac1	Ras-related c3 botulinum toxin substrate 1
RB	Retinoblastoma
RFC3	Replication factor C (activator 1) 3
RPTPs	Receptor protein tyrosine phosphatases
RTKs	Receptor Tyrosine Kinases
RT-PCR	Reverse transcriptase polymerase chain reaction
SCP2	Sterol carrier protein 2
SMARCA2	SWI/SNF related, matrix associated, actin dependent regulator of chromatin, subfamily a, member 2
SNP	Single nucleotide polymorphism
STATs	Signal transducer and activator of transcription
TKi	Tyrosine kinase inhibitors
TMZ	Temozolomide
TP	Tyrosine phoshphorylation
VEGF	Vascular endothelial growth factor
VEGFRs	Vascular endothelial growth factor receptors

CHAPTER I

INTRODUCTION

1.1 Biology of malignant gliomas

1.1.1 Glioma classification

Gliomas are tumors of neuroepithelial tissue which account for large proportion of brain tumor related deaths. They are the most frequent type of primary brain tumors that tend to aggressively invade into surrounding healthy brain tissue. Exact cellular origin of gliomas is not as yet known, although recent studies suggest that glioma arises from neoplastic transformation of either neural stem cells or progenitor cells (1-3). Nonetheless, they are still clinically considered as malignant transformation of normal glial cells and are thus classified, in part, based on their morphological similarities to glial cells (4). They are divided into two main histological types: 1) astrocytoma, tumors of astrocyctic origin, and 2) oligodendroglioma, which are tumor of oligodendocytic origin. Moreover, according to the World Health Organization classification of central nervous system tumors (5), gliomas are further classified into four grades based on degree of differentiation and anaplasia (Figure 1.1). Grade I tumor include mostly pediatric pilocytic astrocytoma. They are non-malignant with limited infiltrative capacity and often curable (6). Grade II to IV gliomas are often aggressive and mainly affect adults (5,6). Grade II tumors are the low grade, well differentiated type of oligodendroglioma (ODG) and astrocytoma (AC) (5). These tumors generally have normal or non-clonal chromosomal pattern (7,8), and thus show the best prognosis and response to therapy. Grade III tumors comprise of anaplastic gliomas which include anaplastic oligodendroglioma (AOD), anaplastic astrocytoma (AAC) and anaplastic

oligoastrocytoma (AOA) (5). The most aggressive and the most frequent type is grade IV glioblastoma (GBM) (4).

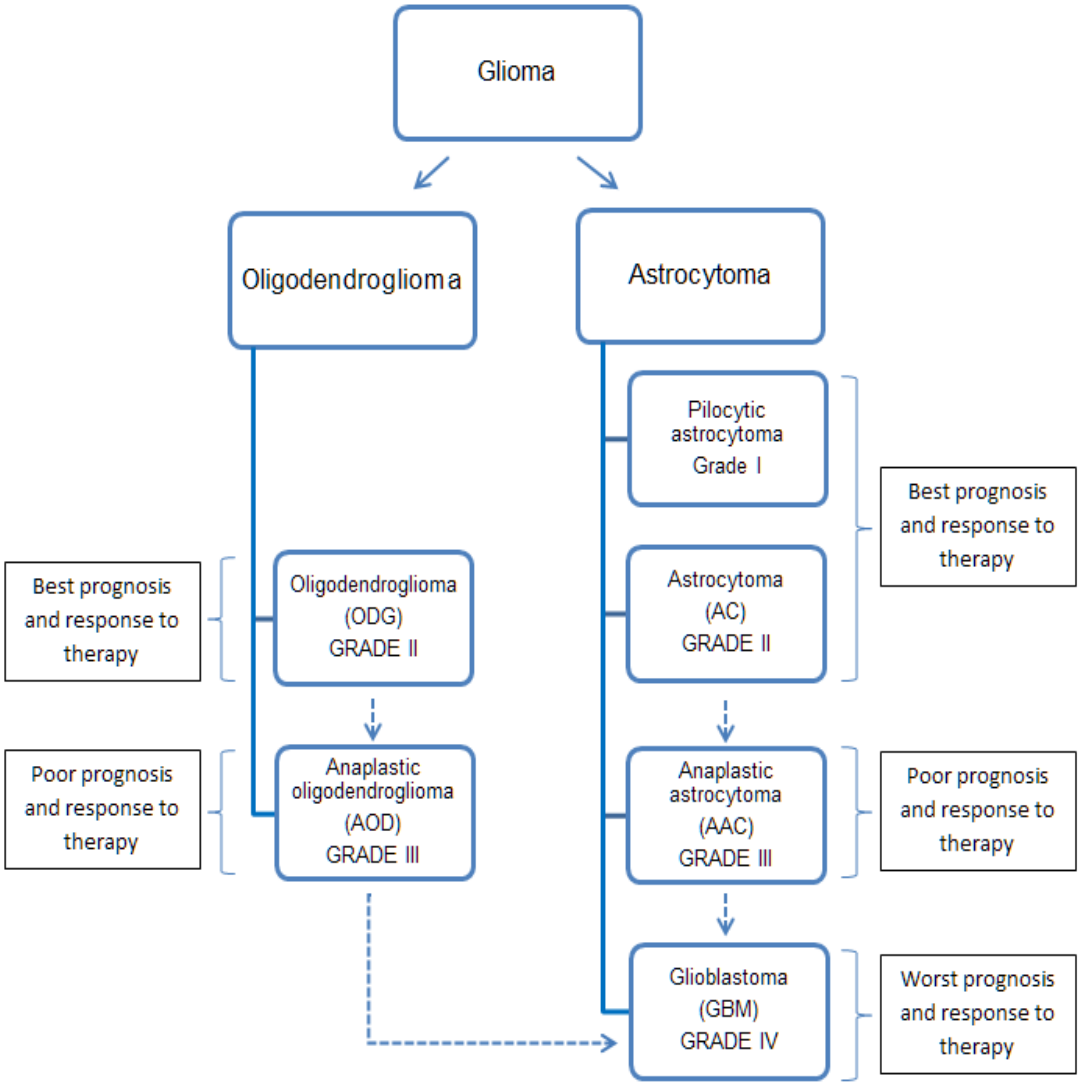

Figure 1.1: Classification of glioma based on histology and malignancy grades. Dotted arrows indicate possible progression of lower grade tumor to higher grade secondary gliomas.

1.1.2 Malignant gliomas

High grade astrocytomas (grade III and IV) are often referred as malignant gliomas because of their tendency to aggressively invade surrounding healthy brain regions (9). In general, tumors with astrocytic components account for three-fourths of all gliomas and represent a significant health burden (4). These malignant tumors can develop *de novo* without any evidence of pre-existing low grade forms (6,9). Accumulation of genetic mutations in low grade astrocytomas can also result in their malignant progression to higher grade, termed as secondary malignant gliomas (9). Secondary GBM tumors, though histopathologically similar to primary GBMs, display distinct molecular profiles (9). Regardless, primary malignant gliomas are the most frequent types and are associated with worse prognosis and poor response to standard therapy (9,10). Their tendency to extensively disperse into the healthy brain tissue hinders complete surgical resection of the tumor and thus results in tumor recurrences (9,10). Additionally, wide range of chromosomal abnormalities occur in high grade astrocytomas (grade III and IV), including complete loss or gain of chromosomes. These genetic abnormalities contribute to multiple subpopulations of cell types within the tumor, which are responsible for the heterogeneous nature of malignant tumors (7-9). This intra-tumor heterogeneity is a major obstacle in establishing correct diagnosis and treatment of malignant gliomas as different cell populations within the tumor tissue respond differently to the treatment (9,10).

The correct diagnosis of these tumors is crucial because some are sensitive to chemotherapy, whereas the majority shows drug resistance (11,12). Current morphology-based guidelines for glioma classification pose a serious challenge in differentiating

between glioma grades (13). In addition, histological reporting of malignant gliomas is highly subjective as wide variations are often observed between pathologists (14). Of note, even correct diagnosis not always translate into better outcome as tumors with similar morphological features can still display distinct patterns of molecular alterations, which have been shown to govern prognosis and response to treatment (1,9,15).

1.1.3 Molecular alterations in malignant gliomas

Several genome wide profiling studies have been conducted to identify clinically relevant genetic signatures of malignant glioma (7,8,16,17). These genomic explorations have provided critical insights into alterations in key signaling pathways that regulate proliferation, migration and invasion of glioma cells. Notably, these genomic aberrations have a specific distribution pattern that correlate with histology and grade, and thus could be useful in improving glioma classification, prognosis and therapeutic prediction (7).

Amplification and gains of chromosome 7 are the most frequent abnormalities detected in high grade astrocytoma (malignant gliomas), particularly GBM (7,18). Whole or partial gains of chromosome 19 and 20 are observed in large number of these tumors (7,18). Further, loss of heterozygosity (LOH) events as well as complete loss of chromosomal regions also occurs frequently in malignant glioma (7,18). Losses of chromosomes 10, 22 and sex chromosome are among the common chromosomal abnormality of GBM (7,18). Interestingly, many chromosomal alterations occur in a specific pattern. Tumors with chromosome 7 amplification also show losses of chromosome 10 and 9p region (7). Further, tumors with whole gains of chromosome 19 often display gains of chromosome 7 and 20 along with chromosome 10 deletions, thus indicating a specific pattern of alterations (7). Several putative tumor suppressor and

oncogenes map to these altered chromosomal regions, and participate in multiple signaling pathways (7,18). Deregulation of associated signaling events contribute to aggressive infiltration of glioma cells into surrounding brain regions, self-sufficiency in growth factor signaling, resistance to apoptotic signals and tumor angiogenesis (7,9,10,15).

Table 1.1: Common chromosomal alterations in gliomas.

Chromosomal region	Type of alteration	Glioma grade
1p	Gains and deletions	Deletions mostly in grade II and III. Gains in grade IV
7	Gains	Grade III and IV
9p	Loss and deletions	Grade IV
9q	Gains	Grade III and IV
10	Loss and deletions	Grade III and IV
19q	Gains and deletions	Deletions in grade II and III. Gains in grade IV
20	Gains	Grade IV
22q	Loss and deletions	Grade III and IV

Malignant gliomas exhibit self-sufficiency in growth signals mainly because of amplification and mutations of several receptor tyrosine kinases (RTKs) such as epidermal growth factor receptor (EGFR), vascular endothelial growth factor receptors (VEGFRs), and platelet-derived growth factor receptor (PDGFR) (Figure 1.2A) (8,9). RTK signaling is constitutively activated due to tyrosine phosphorylation in more than 80% of gliomas (8). Auto-phosphorylated RTKs activate downstream pro-mitotic signaling molecules such as PI3K and RAS (8-10). Moreover, PTEN, that inhibits PI3K activity, is frequently inactivated in more than 50% of malignant gliomas (8). Another critical component of RTK mediated proliferation is the activation of RAS signaling (8).

The protein encoded by *NF1* gene that functions as a negative regulator of RAS is also frequently inactivated in malignant gliomas (8-10). Parallel to growth signals, resistance to anti-growth signals can be attributed to the inactivation of key cell cycle regulator gene, *RB* (9,10). Hypo-phosphorylated form of Rb prevents cell cycle progression by inhibiting E2F transcription factors (9,10). Phosphorylation of Rb by overactivated cyclin D1 and its associated cyclin-dependent kinases, CDK4 and CDK6, induces release of E2F transcription factors and promotes unchecked cell cycle progression (Figure 1.2B) (9,10). Amplifications of cyclins and their kinases along with mutations in their negative regulators disrupt Rb function in about 80% of malignant gliomas (8-10).

Another frequently altered pathway in glioma is related to their acquired capacity to evade apoptotic signals (8-10). Frequent mutations in the p53 pathway, including inactivating mutations of p53 and P14ARF, and amplifications of MDM2 and MDM4 have been reported in gliomas (Figure 1.2C) (8-10). All these genes influence cell apoptosis and are key regulators of cell cycle, cell senescence and DNA repair (9,10).

Finally, widespread diffusion into surrounding healthy brain tissue, extensive vascularization and presence of cancer stem cells are common phenotypes in high grade astrocytomas (8-10). Specifically, abnormal microvascular proliferation and necrosis are key pathological signatures of GBM (9). Increase in tumor bulk creates hypoxic conditions which leads to focal or extensive necrosis and induces ‘hypoxia inducible factor 1- alpha’ (HIF1-α) (9). Subsequent increase in HIF1-α levels result in angiogenic burst through activation of vascular endothelial growth factor (VEGF) which is critical for endothelial cell proliferation (9). Recent reports have also shown an upregulation of VEGF by EGFR in both HIF1-α dependent and independent manner (19). In addition,

inactivation of p53 and RB has been shown to activate VEGF (20). This indicates that key regulators of growth and apoptosis also interact with angiogenesis related signaling processes and therefore play central role in tumor development and progression.

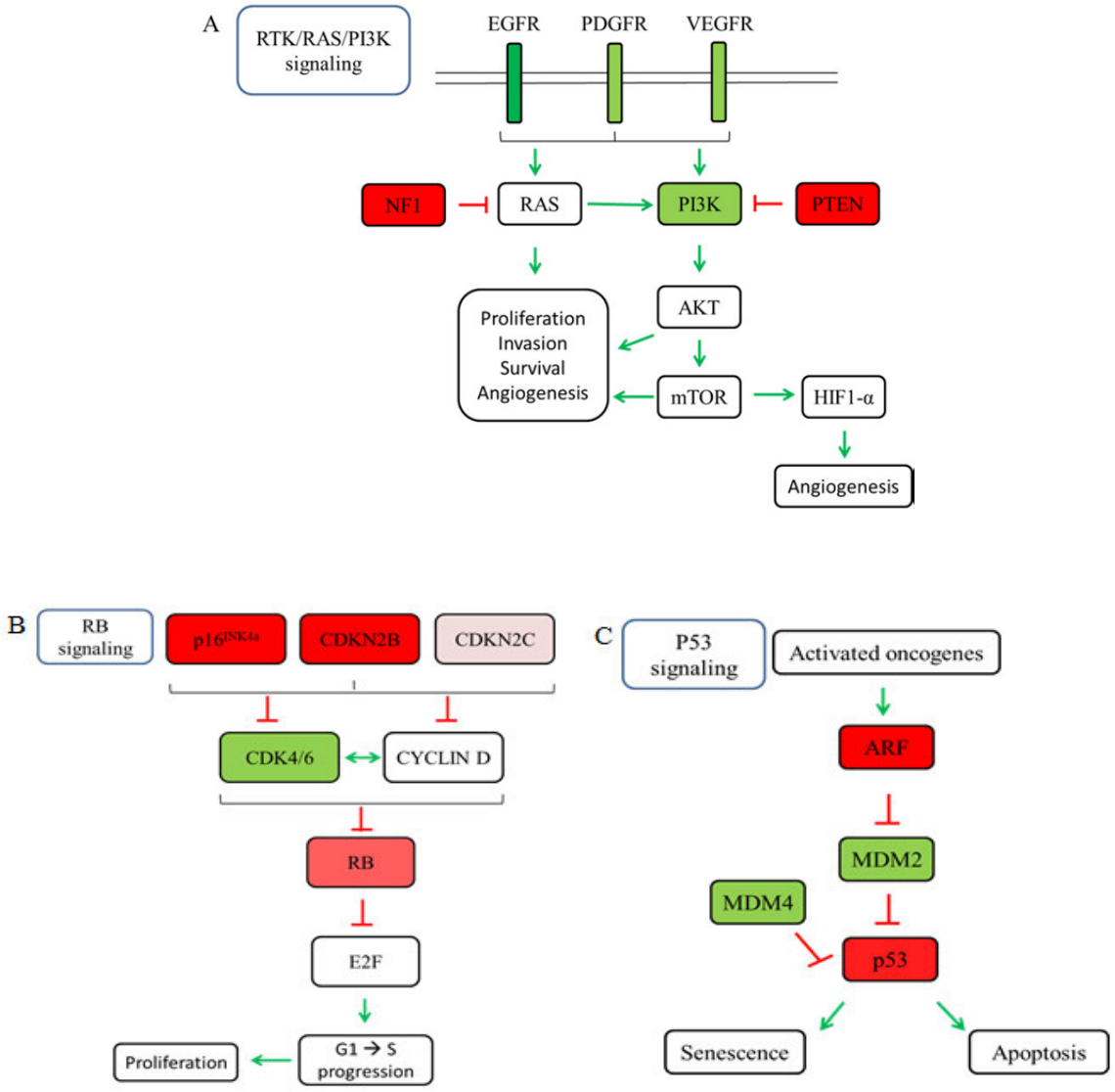

Figure 1.2: Major genetic alterations in three key pathways. Mutations, deletions and amplifications in (A) RTK/RAS/PI3K, (B) RB and (C) p53 signaling pathways are shown. Green boxes indicate activating mutations, amplifications with frequently overactivated genes in darker shade of green. Boxes in color red indicate inactivating alterations such as mutations and deletions, with frequently inactivated genes in deeper shades of red (8).

1.1.4 Migration and invasion of malignant gliomas

The aggressive phenotype of high grade astrocytomas, especially GBM, can mainly be attributed to rapid infiltration of tumor cells into the healthy brain parenchyma. The extensive infiltration has been a major clinical obstacle in treatment of these tumors (9,10). Widespread diffusion of tumor cells makes complete tumor resection virtually impossible as migrated cells are hard to detect and often tumor recurs within several centimeters of the resection margin, causing fatal outcomes (21,22). Notably, grade II astrocytomas are also invasive in nature, though less aggressive than grade III and IV (6,9). Cells of these low grade tumors have been histologically observed at least few centimeters from the tumor mass (22). Thus, invasive characteristic of gliomas is a major clinical problem. Extreme invasive behavior is also a hurdle to complete eradication of the tumor mass with radiation and chemotherapy as normal brain cells are equally sensitive to such therapies (23,24). Extensive cell migration is one of the major reasons for very poor prognosis of GBM patients, with median survival of less than a year even after aggressive therapy (4,24).

Therefore, the general therapeutic goal has been to effectively target glioma cell migration and invasion via novel strategies, to allow subsequent treatment of the tumor bulk with standard therapies (23,25). Knowledge of molecular mechanisms that modulate glioma cell motility is highly important for the identification of potential molecular targets that can be therapeutically regulated to limit invasion.

1.1.5 Molecular mechanisms of glioma cell migration

Migratory capacity of high grade astrocytomas perhaps can simply be attributed to their possible origin from astrocytes which are inherently migratory in nature, as they migrate to the injured brain regions under normal physiological conditions (26). Nonetheless, invasion and subsequent migration of glioma cells into the surrounding healthy brain region involve complex and coordinated interaction between cytoskeletal proteins, cell adhesion molecules and extracellular matrix (24,27). Glioma cells first need to detach from the tumor bulk, then adhere to the extracellular matrix (ECM), induce degradation of surrounding ECM by proteases and thereby migrate into healthy brain tissue (Figure 1.3) (24,27).

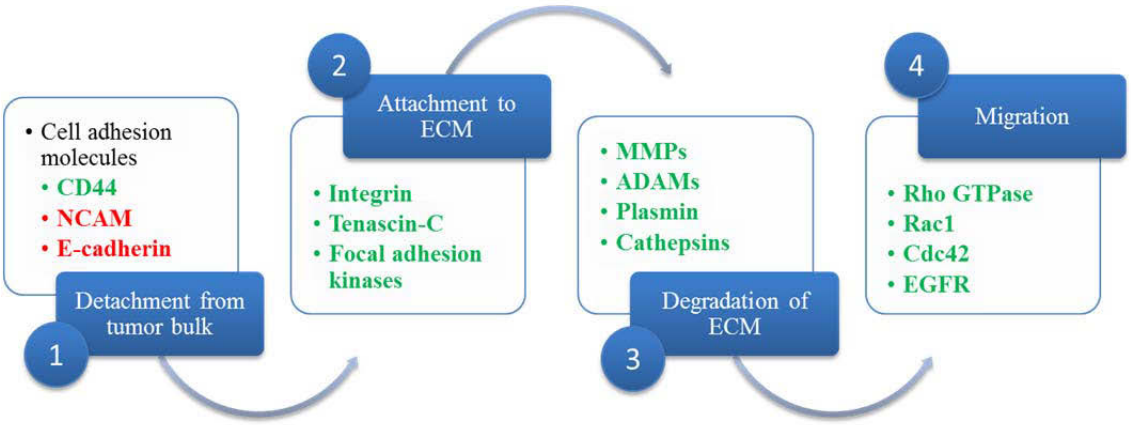

Figure 1.3: Mechanism of glioma cell migration. Major molecules that play important role in each step of glioma cell migration are listed. Green indicates upregulation whereas color red indicates downregulation of molecules.

Detachment of glioma cells requires alteration of several cell adhesion molecules such as CD44, neural cell adhesion molecules (NCAM) and cadherins (24,27).

Downregulation of NCAM and E-cadherin along with upregulation of CD44 and N-cadherin promotes cell motility through cytoskeletal reorganization (22,27-29). Although the role of N-cadherin in glioma invasion has been controversial, general consensus is that destabilization of cadherin-catenin complexes results in increased cellular motility (27). Subsequent attachment to the brain ECM is mostly mediated by extracellular matrix proteins, integrins and tenascin-C, which are upregulated in invading glioma cells and form focal adhesion complexes along with other cytoskeletal proteins (27,30,31).

The next step in glioma invasion requires remodeling of ECM which functions as a barrier to invading cells (27). Invading glioma cells express high levels of ECM-degrading proteases including matrix metalloproteinases (MMPs) (32,33), 'a disintegrin and metalloproteinases' (ADAMs), plasmin and cathepsins (33,34). Turnover of ECM by these proteases provides space for invading cells to migrate into healthy regions.

The last step of brain tumor migration involves rearrangement of the cytoskeleton and formation of extended membrane protrusions from the leading edge of invading glioma cells (24,27). Migrating cells display changes in cell morphology: the cell becomes polarized which directs movement and have extended membrane projections from the leading edge of the cell (24,27). Rho family of GTPases plays an important role in cell movement (24,27). In this process, Rho GTPase stimulates formation of stress fibers and focal adhesions at rear end of the migrating cell (35). In contrast, Rac1 directs formation of lamellipodia (membrane projections) at the leading edge of migrating glioma cell (35). Another member of Rho family, Cdc42, regulates cell polarity and filopodia formation to promote movement of cells in a defined direction (24,27,35).

It is interesting to note that gain of function mutations in the cell adhesion molecules, proteases and other ECM components that promote glioma cell invasion have not been detected in 600 analyzed glioblastoma patients documented in The Cancer Genome Atlas database as of yet (8). However, many genes involved in cell migration are under the transcriptional regulation of tumor suppressors- p53 and RB (9,10). Both these tumor suppressors are frequently inactivated in malignant gliomas (8). Mutations of p53 have indeed been shown to promote invasion by facilitating integrin recycling (36). In addition, alterations in cell-matrix and cell-cell adhesion dependent processes have been linked to amplifications and activating mutations of receptor tyrosine kinases such as EGFR (28,37). Overactivated EGFR signaling stimulates phosphorylation of key molecules of cell-adhesion complexes that destabilizes adheren junctions, ultimately leading to cell invasion and migration (37,38). In particular, high expression of cadherins and associated catenins (β-catenin, p120catenin) along with increased phosphorylation of catenins is observed at the borders of glioblastoma tumors (25,29). Tyrosine phosphorylation of catenins such as β-catenin, not only dissembles adheren junctions but also promotes β-catenin mediated transcriptional activation of several proto-oncogenes such as cyclin D1 and c-Myc (29,39,40). Moreover, aberrant EGFR signaling has been shown to promote invasion through indirect upregulation of proteases such as MMP-1 (22). EGFR downstream targets such as PI3K/AKT pathway regulate several invasion mechanisms, which are also activated in malignant gliomas by mutations and amplifications (25). Overall, receptor tyrosine kinase mediated signaling plays a central role in driving aggressive phenotypes of malignant glioma.

1.2 Treatment strategies for malignant gliomas

Table 1.2: Summary of current treatment approaches for malignant gliomas.

Tumor type	Current treatment approach
Newly diagnosed	
Glioblastoma (Grade IV)	Surgical resection followed by radiotherapy, plus concurrent and adjuvant TMZ or Gliadel wafers (carmustine)
Anaplastic astrocytoma (Grade III)	Surgical resection followed by radiotherapy, plus concurrent and adjuvant TMZ or adjuvant TMZ alone (no standard treatment protocol following surgery)
Anaplastic oligodendroglioma (Grade III)	Surgical resection with either radiotherapy alone, TMZ or PCV with or without subsequent radiotherapy, radiation plus concurrent and adjuvant TMZ, or radiation plus adjuvant TMZ (no standard treatment protocol following surgery)
Recurrent tumors	Re-surgery in some patients, Gliadel wafers, various chemotherapy (PCV, irinotecan, etoposide, carboplatin, bevacizumab and other experimental therapies)

Note: TMZ stands for temozolomide, PCV for combination of procarbazine, lomustine and vincristine.

Current standard of treatment for malignant gliomas include various combinations of surgery, radiation and chemotherapy to improve symptoms and prolong life of patients (Table 1.2). Surgery is mostly incurable because of early infiltration of tumor cells into areas of normal brain resulting in tumor recurrences (9,10). Nonetheless, surgical resection is effective in reducing tumor volume to be further treated with radiation and/or chemotherapy. It is also helpful in removing necrotic core of malignant gliomas (GBM) which is resistant to radiation and poorly accessible to chemotherapeutics (9,10). Surgical

resection, however, can worsen neurologic deficits in cases where a tumor has extensively infiltrated, resides too deep or is in close proximity to eloquent brain region (11). Decision for surgery is generally based on patient's age, performance status and proximity of the tumor to eloquent brain areas. Patients with good performance status and tumor distant from eloquent areas are often offered surgical resection as first line of treatment which also allows time for additional therapy (11). When meaningful tumor debulking is not possible, stereotactic brain biopsy is generally recommended to at least establish diagnosis (11).

To determine best treatment option following surgery, neuro-oncologists often categorize patients with malignant glioma into prognostic groups. Several clinical studies have established age less than 50, good performance status and histological diagnosis as favorable prognostic factors (14,22,41-43). Younger patients with favorable prognosis are almost always offered radiotherapy as first line of treatment. Elderly patients are more likely to develop radiation related toxicity (11). In particular, radiotherapy in elderly patients with poor performance status and histological diagnosis of GBM may not be beneficial as their life expectancy is generally only of few months. Abbreviated radiotherapy or only supportive care without any radiotherapy is offered to these patients (11). However, establishing correct diagnosis based on histology is a major challenge and often results in early radiotherapy leading to radiation related toxicity. Absence of valid diagnostic and predictive markers further compounds to the problem. Combined chromosome 1p and 19q loss mainly in tumors of oligodendrocytic origin is the best known predictive marker as of yet (14). Such patients generally respond better to chemotherapy and may not require post-operative radiotherapy (14,41). Thus, radiation associated adverse effects can be avoided in these patients. Additional markers are needed to further enhance predictive therapeutic accuracy.

Until recently, the most commonly used chemotherapeutic regimen for newly diagnosed malignant glioma patients was carmustine or combination of procarbazine,

lomustine and vincristine (PCV) because of their lipid solubility and ability to cross blood brain barrier (11). However, prospective clinical trials with PCV regimen have shown only modest improvement (less than 1 month) in survival of patients with malignant glioma (9,11). PCV regimen though is still used particularly for low grade gliomas, treatment with temozolomide (TMZ) chemotherapy has now become a standard of care for newly diagnosed gliomas either alone or in combination with radiotherapy. TMZ is an alkylating agent that readily crosses blood brain barrier and has an excellent bioavailability. It produces only mild adverse effects such as nausea and constipation except myelotoxicity and leukemia in rare cases (11). However, response to TMZ varies in patients with glioma. Patients with methylated *MGMT* are sensitive to TMZ treatment whereas patients without *MGMT* promoter methylation are often resistant to TMZ (9). Further studies are required to determine clinical utility of *MGMT* methylation status as a marker of response to alkylating agents. Clinical trials with *MGMT* inhibitors (O6-benzylguanine) and inhibitors of other important resistance enzymes such as PARP (iniparib, olaparib) in combination with TMZ are in progress. Further, response to TMZ treatment in patients with recurrent malignant glioma has been modest. Phase II trials didn't show significant response rate (44-46). Other agents such as carmustine, irinotecan and PCV therapy have also not shown significant survival benefits for these patients (11). Thus further evaluation of alternative regimens and therapies is required.

Chemotherapy is also administered interstitially by placing carmustine wafers (Gliadel) into the tumor resection cavity. The biodegradable polymer wafers release carmustine over several weeks, resulting in higher concentrations of chemotherapy at the site of the tumor with minimal systemic toxicity. These wafers were found to improve median survival of newly diagnosed malignant glioma patients by 1.5 months in a phase III trial but have a limited role in patients with recurrent malignant glioma (47,48).

Overall, survival of malignant glioma patients has not improved over the past decade despite advances in surgical procedures and radio- and chemo- therapeutic

approaches (4). This has resulted in significant interest in exploring alternative therapeutic strategies. Improved understanding of the genetic changes and associated molecular events underlying malignant gliomas has highlighted several therapeutic targets to suppress extensive proliferation and migration of glioma cells (Figure 1.4 and Table 1.3). Several targeted therapies have thus been developed and being evaluated in clinical trials.

Molecular characterization of high grade gliomas has shown a central role of RTK dependent signaling in proliferation, migration, angiogenesis and refraction to apoptosis (8,9). In particular, amplification and activating mutations of EGFR are found in 80% of glioblastoma patients, suggesting that gliomas are kinase-driven cancers (8). Several of these tumors also have a constitutively active EGFR mutant form (EGFR vIII) (8,9). EGFR-targeted therapies have thus been tested to treat malignant gliomas. Small molecule EGFR inhibitors such as gefitinib and erlotinib are generally well tolerated but have largely failed in clinical trials (11,49,50). Molecular alterations such as EGFR vIII expression in combination of PTEN loss has been associated with resistance to EGFR inhibitors (7,11).

PDGF signaling is also frequently upregulated in high grade gliomas and thus is a potential therapeutic target (9,10). Phase II trials with small molecule TK inhibitor, imatinib mesylate, showed only minimal response with no significant improvement in survival of patients with recurrent GBM (51,52). Clinical trials involving combination of imatinib with TMZ and other anti-cancer drugs are in progress. A number of other PDGFR inhibitors are also being considered for treatment of malignant gliomas (Table 1.3).

Another attractive therapeutic target in malignant gliomas is vascular endothelial growth factor (VEGF) and its receptors (VEGFR). VEGF is a critical driver of glioma tumor angiogenesis and is strongly associated with the production of peritumoral edema (9,10). Several anti-angiogenic agents are being evaluated in clinical trials for malignant

glioma (Table 1.3). Bevacizumab, a humanized monoclonal antibody against VEGF, has been approved by FDA as a second-line treatment for patients with GBM. Survival benefits of bevacizumab in combination with other anti-cancer drugs are being evaluated in clinical trials mainly for patients with recurrent malignant gliomas. However, there is no general consensus on optimal treatment schedule and duration of bevacizumab therapy. Scientific rationale for using bevacizumab in combination with other therapeutic agents is lacking. Early clinical trials in recurrent GBM have not shown any additional clinical benefits in patients treated with bevacizumab and irinotecan compared to those treated with bevacizumab monotherapy (53-55). Moreover, markers to predict response to anti-angiogenic therapies have not been identified yet.

In addition, several other inhibitors targeting Ras/MAP kinase pathway (such as farnesyltransferase inhibitors and Raf inhibitors), PI3K/Akt pathway and proteosome degradation pathway are being evaluated in clinical trials (Figure 1.4 and Table 1.3).

Despite tremendous progress in our understanding of tyrosine kinases function and successful *in vitro* studies with several tyrosine kinase inhibitors, therapeutic targeting of kinases has largely failed in clinical trials for heterogeneous solid tumors such as glioblastoma (11,49,50). This is because tumors develop resistance mechanisms to tyrosine kinase-targeted therapies. The principle reason of limitations of anti-kinase agents is that the tyrosine kinase signaling pathways are complex interacting networks instead of being simple isolated systems (50). Several tyrosine kinases are found to be overexpressed in tumors upon treatment with EGFR inhibitors (56). Activation of downstream signaling pathways due to amplification of oncogenic molecules such as PI3K, Ras, STATs and others, along with inactivation of tumor suppressors such as PTEN, together contributes to ineffectiveness of tyrosine kinase inhibitors in GBM (56,57). Moreover, blood brain barrier is a major obstacle to targeted therapies in glioma. Ability of the new targeted inhibitors to cross blood brain barrier is not well established.

Adequate intra-tumor concentration of these inhibitors to alter targets in glioma is unknown. Further, optimal treatment schedule and duration is not clear.

To address genetic heterogeneity of malignant gliomas, treatment strategies simultaneously inhibiting several critical pathways is of significant interest. Genome wide profiling of glioma tumors can allow selection of the most important molecular targets prior to treatment of malignant glioma patients. Genome wide analysis also provides an opportunity to identify novel molecular players in glioma cell migration with potential to modulate tyrosine kinases activity. It will allow discovery of genomic predictors of chemotherapeutic sensitivity that will direct the usage of anti-cancer drugs to the patients that are more likely to respond, avoiding thus toxicity and inefficient toxic drugs. Such genetic markers can even improve diagnostic and prognostic accuracy along with therapy response prediction.

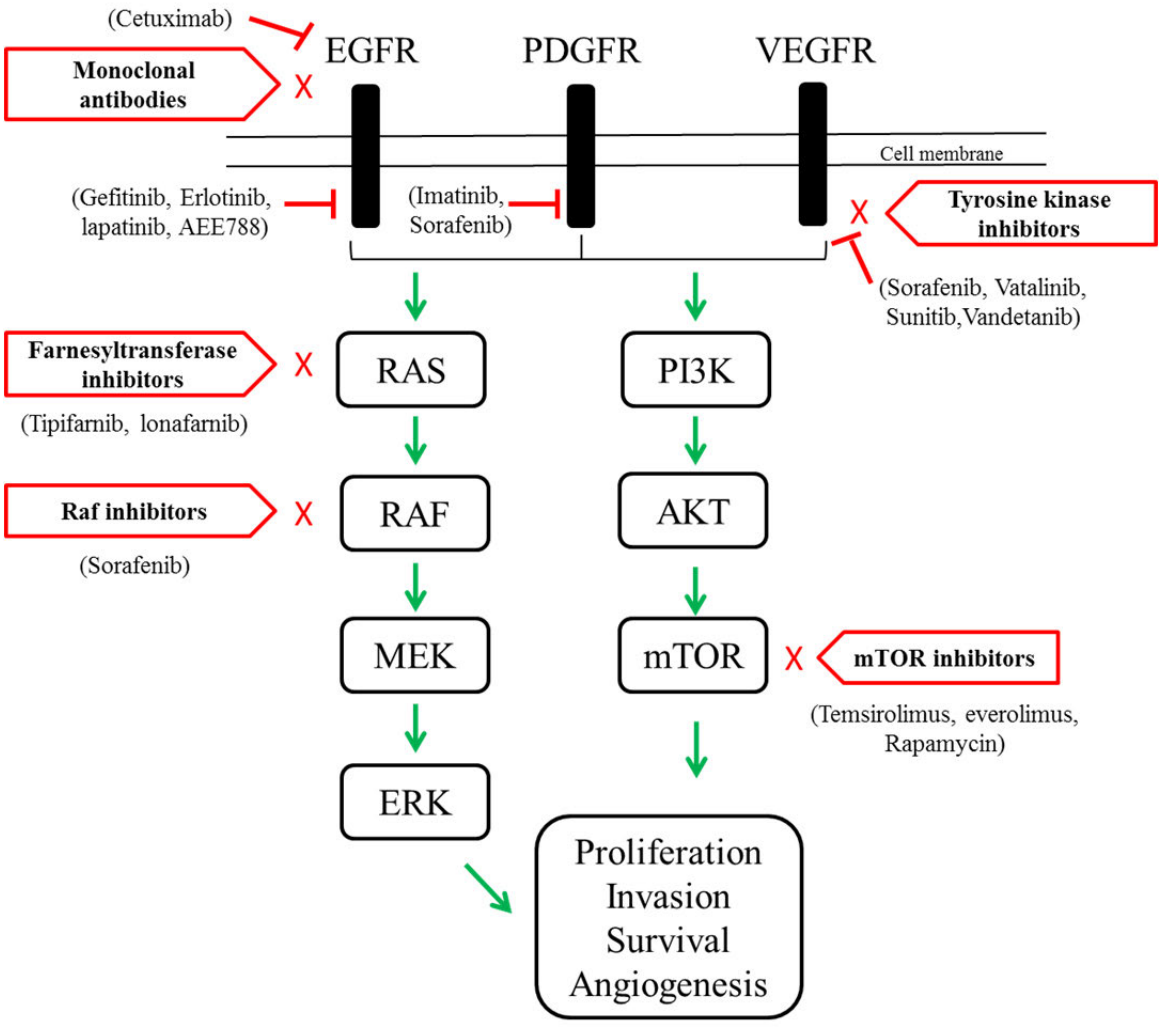

Figure 1.4: Small molecule inhibitors and monoclonal antibodies currrently being evaluated to target glioma relevant RTK-signaling pathways.

Table 1.3: Targeted therapeutic agents in clinical trials for patients with malignant gliomas.

Target	Class	Name	FDA approval
EGFR	Tyrosine kinase inhibitors	Gefitinib (Iressa®)	For advanced non-small cell lung cancer
		Erlotinib (Tarceva®)	For advanced non-small cell lung cancer and pancreatic cancer
		Lapatinib (Tykerb®)	For breast cancer as combination therapy
		AEE788 (also a VEGFR inhibitor)	-
		Vandetanib (Caprelsa®, also a VEGFR and RET inhibitor)	For metastatic medullary thyroid cancer
	Monoclonal antibodies	Cetuximab (Erbitux®)	For KRAS wild-type metastatic colorectal cancer and squamous cell carcinoma of the head and neck
Ras	Farnesyltransferase inhibitors	Tipifarnib (Zarnestra®)	-
		Lonafarnib (Sarasar®)	-
Raf	Tyrosine kinase inhibitors	Sorafenib (Nexavar®, also a VEGFR and PDGFR inhibitor)	For advanced renal cell carcinoma and hepatocellular carcinoma
PDGFR	Tyrosine kinase inhibitors	Imatinib (Gleevec®)	For treatment of multiple cancers, most notably Philadelphia chromosome-positive chronic myelogenous leukemia
		Dasatinib (Sprycel®)	For chronic myelogenous leukemia and Philadelphia chromosome-positive acute lymphoblastic leukemia
		Sunitinib (Sutent®, also a VEGFR inhibitor)	Mainly for treatment of renal cell carcinoma and imatinib-resistant gastrointestinal stromal tumors
		Vatalanib (also a VEGFR inhibitor)	-

Table 1.3: Continued

mTOR	mTOR inhibitors	Temsirolimus (Torisel®, also a VEGF inhibitor)	For treatment of renal cell carcinoma
		Everolimus (Zortress®)	For several advanced cancers
		Sirolimus (Rapamune®)	Approved as an immunosuppressant in kidney transplants
VEGF	Monoclonal antibodies	Bevacizumab (Avastin®)	For several advanced cancers including glioblastomas
VEGFR	Tyrosine kinase inhibitors	Vatalanib, AEE788,Vandetanib, Sorafenib, Sunitinib	(Discussed above)
Protein kinase C	Protein kinase C inhibitors	Enzastaurin	-
Proteasome	Proteasome inhibitors	Bortezomib (Velcade®)	For relapsed multiple myeloma

CHAPTER II

GENOMIC PROFILING OF GLIOMA BIOPSIES REVEALED PROTEIN TYROSINE PHOSPHATASE RECEPTOR TYPE KAPPA AS A NOVEL TUMOR SUPPRESSOR OF PROGNOSTIC VALUE

2.1 Summary of chapter

The majority of patients with malignant glioma die within a year of diagnosis because of operative and therapeutic complications mainly resulting from extensive invasion of glioma cells (9,23). Conventional therapeutic interventions including surgery, radiotherapy and chemotherapy have fallen short of expectations (9,11). Shortcomings of the conventional therapies call for better understanding of glioma genetics particularly as it relates to key regulatory signals that control cell invasion and migration. Several studies in the past decade have focused on genome-wide screening for genetic changes and associated signaling pathways in cancer, for effective and informed therapeutic strategies. Most of the genomic profiling studies in glioma have pointed to the central role of receptor tyrosine kinases (RTKs) mediated tyrosine phosphorylation in driving the aggressive phenotypes of malignant glioma (7-10,43,58). However, limitations of RTK-targeted therapy particularly for heterogeneous tumors such as high grade glioma have prompted search for alternative strategies. New insights into regulatory signals that play a vital role in glioma migration and invasion are of major interest.

We hypothesized that in-depth genomic explorations will improve our current understanding of the molecular mechanisms underlying glioma migration in relation to tyrosine phosphorylation signaling events and will allow discovery of novel glioma

migration markers with prognostic and predictive significance. We aimed to identify genomic alterations in glioma that substantially influence cell migration and invasion.

In this study, we screened for genome wide alterations in a representative population of glioma patients using mapping arrays. Copy number alterations (CNAs) and loss of heterozygosity (LOH) events were detected at several chromosomal loci. Interestingly, these regions harbor multiple candidate genes with delineated roles in the development and progression of cancer. These genes are involved in key regulatory pathways which include phosphorylation/dephosphorylation dependent signaling, DNA replication, transcription, cell adhesion, proliferation and apoptosis. Out of these pathways the most relevant in glioma are the phosphorylation/dephosphorylation- and cell adhesion- dependent signaling networks. This is because loss of cell-adhesion as well as activation of tyrosine phosphorylation signaling pathways via RTKs are the most frequent molecular events in malignant gliomas (7-10,43,58). Since aberrant tyrosine phosphorylation signaling drives cell growth and migration, it is critical that cellular tyrosine phosphorylation levels are strictly regulated. In our analysis, we observed frequent alterations (23%) of the Protein Tyrosine Phosphatase Receptor type Kappa (PTPRK) locus (6q22-23), a gene involved in both tyrosine phosphorylation and cell-adhesion signaling. PTPRK locus alterations were among the top significant and also correlated to overall survival of glioma patients. Receptor protein tyrosine phosphatases (RPTPs) have indeed emerged as key counter-regulators of RTKs-dependent signaling pathways by dephosphorylation at tyrosine residues (Figure 2.1) (59). Inhibition of aberrant phosphotyrosine signaling by RPTPs could ultimately negatively regulate multiple RTKs. Since, RPTPs can inhibit both ligand-activated and ligand independent

RTKs' activities (60), better understanding of their physiological role in malignant glioma can improve response to conventionally used kinase inhibitors and open new doors to design improved therapies. Recent genomic analyses of human neoplasms have shown importance of RPTPs in many cancers (61-64). In fact, several RPTP loci map to chromosomal regions frequently deleted in cancers (62,65). However, glioma specific function of RPTPs in regulation of tyrosine phosphorylation has not been well studied.

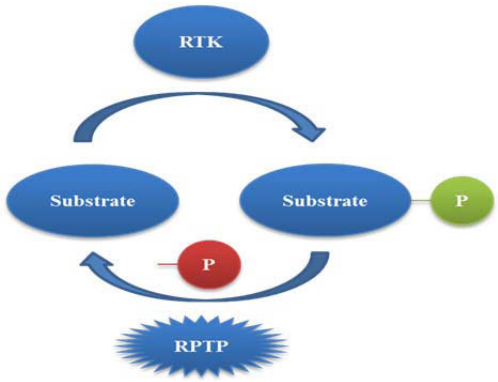

Figure 2.1:Regulation of receptor tyrosine kinase (RTKs) mediated phosphorylation by receptor protein tyrosine phosphatases (RPTPs). RTKs phosphorylate substrate at tyrosine residues to activate signaling processes whereas RPTPs dephosphorylate these tyrosine residues.

Alterations of PTPRK appear very relevant to glioma cell migration because PTPRK is a cell adhesion molecule that is highly expressed in brain. However, PTPRK function has not been described before in gliomas. It is a homophilic adhesion receptor that can directly regulate cell-adhesion dependent processes and can potentially inhibit phosphorylation-mediated signaling events of several receptor tyrosine kinases via tyrosine dephosphorylation activity (59,66). Such receptor like-PTPs play important role in intracellular transduction of changes in the extracellular environment via their

phosphatase activity (67). Interestingly, PTPRK locus (6q22-23) is a common region of allelic deletion at chromosome 6 in several cancers (68-70). Alterations of PTPRK locus have been observed in pancreatic cancer, primary CNS lymphoma and melanoma, and were associated with poor survival of cancer patients (59,68,69,71,72). In particular, study in primary CNS lymphoma found LOH at 6q region and subsequent loss of PTPRK expression to be associated with poor survival of lymphoma patients (69). Moreover, inactivation of PTPRK by sleeping beauty procedure resulted in development of colorectal cancer in mice and was associated with worst outcome (73). These findings suggest that PTPRK is a tumor suppressor that is lost in cancers. Accordingly, we hypothesized that PTPRK is a potential prognostic marker and a functional tumor suppressor gene downregulated in gliomas. Understanding PTPRK function in glioma relevant biological processes will provide novel insights into glioma cell growth and migration.

2.2 Materials and Methods

2.2.1 Sample isolation

We collaborated with Dr. Timothy Ryken at the Deparment of Neurosurgery, University of Iowa Hospital and Clinics and collected several human glioma biopsy specimens (patients provided written informed consent). The study was approved by the University of Iowa institutional review board HawkIRB; IRB#200707727. These biopsies were snap-frozen immediately. Sixty glioma specimens were analyzed in this study. Tissues from epileptic patients undergoing cortical resections were obtained for use as non-tumor tissue (normal) samples.

2.2.2 Microarray analysis

Affymetrix GeneChip^{R} Human SNP Mapping array 6.0 was used to genotype glioma biopsies according to the GeneChip mapping assay manual (Affymetrix, Santa Clara, CA). This microarray allows genotyping of approximately 1.8 million SNPs and copy number alterations (CNAs), which thus permits detection of abnormalities with a median inter-marker distance of around 1Kb. Briefly, DNA was extracted from the glioma biopsies using DNeasy Blood & Tissue kit (Qiagen, Germany). Integrity of the extracted DNA was verified on 1% agarose gel. 250 ng of DNA was then digested by a restriction enzyme (*Sty*I or *Nsp*I) (New England Biolabs, Ipswich, MA). Digested DNA was ligated with *Sty*I or *Nsp*I specific adaptors using T4 DNA ligase (New England Biolabs, Ipswich, MA). These ligated DNA fragments were PCR amplified with Titanium *Taq* (Clontech, Mountain view, CA) and a single primer complementary to the adaptor sequence. PCR products were then purified from excess primer and salts by column filtration. The eluted products were fragmented using DNaseI. An aliquot of the fragmented DNA was separated and visualized on a 4% agarose gel in 1× TBE buffer to ensure that bulk of the product had been properly fragmented to a size less than 200 bp. The fragmented samples were end-labeled with biotin using terminal deoxynucleotidyl transferase prior to the hybridization of each sample to Genome-Wide Human SNP Array 6.0 for 16 h at 50°C. Following hybridization, the arrays were washed and stained using an Affymetrix Fluidics Station 450. The most stringent wash was 0.6× SSPE, 0.01% Tween-20 at 45°C and the samples were stained with R-phycoerythrin (Life Technologies, Carlsbad, CA). Imaging of the microarrays was performed using a GCS3000 high-resolution scanner (Affymetrix, Santa Clara, CA). The probe intensity

data were collected using Affymetrix GCOS v1.4 software. PartekGS software (Partek, St. Louis, MO) and Nexus (BD Biosystems, El Segundo, CA) were used to evaluate copy number abnormalities and loss of heterozygosity (LOH) status. Tumor data files (.Cel files) were compared to a baseline generated with 270 normal HapMap samples (www.HapMap.org) (for Partek) or with NCBI built 36.1 (for Nexus). Hidden Markov model-based method was used to identify LOH at chromosomal regions from unpaired tumor samples by calculating and comparing SNP intermarker distances, documented SNP-specific heterozygosity rates and the haplotype structure of the human genome. Other comparisons were made using matched blood samples from 24 recent patients for baseline and pair-wise comparisons between paired blood and tumor samples. Significant results from genomic analysis were subsequently confirmed by semi-quantitative reverse transcriptase -PCR (RT-PCR) and real-time quantitative-PCR (Q-PCR).

2.2.3 RT-PCR and real-time Q-PCR

RNA from glioma biopsies and normal (non-tumor) tissue samples were extracted with Trizol according to the manufacturer's protocol (Life Technologies, Carlsbad, CA). Integrity, quality and quantity of these RNA were assessed on 1% agarose gel and using Nanodrop 2000 Spectrophotometer (ThermoScientific, Huntsville, AL). Next, 5 µg of the RNA was reverse transcribed into cDNA using MuMLV retrotranscriptase and oligo dT using standard protocol (Life Technologies, Carlsbad, CA). The cDNA quality was verified by running them on 1% agarose gel. 50 ng of cDNA was then used for further analyses. PTPRK transcript levels were analyzed using RT-PCR and real-time Q-PCR analysis. cDNA from primary glioma cell lines were amplified for detection of full length PTPRK transcript using Expand Long Template PCR System (Roche Diagnostics,

Indianapolis, IN). GAPDH was used as a housekeeping gene. Primer sequences are listed under Table 2.1. Real-time PCR reactions were performed under the following conditions: 95 °C for 30 sec, 58 °C for 30 sec and 72 °C for 30 sec, for 40 cycles of amplification.

Table 2.1: List of primers used in this study.

Gene name	Primer	Sequence
PCR primers		
PTPRK	Forward	5- TGGAGAAAAAGCCAGACTTCA-3
	Reverse	5- AGCCAATCTCTACCCGTGAAT-3
Full length PTPRK amplification primers		
PTPRK	Forward	5- CTTTCGCCCCTGAGGTAGTTT-3
	Reverse	5- CTGCTGGCTCAATAGATGGAC-3

2.2.4 Western blotting

Lysates from glioma and non-tumor specimens were prepared by adding 10 volumes of lysis buffer to cryopreserved tissues. The lysis buffer composed of 150 mM sodium chloride, 1.0% Triton X-100, 0.5% sodium deoxycholate, 0.1% sodium dodecyl sulphate (SDS), 50 mM Tris, pH 8.0, 1x protease inhibitor cocktail, 1 mM EGTA, 5 mM EDTA, 5 mM sodium fluoride, 1 mM PMSF and 1 mM sodium orthovanadate. Glioma tissues were disrupted by incubating them on ice for 30 minutes with frequent vortexing and then centrifuged at 10,000 rpm for 10 minutes at 4^{o}C. Supernatant was collected and the concentration of protein was measured using bicinchoninic acid assay (Pierce, Rockford, IL). Equal volume of 2x SDS laemmli sample buffer (Bio-Rad, Hercules, CA) was added to the lysates. Lysates were then heated at 95^{o}C for 5 minutes prior to loading

them on SDS-polyacrylamide gel. 50 µg of the homogenates were loaded on a 7.5% polyacrylamide gel. Lysates from glioma cell lines were prepared similarly. PTPRK expression was analyzed by immunoblot with two antibodies, one recognizing an epitope on the intracellular domain (ab13225, Abcam, Cambridge, MA) and the other targets the extracellular domain (gift from Dr. Fisher at the University of Michigan, Ann Arbor, MI). GAPDH (6C5, Abcam, Cambridge, MA) was used as a loading control. Nitrocellulose membranes were developed with the ECL detection system (GE Healthcare, Piscataway, NJ).

2.2.5 Cell lines, transfection and transduction

Primary cell lines were generated from the glioma tumor biopsies. Briefly, the tumor biopsies were digested with trypsin for different time periods depending on the preliminary diagnosis (normal brain tissue ~4 hours; low grade tumors ~4 – 8 hours; high tumors ~6 – 12 hours). The digested tissues were then homogenized and incubated at 37°C in proliferation permissive DMEM/F12 media supplemented with 15% fetal bovine serum, 15mM HEPES buffer (pH = 7.5), 1 mM sodium pyruvate, 10 µg/ml insulin, 100 ng fibroblast growth factors and 1% penicillin/streptomycin. Several early passages were frozen down for future studies. These cell lines were characterized at the molecular level to assess their lineage origin and genetic signatures, using microarray profiling. Four primary high grade astrocytic cell lines (AAC-206, GBM-379, GBM-417, GBM-440) were used for this study. These cell lines were selected based on their PTPRK status and proliferative capacity in *in vitro* cell culture conditions. The primary cell lines were maintained in DMEM/F12 media supplemented with 15% fetal bovine serum, 15mM HEPES buffer (pH = 7.5), 1 mM sodium pyruvate, 10 µg/ml insulin, 100 ng fibroblast

growth factors and 1% penicillin/streptomycin, at 37°C in 5% CO_2. Additionally, U87-MG cell line from ATCC (Manassas, VA) was used and maintained in DMEM supplemented with 10% fetal bovine serum at 37°C in 5% CO_2.

Wild-type PTPRK was cloned into the expression plasmid pIRES-hrGFP-II (Stratagene, La Jolla, CA) and transfected into malignant glioma cell lines using Xfect transfection reagent (Clontech, Palo Alto, CA). Cells transfected with the empty vector were used as control for each cell line (Mock).

For lentiviral transduction**,** five shPTPRK-containing pLKO.1 plasmids were initially used to identify the best shRNA(s) with maximum knockdown of PTPRK mRNA levels (ThermoScientific-OpenBiosystems, Huntsville, AL). Recombinant lentiviral vectors carrying human shPTPRK were produced as previously reported (74). In brief, shRNA constructs were co-transfected with pPAX2 packing and pVSVG envelope plasmid into TSA201 cells. The recombinant lentivirus was filtered and tittered in NIH3T3 cells by conventional protocols (74). 2 x 10^5 U87 malignant glioma cells were then transduced with either shPTPRK or scrambled lentivirus in 60-mm tissue culture dish, twice 24 hours apart. Polybrene at concentration 8 μg/ml was used to enhance efficiency of lentiviral transduction. Stable transduced colonies of U87 malignant glioma cells were subsequently selected with puromycin (1 μg/ml; Sigma Aldrich, St. Louis, MO). Retention of the insert was periodically monitored by western blot analysis of PTPRK expression following transient transfection of the shPTPRK expressing stable cell line with wild-type PTPRK clone for 96 h. For primary cell lines (GBM-417, GBM-440) all assays were performed 4 days post-transduction, with 2 days of puromycin selection.

2.2.6 Proliferation assay

MTT colorimetric assay (Sigma-Aldrich, St. Louis, MO) was used to measure proliferation of glioma cell lines (U87-MG, AAC-206 and GBM-379) transfected with control-empty vector or wild-type PTPRK expression plasmid. The assay is based on ability of live cells to reduce yellow color tetrazolium salt (MTT) to insoluble purple formazan crystals, which can then be solubilized in DMSO and quantified by spectrophotometric means. The amount of formazan produced is directly proportional to the number of living cells. For this assay, cells were harvested with 0.05% trypsin after 24 h of transfection. 4000 malignant glioma cells per well were then seeded in a 96 well plate in 12 replicates and incubated at 37°C in 5% CO_2. After 72 h, 20 µl of MTT solution (final concentration 0.5 mg/ml, Sigma Aldrich, St. Louis, MO) was added to each well and the plate was incubated for 4 h at 37°C. The purple formazan product thus produced was dissolved in 200 µl of DMSO. Absorbance of the purple color was measured at 540 nm with background absorbance at 690 nm using a microplate spectrophotometer (Spectra Max Plus, Molecular Devices, CA). The results represent average from three independent experiments and have been expressed as percentage of viable cells relative to mock cells.

2.2.7 Flow cytometry

Cell cycle analysis was performed by flow cytometry with propidium iodide (PI). Briefly, malignant glioma cells transfected with empty or wild-type PTPRK vector were serum arrested at 24 h post-transfection. After 24 h, serum free media was replaced with complete culture media for an additional 24 h period. Cells were then trypsinized with

0.05% trypsin (Invitrogen, Carlsbad, CA) washed with phosphate buffer saline (PBS) and counted. 500 µl of cold hypotonic PI staining solution was added to 5 x 10^5 cells. Cells suspended in hypotonic solution were stored for 30 minutes on ice with frequent vortexing. The resulting nuclei suspension was analyzed on flow cytometer. Staining solution contained 50 µg/ml propidium iodide (Sigma Aldrich, St. Louis, MO) and 0.1% Triton-X-100 in 0.1% sodium citrate solution. 10 µg/ml RNase A (ThermoScientific, Huntsville, AL) was added to the staining solution to eliminate staining of RNA. Cell cycle analysis was performed using Becton Dickinson LSR II flow cytometer and ModFit^{TM} software through the flow cytometry core facility at the University of Iowa.

2.2.8 Soft agar assay

Anchorage independent growth of mock or wild-type PTPRK expressing U87-MG cells was analyzed with soft agar colony formation assay as described previously (75). Cells were seeded at a concentration of 40,000 per ml in 0.4% agarose and plated over the bottom layer of 0.8% agarose in a six-well plate. The plate was incubated at 37°C for 3 weeks. Colonies thus formed were stained with 0.05% crystal violet solution, imaged and counted in 10 random 4x fields under a Jenco microscope (Jenco, Portland, OR) attached to a Mightex CCD camera. Graphs were plotted as average colony count relative to mock cells in triplicates from at least three independent experiments.

2.2.9 Migration assay

Migration capacity of glioma cell lines was analyzed by scratch wound assay after overexpression and knockdown of PTPRK. Individual wounds were induced by scratching confluent monolayers of cells with a 10 µl pipette tip. Prior to creating the

wound, culture media was replaced with serum-free media to control for proliferation. Images of the wounds were taken with a 4x objective at 0 and 24 h using a Jenco microscope (Jenco, Portland, OR) equipped with a Mightex CCD camera. Image analysis was done using TScratch software (CSElab, ETH Zurich, CH) and changes in wound areas were measured over 24 h period. The results represent average of three independent experiments, shown as percentage of migrated cell relative to mock cells.

2.2.10 Statistical analysis

Survival curves were plotted according to Kaplan-Meier analysis and median survival was compared using the Log-Rank test. Significant variables in univariate analyses of overall survival were also analyzed using multivariate regression analyses (KPS, age and molecular events). Unpaired Student's t-test was used to analyze statistical significance of *in vitro* cell-based experiments. $P<0.05$ was considered for statistical significance. All statistical analysis was performed using Excel or SAS version 9.3.

2.3 Results

2.3.1 Clinical data

The study sample of sixty glioma biopsy specimens was representative of patients with grade II to IV glioma subtypes. Majority of these patients were diagnosed with aggressive grade III and grade IV gliomas. Only 11 out of 60 patients were grade II gliomas (ACG and ODG) (Table 2.2). This distribution of patients based on grade is also in line with overall glioma patient population which mainly comprises of patients with high grade gliomas. Clinical features such as histology, diagnosis, age at diagnosis and Karnofsky Performance Status (KPS) of the patients were recorded for evaluating

association among clinical and biological factors (Table 2.2). The median age at diagnosis was 51 years with range from 18 to 79 years. Patients did not receive any therapy prior to surgery. Following surgery, patients were treated with radiotherapy, chemotherapy or their combination (conventional approach as indicated in Table 1.2) and survival was followed up to 15 years from the time of diagnosis. Patient specific therapy was given depending upon various clinical features such as pathology, diagnosis, age at diagnosis and KPS. Dose of radiation (range 17.5 Gy to 60 Gy in 24 to 34 fractions) over period of 5-6 weeks was administered, accordingly. Concomitant temozolomide (TMZ) chemotherapy was administered at a dose of 75 mg/m^2/day with radiotherapy. Adjuvant TMZ, after 4 weeks of radiotherapy, was given at a dose of 150 mg/m^2/day on days 1 to 5 of the first 28-day cycle. If the first cycle of chemotherapy was well tolerated, it was followed by 200 mg/m^2/day on days 1 to 5 of each subsequent 28-day cycle. Total number of cycles varied depending upon patient's clinical features.

All grade II astrocytic patients received radiotherapy and one cycle of adjuvant treatment with TMZ. Grade II oligodendroglioma patients also mainly received radiotherapy along with adjuvant TMZ chemotherapy (150 mg/m^2/day on days 1 to 5 for 1 cycle and 200 mg/m^2/day on days 1 to 5 for 2 cycles). Three patients with chromosome 1p/19q deletion signature were offered Gliadel wafer (carmustine) implants and one patient with chromosome 1p/19q deletion was treated with TMZ directly (150 mg/m^2/day on days 1 to 5 for 1 cycle and 200 mg/m^2/day on days 1 to 5 for 5 cycles) instead of radiotherapy. Patients with chromosome 1p/19 deletion signature respond much better to chemotherapy and thus are generally administered chemotherapy without any post-operative radiotherapy (14,41). Further, majority of the patients with grade III anaplastic

oligodendroglioma and anaplastic astrocytoma received standard therapy of radiation followed by adjuvant TMZ. Dose of adjuvant chemotherapy varied between patients (150 mg/m^2/day for 5 days - 3 cycles or 200 mg/m^2/day for 5 days - 6 cycles or 150 mg/m^2/day for 5 days - 1 cycle followed by 200 mg/m^2/day on days 1 to 5 for 5 cycles). Two elderly patients with age ≥ 77 years received surgery with Gliadel wafer implants instead of prior radiotherapy. Early chemotherapy instead of radiotherapy can avoid radiation related adverse effects in such patients with low life expectancy. Moreover, one of the elderly patients with anaplastic oligodendroglioma displayed chromosome 1p deletion signature and therefore was likely to benefit more with chemotherapy (14,41). Further, patients diagnosed with GBM received surgery with Gliadel wafer implants followed by combination of radiotherapy, and concomitant and adjuvant TMZ chemotherapy as mentioned in Table 1.2. Standard dose of concomitant and adjuvant TMZ was administered.

In order to verify that our study population is representative of actual glioma population and to avoid bias results we correlated overall survival to known prognostic predictors such as age and glioma grade. Patients were divided into two age groups for overall survival analysis; patients with age less than or equal to the median age (≤51) and those older than the median age. Significant correlation was found between age and survival (cut-off age=51 years, p=0.003, Log-Rank test) (Figure 2.2A). Patients with age less than 51 years have longer survival (38 months vs. 18 months) in glioma. This is in accordance with many previous clinical studies which have established age at diagnosis as an independent prognostic parameter indicating that young age at the time of diagnosis is associated with better survival of glioma patients (14,22,41-43).

Table 2.2: Clinical data for glioma patients in this study.

Glioma	Grade	# of Patients	% of females	Age at diagnosis in years		Survival in months	Tumor Recurrence cases		KPS score
				Median	Range	Median	#	%	Median
AC	II	5	38	32	20-54	26	0	0	94
ODG	II	6	29	40	24-58	56	4	43	85
AOD	III	7	33	39	20-79	29	6	67	84
AAC	III	13	20	48	18-77	25	5	31	92
GBM	IV	29	55	59	28-72	16	17	48	85

Note: AC = Astrocytoma, ODG = Oligodendroglioma, AOD = Anaplastic oligodendroglioma, AAC = Anaplastic astrocytoma, GBM = Glioblastoma. KPS stands for Karnofsky Performance Status.

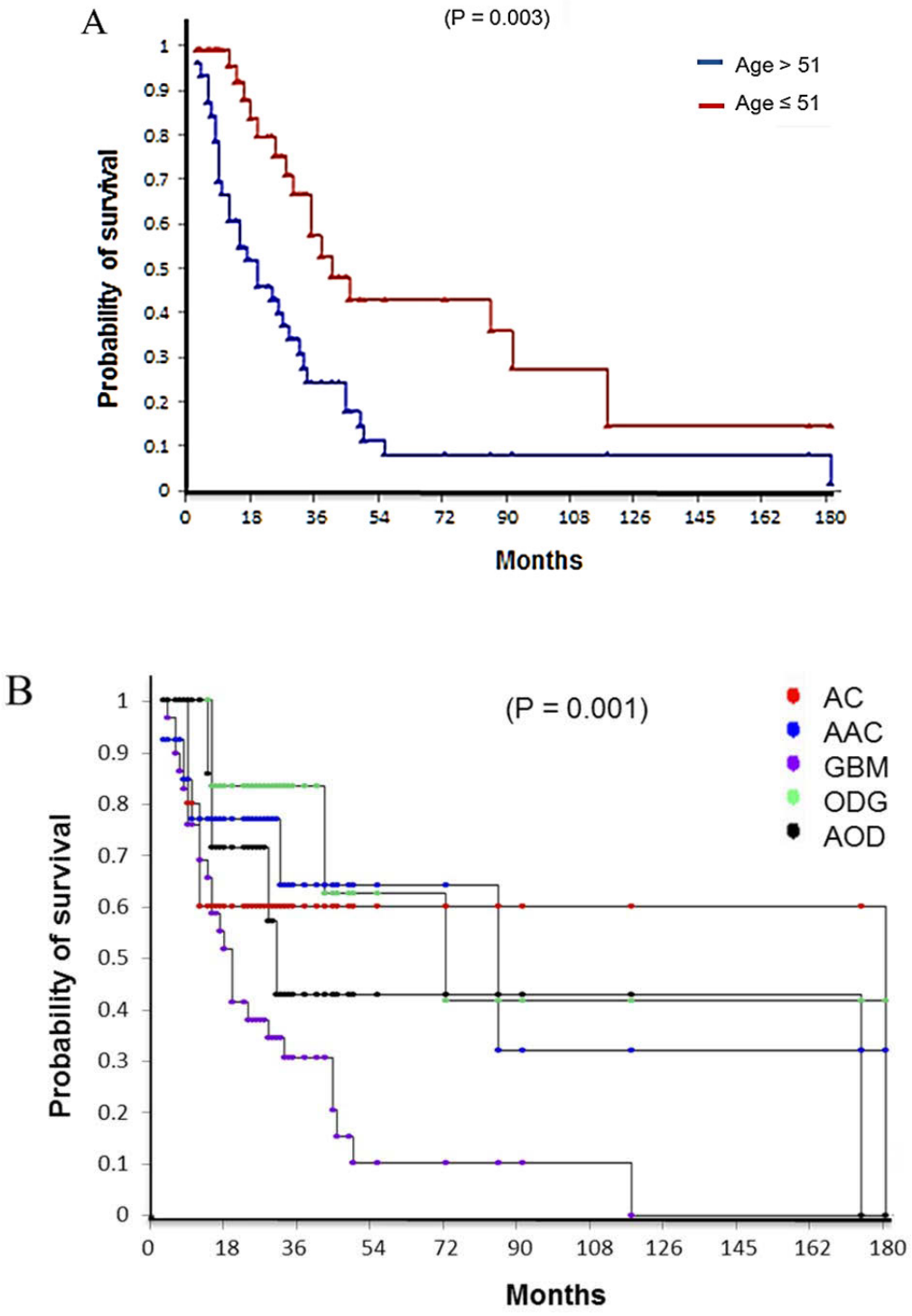

Figure 2.2: Kaplan-Meier curves of overall survival according to age and diagnosis. Kaplan-Meier estimates of probability of survival stratified according to (A) median age (51 year) and (B) glioma type were plotted against survival in months. ODG= Oligodendroglioma, AOD=Anaplastic oligodendroglioma, AC=Astrocytoma, AAC =Anaplastic astrocytoma and GBM = Glioblastoma.

Moreover, Kaplan-Meier estimates of probability of survival stratified according to recorded clinical diagnosis were plotted. Patients that were diagnosed with grade II and grade III gliomas showed similar survival however grade IV patients showed the worst survival (p=0.001, Log-Rank test) (Figure 2.2B). Specifically, median survival in patients with GBM was 18 months compared to low grade glioma patients with median survival of 56 months. Thus, patients with low grade glioma have better survival chances after surgery and treatment. Significant correlations with age and diagnosis suggest that the study population is representative of general characteristics of patients with glioma.

2.3.2 LOH analysis revealed multiple tumor suppressor candidates with PTPRK locus among the top significant alterations

To identify genetic changes in our representative population of glioma patients, we performed genome wide screening of CNAs and LOH events in biopsy specimens using mapping arrays. Using Partek and Nexus algorithms, we detected significant LOH (copy neutral or with deletion) at several chromosomal regions ($P<0.0001$) (Table 2.3). These regions harbor potential tumor suppressor genes with important role in several signaling pathways that regulate transcription, proliferation, apoptosis, tyrosine phosphorylation and cell adhesion. Among these signaling pathways, alterations in cell-adhesion and tyrosine phosphorylation signaling are the most relevant to biology of glioma. This is because genomic analyses have shown activation of tyrosine phosphorylation signaling pathways and loss of cell adhesion as frequent events in glioma (7-10,43,58). In particular, aberrant tyrosine phosphorylation via overactivated

receptor tyrosine kinases is observed in more than 80% of malignant gliomas that lead to cell proliferation, migration and invasion (8).

Table 2.3: Chromosomal regions with highly statistically significant loss of heterozygosity (LOH) in analyzed glioma biopsies.

Chr.	Starting site	Ending site	RefSeq ID	Gene Symbol	Function	Frequency (%)
1	53165535	53289870	NM_002979	SCP2	Metabolism	7
2	162988002	163403486	NM_173162	KCNH7	Transcription	4
2	209997015	210307079	NM_001039538	MAP2	MAPK signaling	7
3	50375234	50515896	NM_006030	CACNA2D2	MAPK signaling	3
6	**128331624**	**128883416**	**NM_002844**	**PTPRK**	**Cell adhesion and tyrosine phosphorylation**	**23**
7	18501893	19003517	NM_178423	HDAC9	Transcription	17
9	2005341	2183623	NM_139045	SMARCA2	Transcription	21
10	74436985	74526630	NM_000917	P4HA1	Metabolism	10
10	97941444	98021323	NM_013314	BLNK	MAPK signaling	10
10	118177413	118227458	NM_001011709	PNLIPRP3	Metabolism	10
12	90063165	90096460	NM_133504	DCN	Cell adhesion, apoptosis	4
13	33290205	33438695	NM_181558	RFC3	DNA replication	10
14	77939845	79400513	NM_004796	NRXN3	Cell adhesion	8

Note: Chr. stands for chromosome, starting and ending site denote genomic region where LOH was detected. Frequency indicates percentage of biopsy specimens with indicated alteration.

In context with cell-adhesion and tyrosine phosphorylation signaling which is mainly responsible for migratory phenotype of glioma cells, we observed alterations of the Protein Tyrosine Phosphatase Receptor type Kappa (PTPRK) locus (6q22.33) among the top significant altered regions (Table 2.3). PTPRK locus alterations are important to glioma biology as PTPRK is a homophilic cell adhesion receptor that is highly expressed in brain. It can directly sense cell-cell contact and regulate intracellular tyrosine phosphorylation signaling by inducing dephosphorylation of tyrosine residues. Prognostic significance of the PTPRK locus alterations was assessed for overall survival after controlling for effects of age at diagnosis, tumor grade and post-operative KPS scores. Kaplan-Meier survival analysis indicated significant association between PTPRK genomic status and median survival in our study population (Figure 2.3, $P<0.0001$, Log-Rank test). Patients with inactivated or deleted PTPRK (23%) had the worst outcome (median survival = 14 months) compared to patients with normal PTPRK locus (median survival = 30 months). Since our analysis was limited by small sample size, prognostic significance of PTPRK genomic status was independently confirmed in a bigger dataset of more than 350 glioma patients (Rembrandt/NCI databank, National Cancer Institute. 2005. http://rembrandt.nci.nih.gov). Genomic profiling of these patients was conducted similar to our analysis. PTPRK genomic status showed prognostic significance in this dataset as well (Figure 2.4A, $P=0.0058$). Patients with normal PTPRK locus (n=286) had better survival than those with altered (deletion/LOH) PTPRK locus (n=42). In addition, gene expression profiles of patients with glioma are also documented in the Rembrandt dataset (National Cancer Institute. 2005. http://rembrandt.nci.nih.gov). Survival analysis based on PTPRK transcript levels in the Rembrandt glioma dataset indicated significant

association between PTPRK expression and outcome (Figure 2.4B, P=0.002). Patients with low PTPRK mRNA levels (129 of 342 patients) had poor survival. Thus PTPRK status at both genomic and transcriptomic level can predict survival of glioma patients.

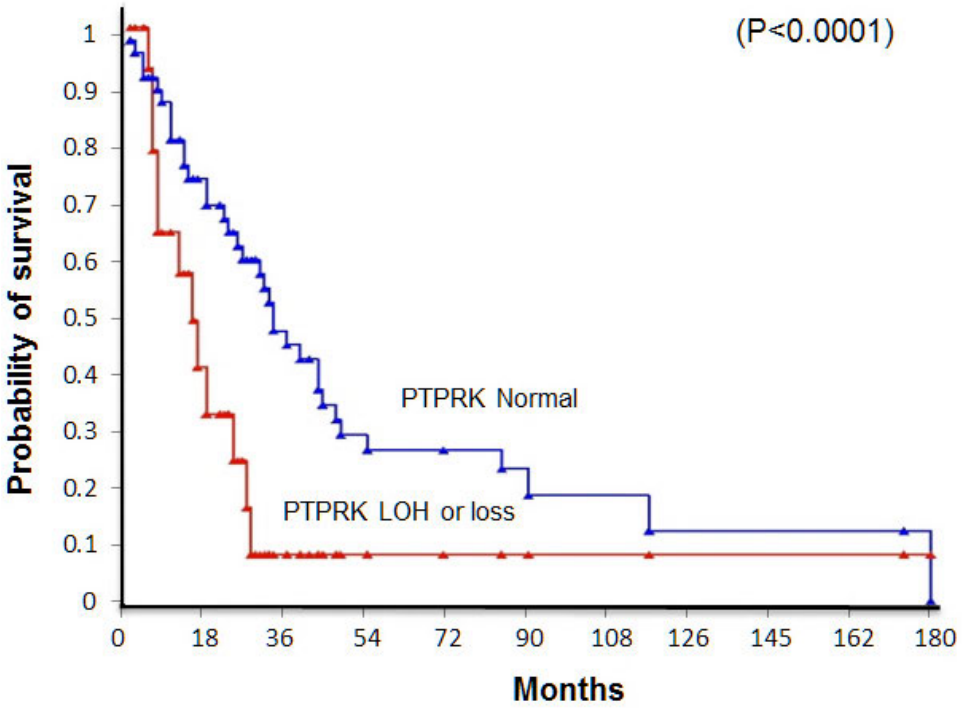

Figure 2.3: PTPRK locus alteration is associated with poor outcome. Kaplan-Meier estimates of probability of survival stratified according to PTPRK locus status were plotted 1) PTPRK normal and 2) PTPRK LOH or loss.

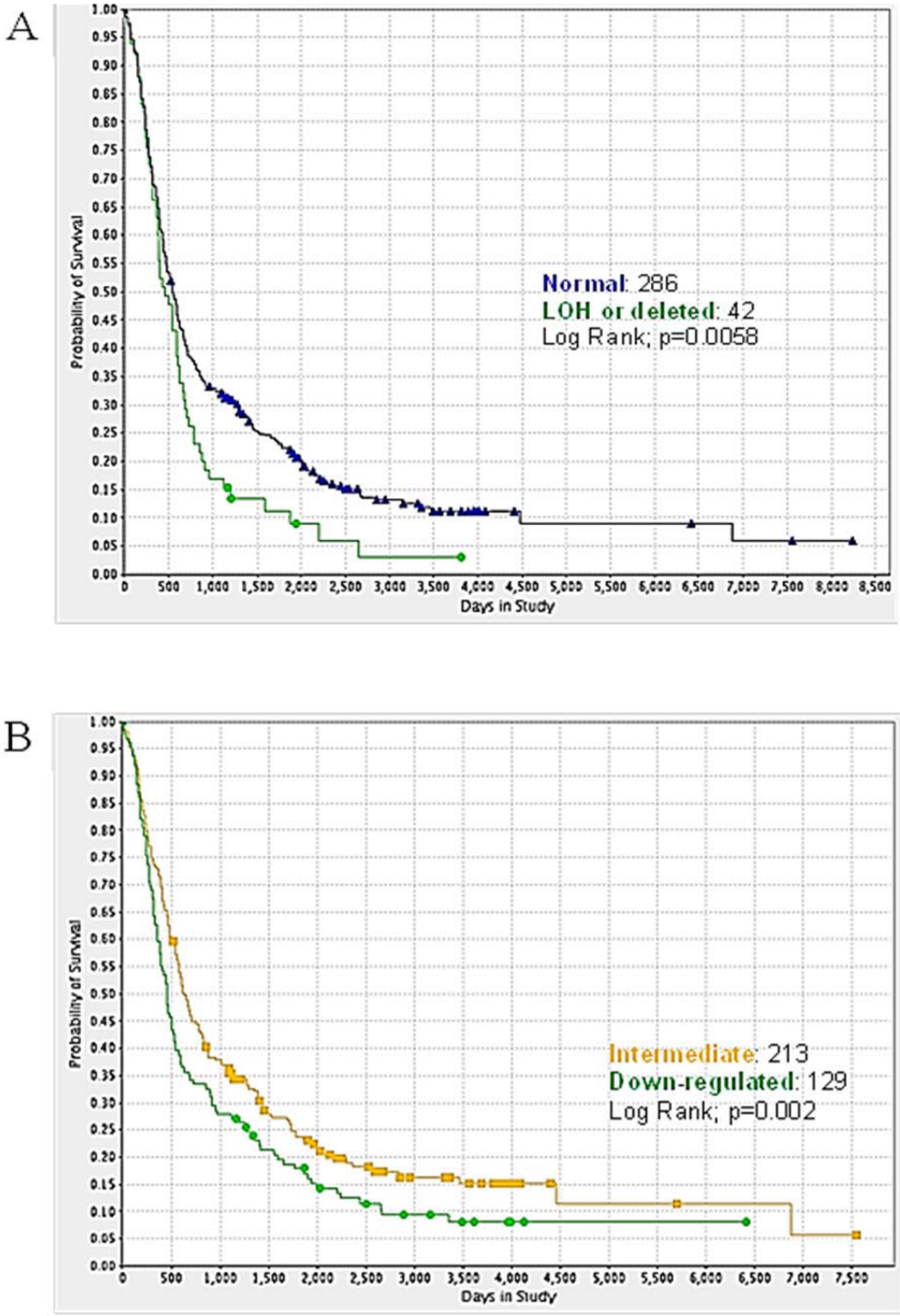

Figure 2.4: PTPRK genomic and transcriptomic status correlated with survival in Rembrandt dataset of glioma patients. Kaplan-Meier curve for overall survival of glioma patients in independent dataset according to (A) PTPRK genomic status and (B) transcriptomic levels were plotted.

2.3.3 PTPRK expression is reduced in malignant glioma

In an effort to better understand PTPRK role in biological processes of glioma we analyzed PTPRK mRNA and protein levels in glioma tumor specimens and normal (non-tumor) brain tissues. Consistent with the observation from Rembrandt dataset, real-time PCR analysis of PTPRK expression revealed significantly lower transcripts in tumor specimens compared to non-tumor biopsies (Figure 2.5A, $P<0.001$). This suggests that inactivation of the PTPRK favors glioma phenotypes. Interestingly, PTPRK mRNA levels also correlated with glioma grade (Figure 2.5B). Five random samples for each glioma grade (grade II to IV) were analyzed by RT-PCR. Despite the fact that GAPDH levels were not similar for all the samples, grade II gliomas showed clear evidence of high PTPRK transcript levels compared to the highly dispersive grade III and grade IV gliomas (GBM).

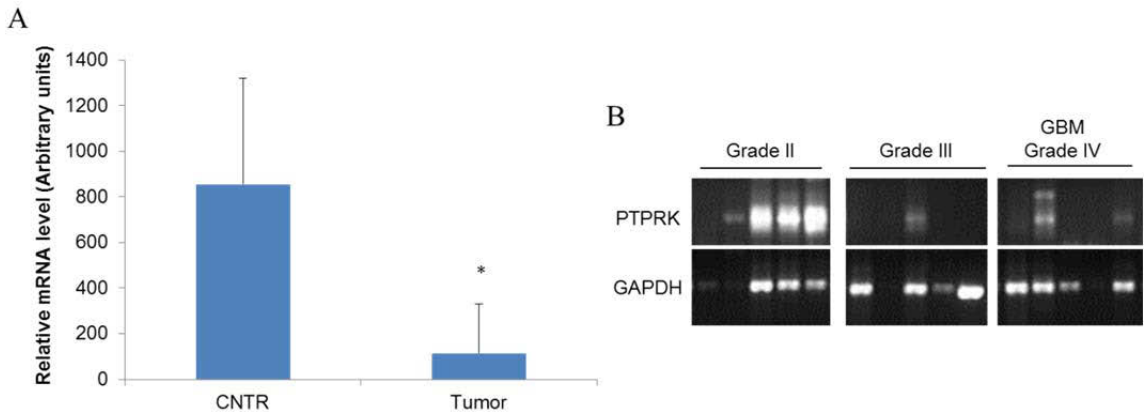

Figure 2.5: PTPRK transcript levels are lower in glioma. (A) PTPRK mRNA levels were analyzed in glioma biopsies and non-tumor brain tissue specimens (control) using real-time qPCR (B) Five tumor specimens per glioma grade were randomly selected and amplified for PTPRK via RT-PCR. PCR products were run on 2% agarose gel. GAPDH was used as a housekeeping gene.

Further, PTPRK protein expression was compared between tumor specimens from different grades of glioma patients and normal (non-tumor) brain tissues. Surprisingly, multiple PTPRK fragments were detected in both normal brain and glioma tissue samples (Figure 2.6A). In fact, all the analyzed glioma specimens showed multiple PTPRK fragments, independent of tumor grade (Figure 2.6A and 2.6B). These fragments can result from post-translational processing of the transmembrane PTPRK protein (Figure 2.6C). Such modification is a common phenomenon for most of the receptor type proteins (76,77). Based on the PTPRK protein sequence, protein bands at ~180 kDa and ~90 kDa correspond to the full length PTPRK and its P-subunit, respectively. Two close bands near 75 kDa seem to be PTPRK intracellular fragments (PΔE and ICD) with cleaved extracellular domain. PΔE (~75 kDa) is a membrane bound fragment whereas ICD fragment (~66 kDa) is released from the membrane. The E-subunit was not detected as the antibody targets intracellular domain of PTPRK. Additional bands of cleaved PTPRK were seen which are yet to be characterized. Regardless, PTPRK protein levels were much higher in normal tissues compared to high grade glioma (grade III and IV) tumors (Figure 2.6A). The major difference between normal and tumor tissues was expression of 180 kDa full length PTPRK (Figure 2.6A, #1). Full length PTPRK expression was lost in majority of high grade gliomas (grade III and IV) (Figure 2.6A). Interestingly, low grade gliomas showed higher levels of total PTPRK as well as full length PTPRK protein in comparison to aggressive grade III gliomas (Figure 2.6B). Altogether, PTPRK expression in glioma is altered not only resulting from mutations but also by post-translational processing of the full length protein. These results suggest that

full length PTPRK has an important functional role in glioma and its downregulation could be a crucial event in glioma progression.

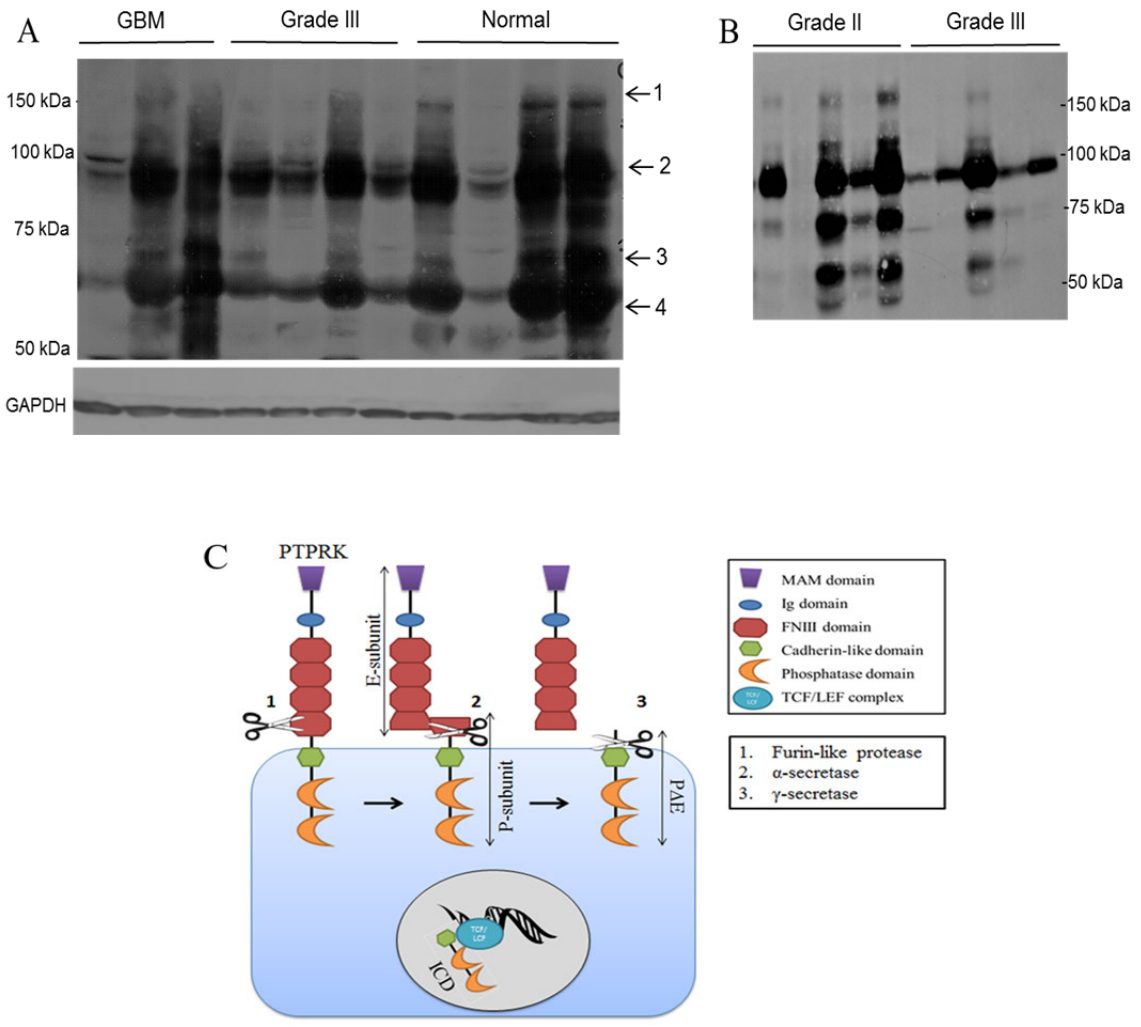

Figure 2.6: Western blot analysis of PTPRK in glioma tissue specimen and normal brain tissue. (A) PTPRK expression was analyzed in high grade gliomas (grade III and grade IV-GBM) with antibody recognizing intracellular PTPRK domain (Abcam 13225). Full length PTPRK and its fragments are shown: 1) Full length cell surface PTPRK, 2) predicted PTPRK P-subunit, 3) predicted PΔE subunit and 4) predicted ICD domain. (B) Expression of PTPRK protein was compared between low grade (grade II) and grade III gliomas. (C) Diagrammatic representation of PTPRK processing by activity of three proteases 1) a furin-like protease yielding a PTPRK P-subunit fragment, 2) an α-secretase yielding a PΔE subunit, and 3) γ-secretase that generates a membrane-free PTPRK-intracellular domain (ICD) fragment.

2.3.4 PTPRK overexpression inhibits both anchorage-dependent and -independent proliferation of malignant glioma cells

Since receptor tyrosine kinases are key mediators of glioma growth and that PTPs are important counterparts of tyrosine kinases activity, frequent inactivation of PTPRK in glioma lead to a hypothesis that cell surface associated PTPRK protein suppresses glioma cell growth. To determine whether wild-type PTPRK affects the proliferative capacity of glioma cells, PTPRK was overexpressed in malignant glioma cell lines and their growth was assessed *in vitro* with the MTT proliferation assay. Three high grade glioma cell lines that do not express full length PTPRK transcript were selected (Figure 2.7). These cell lines were U87-MG cells and two primary cell cultures of high grade glioma - AAC-206 and GBM-379. Wild-type PTPRK was overexpressed in these malignant glioma cell lines and the efficiency of PTPRK transfection was verified by western blot (Figure 2.8A)**.** Full length PTPRK expression was observed in all the cell lines after transfection with wild-type PTPRK vector compared to mock cells. PTPRK overexpression induced marked decrease in proliferation of all the three cell lines by 50-60% compared to mock cells (Figure 2.8B; P=0.003, U87-MG; P=0.005, AAC-206; P=0.008, GBM-379). Significant decrease in proliferation of the wild-type PTPRK expressing malignant glioma cells indicate that the cell surface PTPRK protein is a negative regulator of glioma cell growth.

We further confirmed PTPRK role in glioma proliferation by analyzing cell cycle profiles of U87-MG, AAC-206 and GBM-379 cells expressing wild-type PTPRK or control vector by flow cytometry. Specifically, cell cycle analysis of PTPRK expressing

primary cell lines (AAC-206, GBM-379) and U87-MG cells showed 12% and 17% higher cell fraction in G1 phase along with lower fraction of S phase than mock cells, respectively (Figure 2.9A, 2.9B and 2.9C). Thus, in accordance with MTT assay results, greater fraction of malignant glioma cells were found in G1 phase after PTPRK overexpression suggesting that wild-type PTPRK inhibits cell cycle progression.

In addition, we examined the effect of wild-type PTPRK on anchorage independent growth of malignant glioma cells. PTPRK expressing and mock U87-MG cells were assessed for their ability to grow unattached in soft agar. Results from soft agar colony assay showed significant 68% reduction in colonies upon wild-type PTPRK expression in U87-MG cells compared with mock cells (Figure 2.10, P=0.003). PTPRK expression reduced the anchorage independent survival of glioma cells and thus can inhibit their malignant transformation.

Together, our results show that wild-type PTPRK suppresses proliferation of glioma cells in monolayer cultures as well as in three-dimensional growth environment.

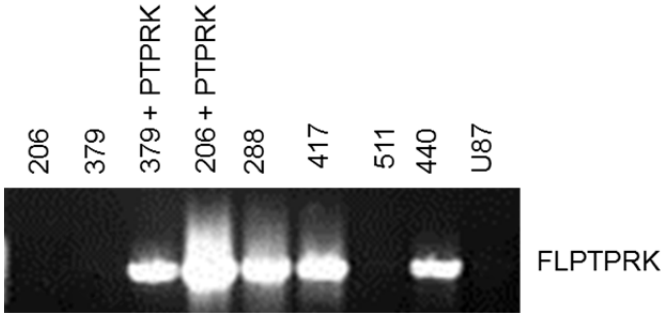

Figure 2.7: RT-PCR detection of full length PTPRK transcripts in primary glioma cell lines. cDNA from primary glioma cell lines and U87-MG cells was amplified for detection of full length PTPRK (FLPTPRK, 4.6 Kb). Numbers indicate patient ID. 206+PTPRK and 379+PTPRK are cell lines transfected with wild-type PTPRK.

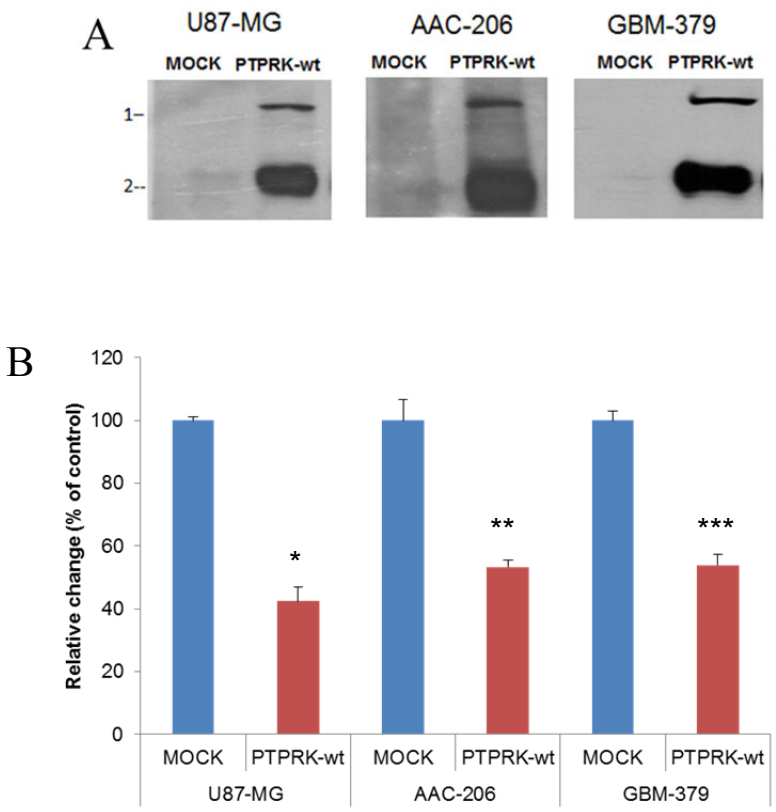

Figure 2.8: PTPRK inhibits proliferation of glioma cell lines. (A) Re-constitution of full length PTPRK in the three glioma cell lines was verified by immunoblotting – 1) Full length PTPRK protein 2) Extracellular domain (E-subunit). (B) Proliferative potential of U87-MG, AAC-206 and GBM-379 cell lines was determined using MTT proliferation assay after transfection with PTPRK expression vector. Cells transfected with empty vector were used as mock for each cell line. The data represent relative average change compared to mock cells from three independent experiments performed in twelve replicates for each cell line. Error bar indicates standard error. * P=0.003, ** P=0.005, *** P=0.008.

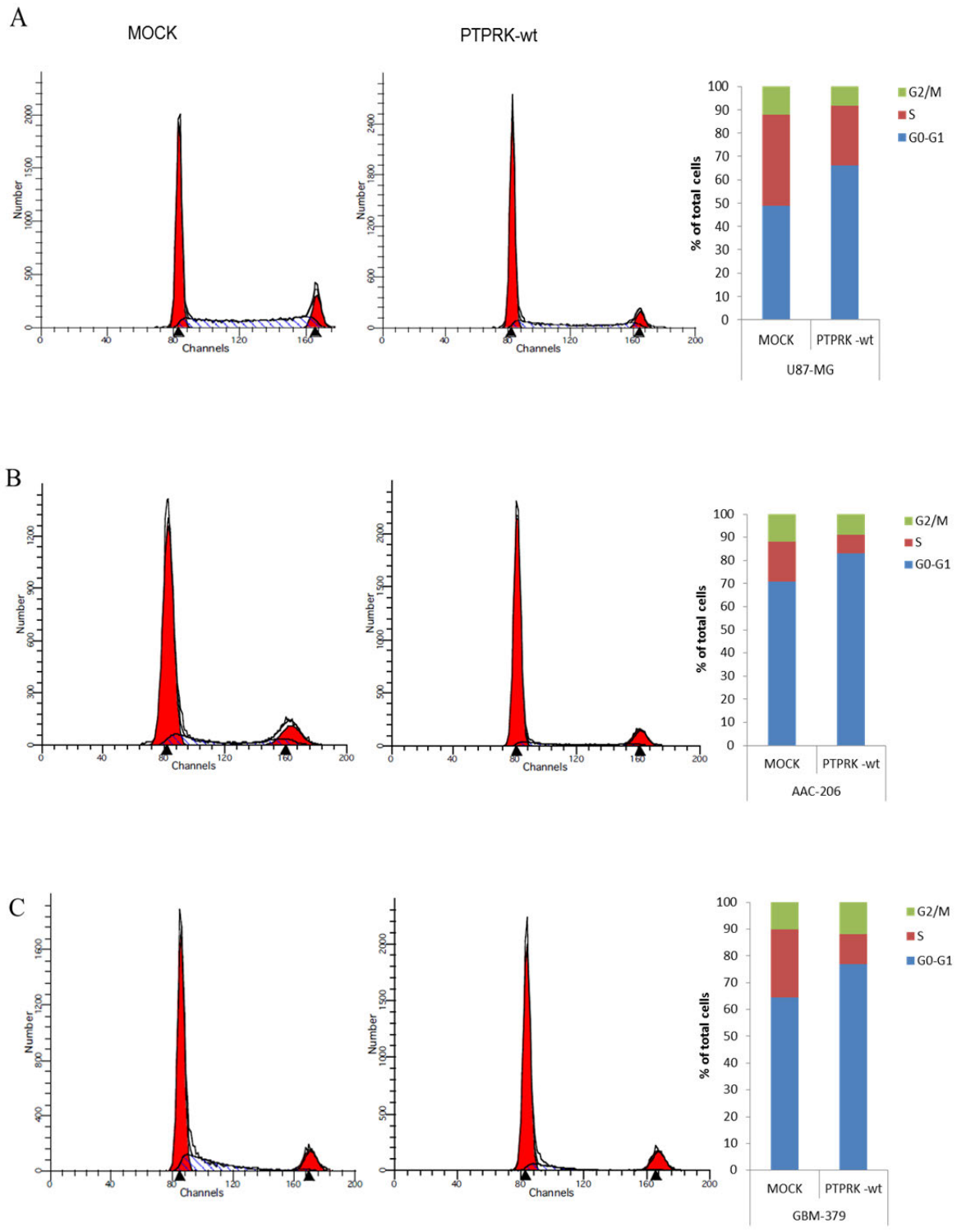

Figure 2.9: PTPRK inhibits cell cycle progression. DNA content of (A) U87-MG, (B) AAC-206 and (C) GBM-379 glioma cell lines was analyzed by flow cytometry. Cell cycle distribution is shown in the bar graphs.

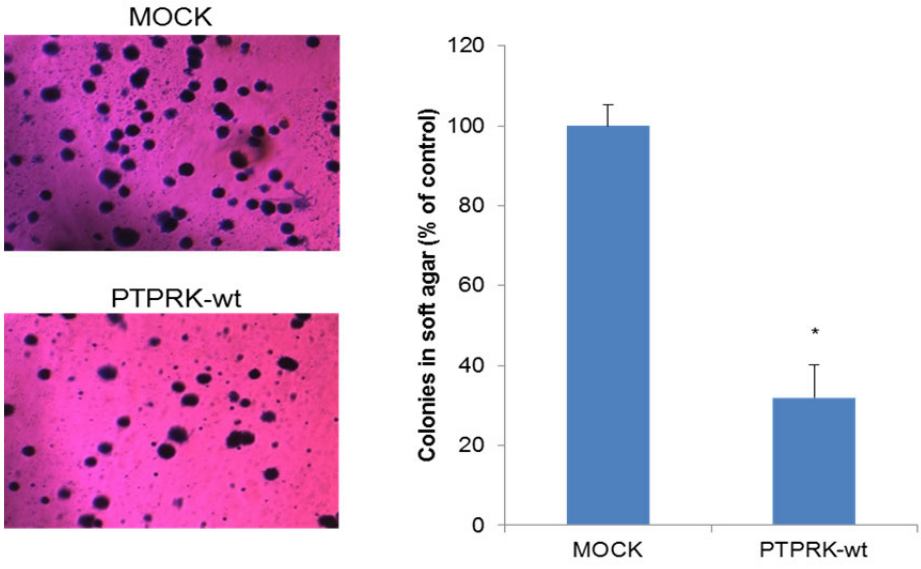

Figure 2.10: PTPRK suppresses anchorage independent growth of U87-MG cells. Anchorage independent growth of U87-MG cells transfected with wild-type PTPRK or empty control vector was analyzed by soft-agar assay. The data represents results from three independent experiments performed in triplicate. *, statistically significant decrease in number of colonies relative to mock cells (P=0.003)

2.3.5 PTPRK suppresses glioma cell migration *in vitro*

Extensive cell migration into the surrounding brain tissue is a hallmark of malignant gliomas. Since, PTPRK can regulate cell adhesion dependent processes (66) and that it is frequently inactivated in malignant gliomas, we hypothesized that PTPRK suppresses glioma cell migration. To determine whether PTPRK expression affects migration capacity of glioma cells, we overexpressed PTPRK in U87-MG, AAC-206 and GBM-379 cell lines, and analyzed their migratory behavior with *in vitro* wound healing assay. Confluent monolayers of mock and PTPRK expressing cell lines were scratched to create a wound. Expression of wild-type PTPRK significantly suppressed migration of all the three malignant glioma cell lines by 50-60% (P=0.001, U87-MG; P=0.004, AAC-206; P= 0.001, GBM-379) as indicated by smaller changes in the wound area size of PTPRK

expressing cells compared to mock cells after 24 h period (Figure 2.11, 2.12A and 2.12B). The mock cell lines migrated more rapidly and almost closed the wound at 24 h. In contrast, PTPRK expression significantly delayed wound closure in the three cell lines.

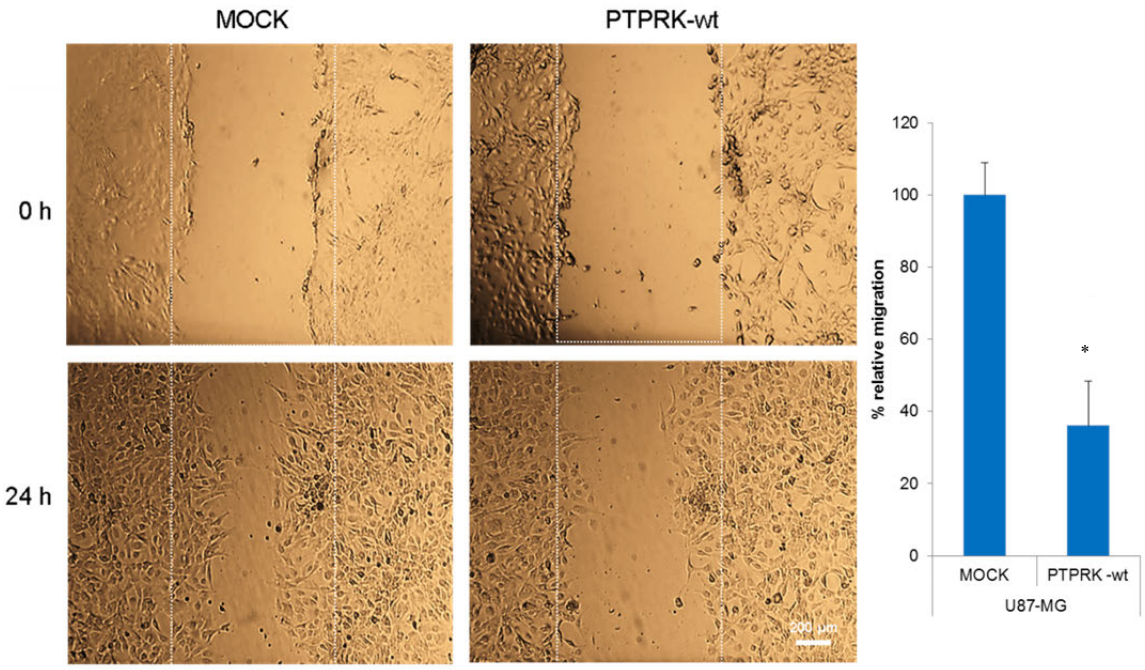

Figure 2.11: Reconstitution of PTPRK inhibits migration of U87 malignant glioma cells. U87-MG cells, transfected with empty vector (mock) or PTPRK were scratched at cell confluence with a pipette tip to create a wound. Wound images were taken at 0 h and 24 h. Changes in wound area were analyzed using TScratch software. Dotted lines indicate approximate position of the wound edge at 0 h. Scale bar=200 µm. Histogram represents changes in wound area per time compared to mock cells from three independent experiments performed in 18 replicates. Statistically significant difference is denoted by *, $P<0.001$ (n=18).

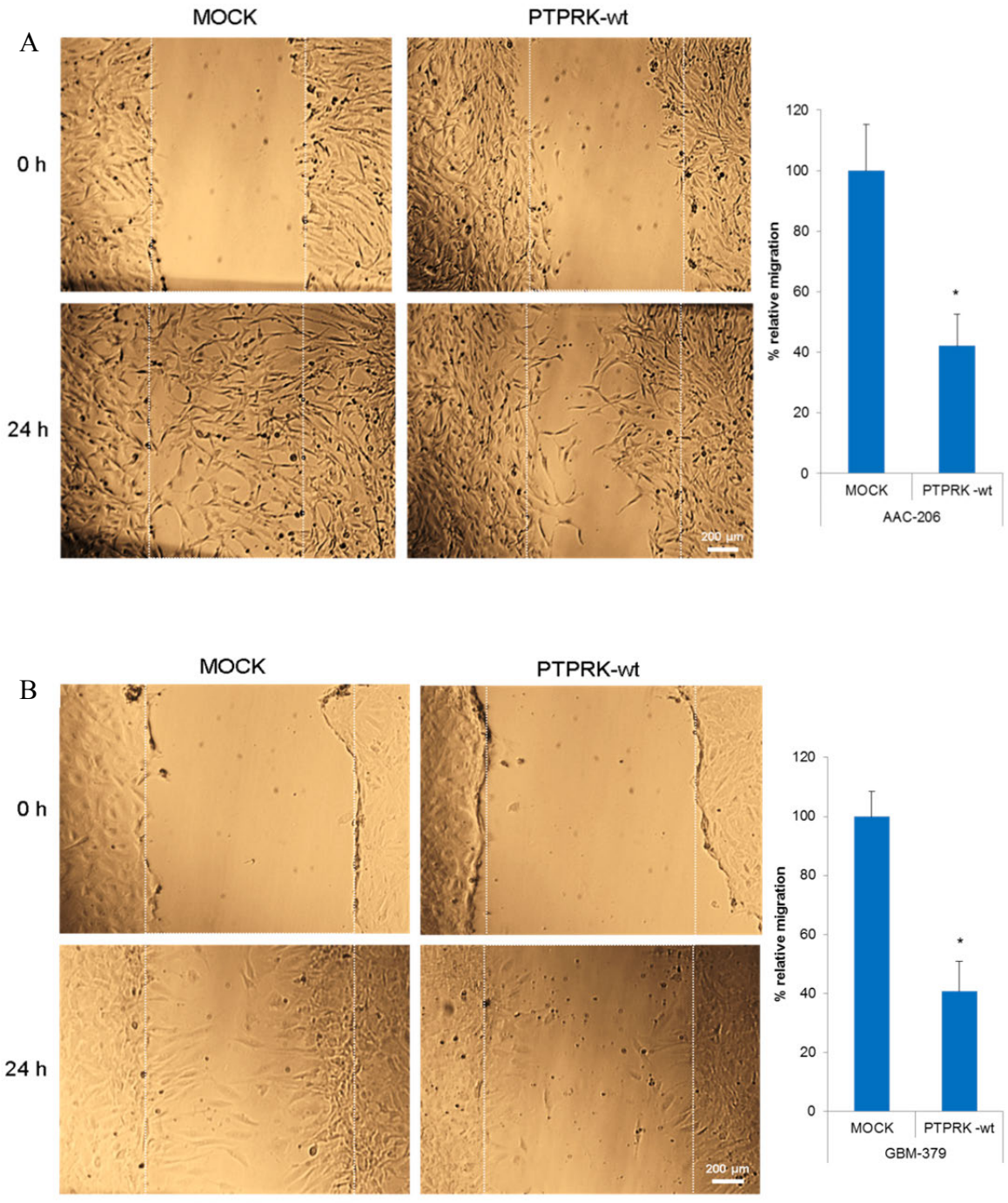

Figure 2.12: PTPRK overexpression suppresses migration of primary malignant glioma cell lines. Wound healing assay was performed as described under the Material and Methods. (A) AAC-206 and (B) GBM-379 cell line. Dotted lines indicate approximate position of the wound edge at 0 h. Scale bar=200 µm, *, P<0.004

To complement these results, the effect of PTPRK knockdown on glioma cell migration was studied. Stable PTPRK specific shRNAs (shPTPRK-1 to 5) or scrambled shRNA expressing U87-MG cell lines were generated as described under the Materials and Methods section. These cell lines were transiently transfected with wild-type PTPRK. The knockdown efficiency of shPTPRKs was analyzed 96 h post-transfection of wild-type PTPRK by immunoblot (Figure 2.13).

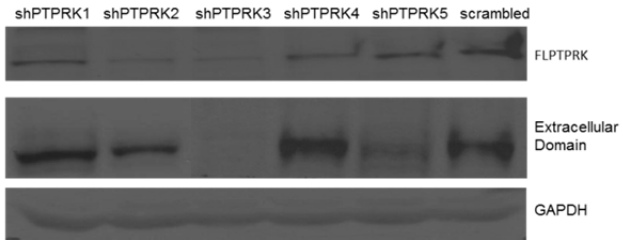

Figure 2.13: Immunoblot analysis of shRNA mediated knockdown of PTPRK. Five shPTPRKs and scrambled shRNA expressing stable U87-MG cell lines were transfected with wild-type PTPRK expression vector for 96 h to analyze their knockdown efficiency by western blotting.

In particular, shPTPRK-3 and shPTPRK-5 expressing stable U87-MG cells showed maximum knockdown and thus were selected for migration studies using wound healing assay. Confluent monolayers of the two PTPRK specific shRNAs or scrambled shRNA expressing stable U87 cells were scratched with a pipette tip to create a wound, 96 h post-transfection of wild-type PTPRK. shPTPRK-3 expressing U87-MG cells showed more than 2 fold greater migration compared to scrambled shRNA expressing cells (Figure 2.14, $P<0.001$). In addition, the effect of PTPRK knockdown on migration was analyzed using another PTPRK specific shRNA, shPTPRK-5, to ensure that migration in response to PTPRK knockdown was not due to an off-target effect.

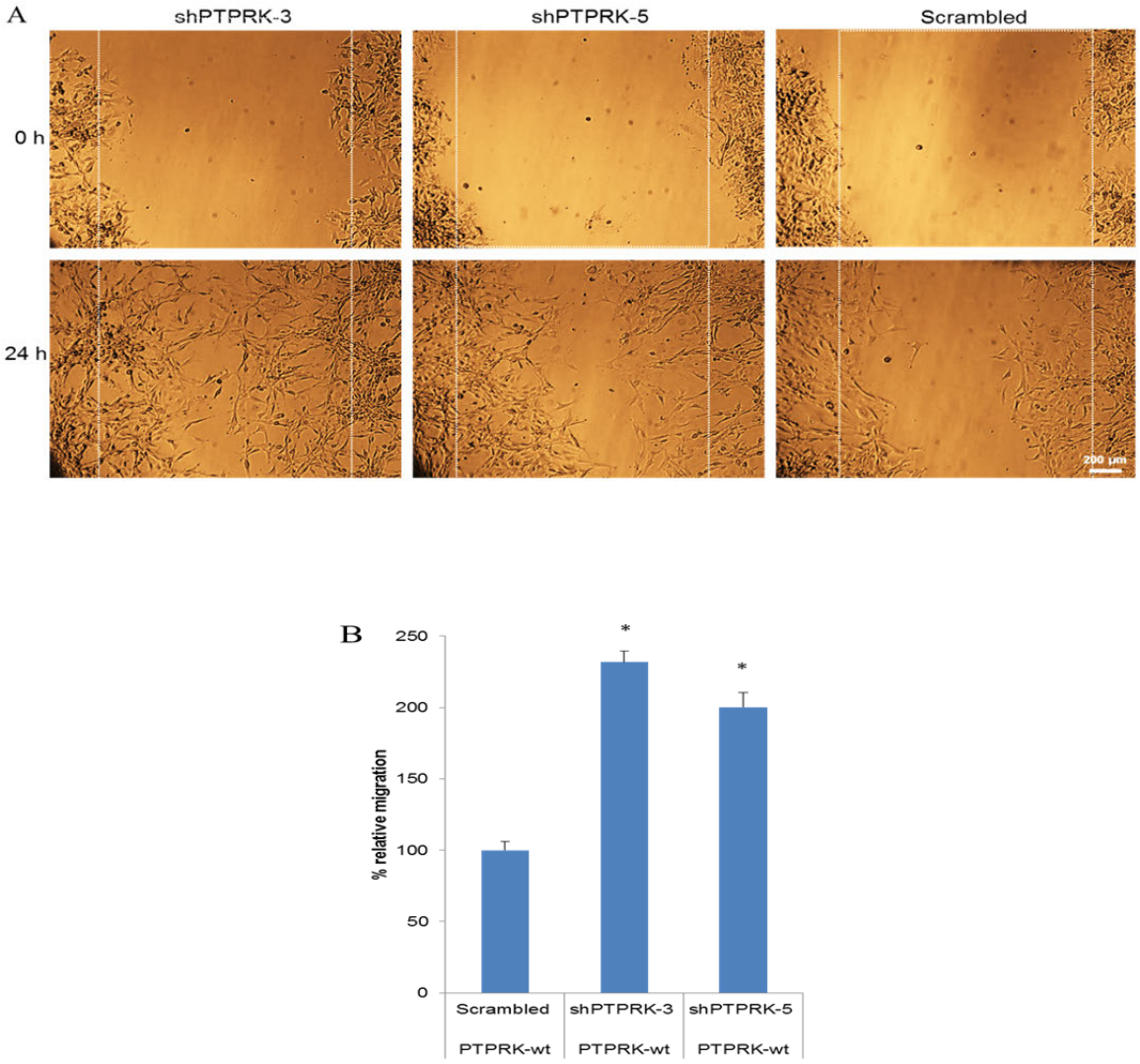

Figure 2.14: Knockdown of PTPRK induces migration of U87 malignant glioma cells. (A) Confluent monolayers of shPTPRK(-3 and -5) and scrambled shRNA expressing U87-MG cells were scratched after 96 h of PTPRK transfection. (B) Data are presented as percentage of migration (change in wound area) relative to scrambled shRNA expressing U87-MG cells from three independent experiments, in twelve replicates. *, $P<0.05$.

U87-MG cells with stable shPTPRK-5 or scrambled shRNA expression were scratched 96 h post-transfection of wild-type PTPRK and the wounds thus created were monitored for 24 h (Figure 2.14A). Similar to shPTPRK-3, shPTPRK-5 expressing U87 cells showed two times higher migration than scrambled shRNA expressing cells (Figure 2.14, $P<0.001$). Overall, these results suggest that wild-type PTPRK inhibits glioma cell migration.

2.3.6 PTPRK proteolysis contributes to glioblastoma cell migration

Western blot analysis of the glioma tumor specimens revealed that membrane bound full length PTPRK is extensively processed post-translationally, particularly in high grade gliomas such as GBM (Figure 2.6). Such post-translational processing mainly occurs due to elevated levels of proteases in GBM (33,34). Consequently, several PTPRK fragments were detected. However, expression of full length PTPRK protein was not observed. Consistent with these observations, a recent analysis of five GBM cell lines showed only processed PTPRK protein isoforms and no full length protein (Figure 2.15A). Other bands around 50 Kda were seen that are not yet well characterized. Membrane bound, full length PTPRK protein was found to inhibit glioma cell migration (Figure 2.11 and 2.12). In contrast, PTPRK fragments, specifically, membrane-free PTPRK-ICD fragment (Figure 2.6C) can potentially translocate to the nucleus and function differently than membrane associated PTPRK due to differences in substrate availability in the subcellular compartments.

Since cell surface associated PTPRK protein was not detected in GBM possibly due to elevated levels of proteases (33,34), we hypothesized that proteolytic fragments of

PTPRK contribute to tumor phenotype. Therefore, we analyzed the effect of PTPRK proteolysis on GBM cell migration in two primary cell lines, GBM-417 and GBM-440, using *in vitro* wound healing assay. We selected these cell lines because they express full length PTPRK at the transcript level (Figure 2.7) but display only proteolyzed PTPRK fragments without any detectable expression of the full length protein (Figure 2.15A). The two primary GBM cell lines were transduced with lentivirus containing scrambled or PTPRK specific shRNAs (shPTPRK-3 and shPTPRK-5). Since these cell lines expressed PTPRK mRNA, use of shRNA to downregulate PTPRK was appropriate. Subsequent reduction in levels of PTPRK-ICD fragment was expected and therefore analyzed via western blot analysis (Figure 2.15B). Based on the PTPRK-ICD levels, knockdown was more efficient in GBM-440 cell line compared to GBM-417 cells. For migration assay, confluent layers of GBM-417 and GBM-440 cell lines transduced with either shPTPRK (-3 or -5) or scrambled shRNA were scratched, and differences in migration rate was analyzed over the period of 24 h. Downregulation of PTPRK by both shPTPRK constructs showed significant reduction in the migration of GBM cells (Figure 2.16 and 2.17, $P<0.05$). Specifically, knockdown by shPTPRK-3 reduced migration of GBM-417 (Figure 2.16) and GBM-440 cells (Figure 2.17) by 45% and 64%, respectively ($P=0.005$, GBM-417; $P<0.001$, GBM-440). Further, shPTPRK-5 mediated PTPRK knockdown also decreased migration capacity of GBM-417 (Figure 2.16, $P=0.01$) and GBM-440 (Figure 2.17, $P=0.001$) cells by 32% and 50%, respectively, but to lesser extent than shPTPRK-3 construct. Differences in migration rates between shPTPRK-3 and shPTPRK-5 transduced cells can be inferred from PTPRK-ICD levels secondary to shRNA mediated downregulation of PTPRK in GBM cell lines. PTPRK-ICD levels were comparatively

lower in shPTPRK-3 transduced GBM cells than those transduced with shPTPRK-5 (Figure 2.15B), thus accounting for greater decrease in migration by the shPTPRK-3 construct. Moreover, reduction in migration was greater for GBM-440 cell line compared to GBM-417. This difference could be because of more efficient PTPRK knockdown in GBM-440 cells than GBM-417 cell line. Nonetheless, this data suggest that extensive proteolysis of PTPRK can contribute to glioblastoma cell migration.

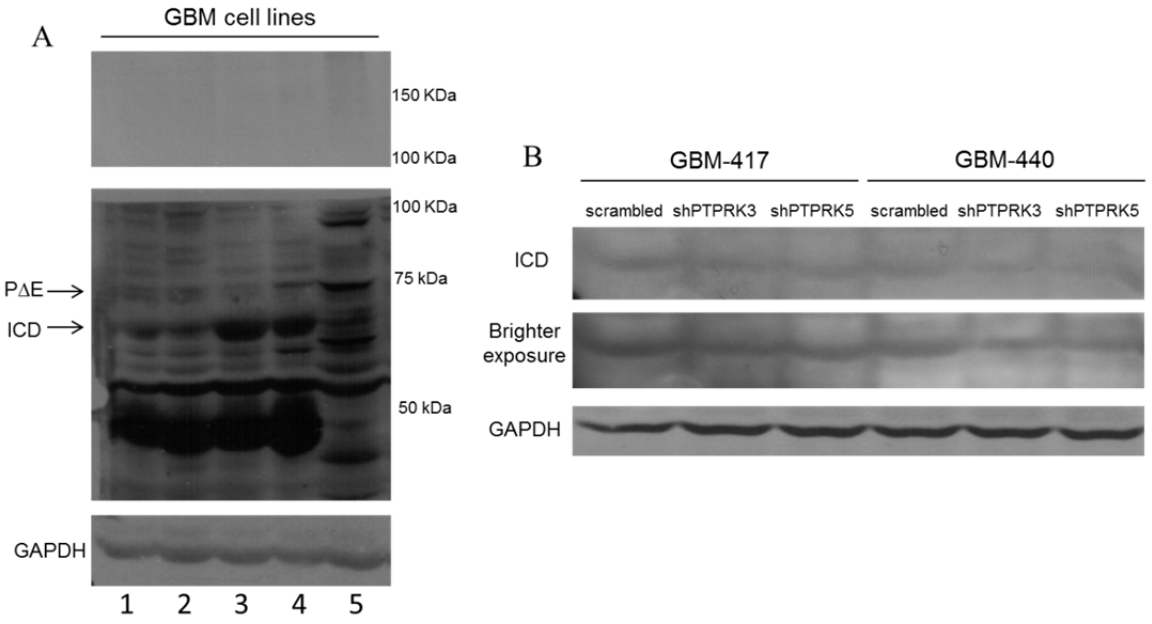

Figure 2.15: Full length PTPRK protein is proteolytically processed in GBM. (A) Five GBM cell lines (left to right – primary cell lines 617, 620, 417, 440 and U251-MG) were analyzed for PTPRK expression by western blot. Antibody recognizing extracellular domain was used to detect full length PTPRK whereas antibody against intracellular domain was used for detection of PTPRK fragments. (B) shPTPRK mediated knockdown of PTPRK in GBM-417 and GBM-440 cell line subsequently reduced PTPRK-ICD levels as detected by western blot.

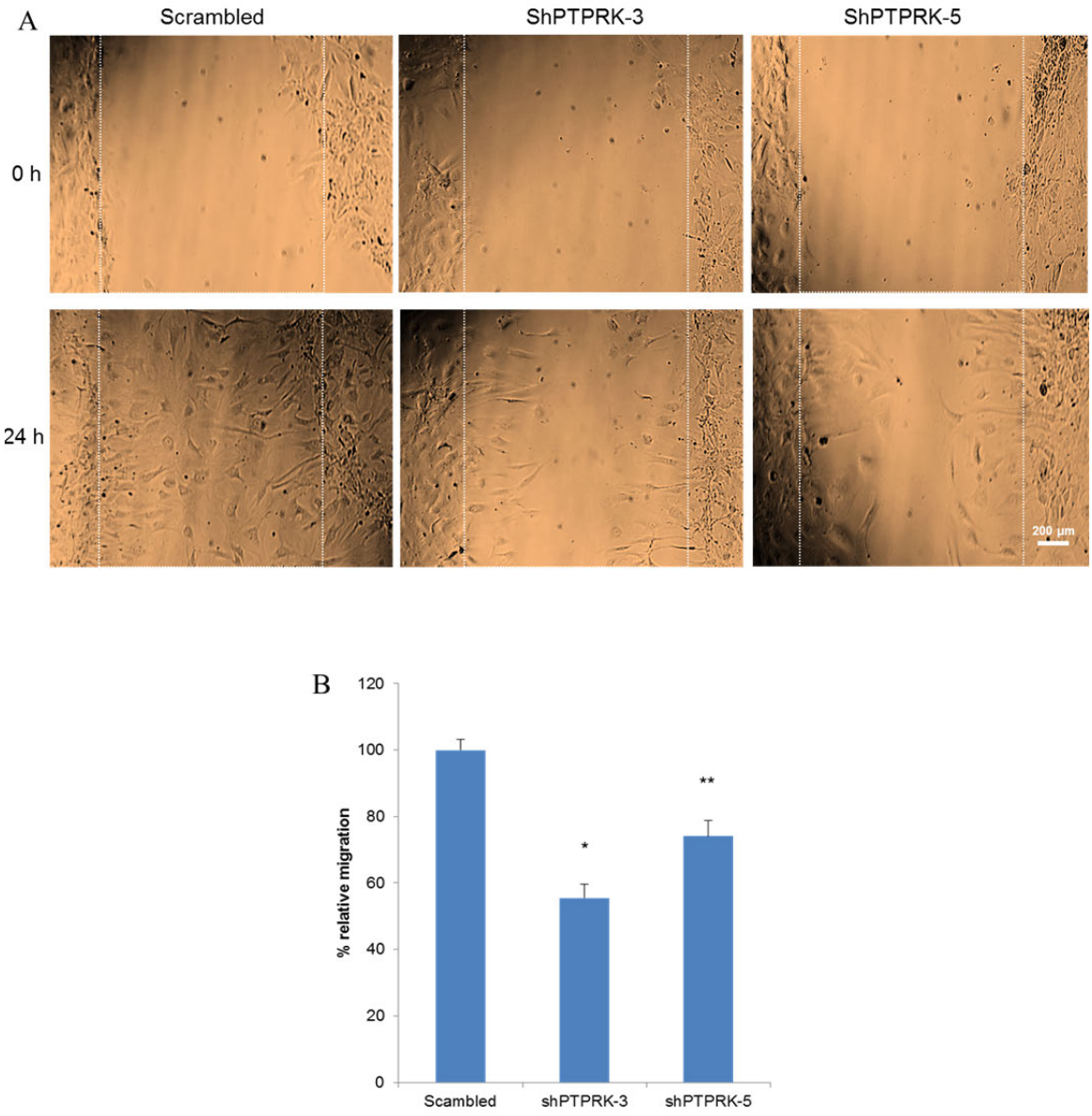

Figure 2.16: Extensive proteolysis of PTPRK in glioblastoma contributes to cell migration. (A) Confluent monolayers of GBM-417 primary cell line transduced with shPTPRK (-3 and -5) or scrambled shRNA were scratched as described under the Material and Methods section to create a wound. Images of the wound were taken at 0 h and 24 h. White lines indicate approximate wound edge at 0 h. Scale bar = 200 µm. (B) The histogram represents percentage of migration relative to scrambled shRNA cells from three independent experiments, in twelve replicates. *, P=0.005; **, P=0.01.

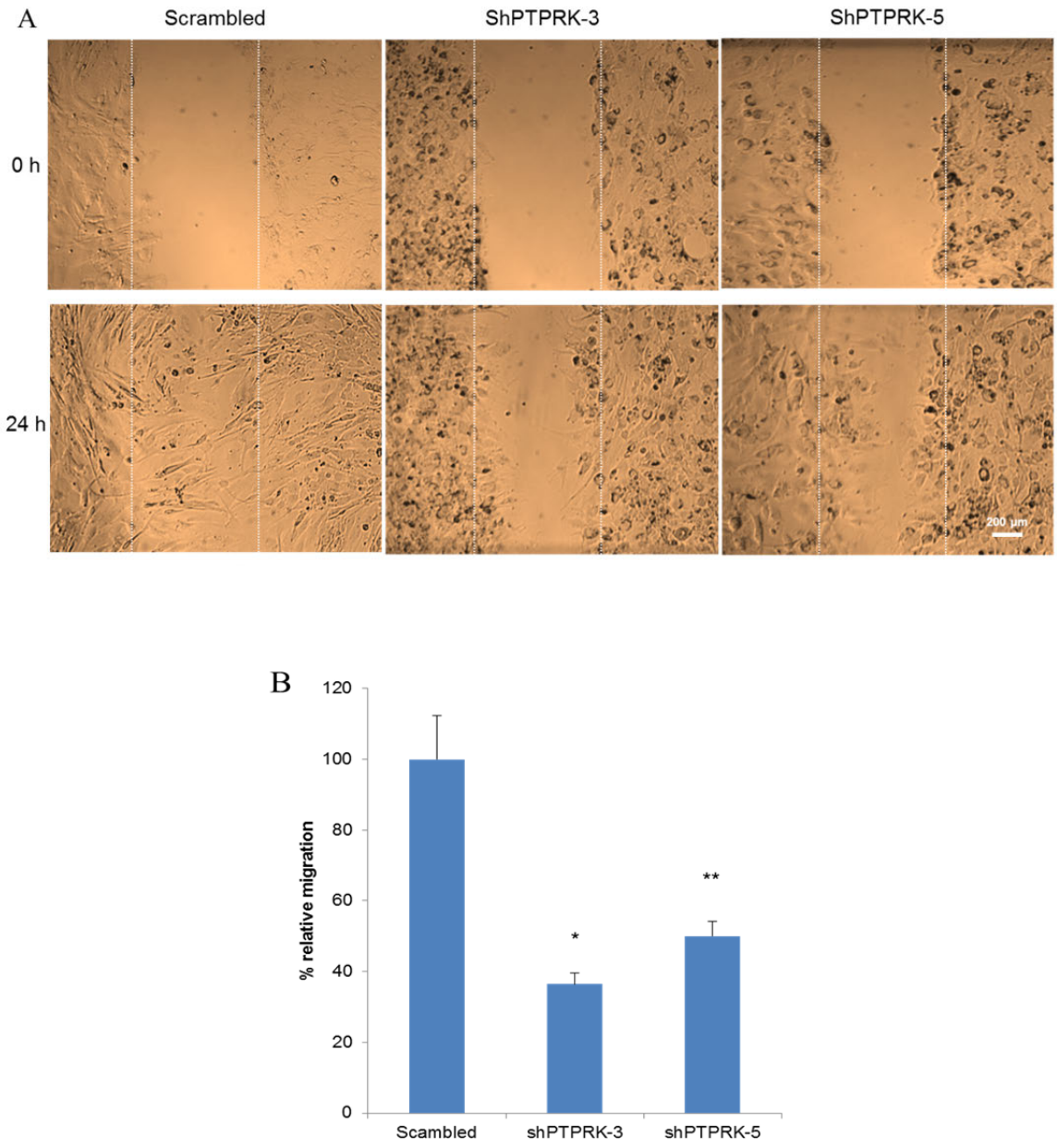

Figure 2.17: PTPRK knockdown reduces migration of GBM-440 cells. (A) Confluent monolayer of GBM-440 primary cell line transduced with two PTPRK specific shRNAs (shPTPRK-3 and -5) or scrambled shRNA were scratched to create a wound. Images of the wound were taken at 0 h and 24 h. White lines indicate approximate wound edge at 0 h. Scale bar = 200 µm. (B) The histogram represents percentage of migration relative to scrambled shRNA cells in terms of change in wound area from three independent experiments, in twelve replicates. *, P<0.001; **, P=0.001.

2.4 Discussion

SNP arrays have great potential as a cancer diagnostic tool. The advantage of SNP arrays over other chip-based methods is their ability to detect LOH. They enable detection of genome-wide patterns of allelic imbalances that could harbor potential tumor suppressors of diagnostic and prognostic utility. They can detect both copy neutral LOH and LOH resulting from deletions. Ideally, LOH is determined by comparing allelic pattern in paired blood samples to that in the tumor. However, bioinformatics based calculations allow identification of LOH events in patients with no corresponding blood DNA sample as control (78). This approach estimates the distribution of allele-specific measurements in chromosomal regions of normal human population such as "270 Hapmap samples data" and uses that estimate to detect genome wide LOH in the study tumor specimens. In our microarray analysis, we relied on this bioinformatics approach as for the majority of glioma tumor specimens paired blood samples were not available.

Genomic explorations can enable the discovery of novel migration-related genetic alterations in glioma with potential prognostic and predictive utility. In our study, LOH analysis and overall survival analyses identified PTPRK as a glioma tumor suppressor candidate with prognostic value. PTPRK is a receptor protein tyrosine phosphatase which mediates trans-homophilic cell-cell interactions. It can directly contribute to contact inhibition of cell growth and migration by transducing downstream signals in response to cell-cell contact (59,66). Loss of contact inhibition, unchecked proliferation and cell migration are typical features of malignant glioma. Since PTPRK is highly expressed in normal brain, its alterations are very relevant to biology of malignant gliomas. However,

physiological role of PTPRK as a putative tumor suppressor and its capacity to influence malignant glioma phenotype has not been studied so far.

In this study, we provide first time evidence for PTPRK as a glioma tumor suppressor. PTPRK transcript and protein levels were significantly lower in malignant glioma tumors compared to normal (non-tumor) brain tissue samples. Interestingly, PTPRK protein and mRNA levels inversely correlated with glioma grade. Higher PTPRK levels were detected in low grade glioma tumors compared to grade III and IV gliomas. This suggest that inactivation of PTPRK might be an important molecular event during glioma progression.

Further, expression of cell surface associated PTPRK protein was lost in high grade gliomas, particularly GBM, due to mutations and post-translational processing events. Several cell surface receptor proteins including PTPRK are sequentially processed by proteases (79-81). Specifically, PTPRK is processed into multiple small fragments by three cleavage events: 1) a furin-like protease, yielding a PTPRK P-subunit fragment which is non-covalently attached to the extracellular domain, PTPRK E-subunit; 2) an α-secretase, yielding a PΔE subunit (P-subunit without most of the extracellular region); and, 3) subsequent processing by γ-secretase ultimately generates a membrane free PTPRK-intracellular fragment (PTPRK-ICD) (Figure 2.6C). Interesting to note was that the expression of full length cell surface PTPRK protein was observed only in low grade gliomas and normal brain tissues. Only multiple small PTPRK fragments were detected in a majority of grade III and IV glioma tissue specimens. This indicates that high protease activity in malignant gliomas (33,34) cleaves membrane bound receptor PTPRK protein into several fragments. Since, both normal brain tissue samples and low grade

glioma specimens also showed PTPRK fragments, it can be concluded that it is the expression of cell surface associated PTPRK form that differs from high grade gliomas. Thus, loss of full length PTPRK protein could be an important event in glioma progression leading to rapid proliferation and migration of malignant glioma cells. Another particularly interesting aspect that is yet to be investigated is that mutations of the PTPRK gene might alter processing events, ultimately leading to loss of full length PTPRK protein expression.

This study shows that the receptor form of PTPRK protein mediates contact inhibition of cell growth and migration. Of note, in the absence of full length PTPRK, proteolytically generated PTPRK fragments play tumor supportive role by promoting migration of glioblastoma cells. Apparently, the balance between cell surface receptor form of PTPRK and its intracellular fragments seems to regulate cell adhesion and migration in normal physiological conditions. This balance is perhaps disturbed in glioblastoma due to high levels of proteases and/or PTPRK mutation events (33,34) which in turn results in selective retention of PTPRK fragments in GBM. A limited number of receptor type PTPs' studies have shown some evidence of the membrane free intracellular domains possessing a potential transcription modulating activity upon nuclear translocation (79,80). Based on these studies, it can be speculated that the membrane free PTPRK-ICD fragment can translocate to the nucleus and contribute to cancer phenotype by influencing gene transcription. This fragment might activate other nuclear proteins by tyrosine dephosphorylation, leading to cell survival and migration. Another possibility is that increase in the nuclear phosphatase levels might result in dephosphorylation at autoinhibitory tyrosine sites of oncogenic transcription factors and thereby activate

signaling processes. Targeting PTPRK-ICD fragment in GBM with specific inhibitors could be a useful therapeutic strategy to suppress cell migration and dispersal.

Migration and invasion of glioma cells is a multi-factorial process that involves several biochemical events. Exact molecular mechanisms of PTPRK dependent regulation of glioma phenotypes have not been established. However, few studies in other cellular systems suggest that PTPRK dephosphorylate EGFR and β-catenin at tyrosine residues (82,83). Deregulation of these signaling networks is among the major driving forces behind glioma proliferation, migration and even treatment resistance (84-88). Thus, PTPRK is implicated in signaling events that are frequently altered in malignant gliomas.

Interestingly, two other RPTPs, PTPRZ1 and PTPRM, have also been found altered in gliomas that were shown to regulate cell growth and migration (89,90). However, alterations of PTPRK were the most frequent of all RPTPs in our population of glioma patients, which suggests that PTPRK is an important regulator of glioma growth and migration. Nonetheless, it is likely that alteration of other RPTPs also contribute to the aggressive phenotype of glioma.

Overall, functional imbalance between tyrosine kinases and tyrosine phosphatases is a major contributor to glioma development and progression. PTPRK is one such tyrosine phosphatase that is frequently altered in malignant glioma. Our results demonstrated for the first time that PTPRK is a tumor suppressor and an independent prognostic marker in glioma which inhibits proliferative and migratory capacity of malignant glioma cells.

CHAPTER III
TUMOR DERIVED MUTATIONS OF PROTEIN TYROSINE PHOSPHATASE RECEPTOR TYPE KAPPA AFFECT ITS FUNCTION AND ALTER SENSITIVITY TO CHEMOTHERAPEUTICS IN GLIOMA

3.1 Summary of chapter

Aggressive behavior of malignant gliomas can be attributed to frequently altered tyrosine phosphorylation signaling (91,92). Genomic profiling studies have indeed shown overactivation of receptor tyrosine kinase (RTKs) pathways via tyrosine phosphorylation (TP) as the most commonly altered phenomena in glioma, with more than 80% of gliomas displaying epidermal growth factor receptor (EGFR) constitutive TP and subsequent tyrosine kinase burst (8,92). Unchecked TP is instrumental in overactivated cellular processes leading to cell growth, invasion, migration as well as resistance to therapy (91). Thus, targeting the TP regulatory signals represents a potential therapeutic approach and is important given the fact that preliminary efficacy results of most clinical trials targeting tyrosine kinase activity have fallen short of expectations (11,49).

Recent studies suggest a key role of protein tyrosine phosphatases (PTPs) mediated dephosphorylation in reducing tyrosine phosphorylation levels in cancer cells (59,91). In particular, receptor type PTPs are increasingly thought to be important regulators of cell-cell contact dependent signaling via tyrosine dephosphorylation of intracellular signaling molecules (59,91). Although functional effects of alterations in PTPs have been recently reported in human tumors (59,93), no single PTP study has as yet shown to influence the malignant phenotype and drug response in glioma. Previously,

we have shown that Protein Tyrosine Phosphatase Receptor type Kappa (PTPRK) is the most frequent altered RPTP in glioma which negatively regulates cell growth and migration. These observations prompted us to further characterize molecular mechanisms of PTPRK function in glioma, its effect on glioma therapeutics and to define biological consequences of mutations in the PTPRK gene.

PTPRK, one of the 21 known receptor type PTPs, is a transmembrane protein that regulates cell-cell contact (62,67). The extracellular region contains a MAM domain, an immunoglobulin like-domain and four fibronectin type III domains, similar to cell adhesion molecules, essential for cell-cell adhesion (59). PTPRK mediates highly specific intercellular homophilic interactions (Figure 3.1). Its expression has been found to increase with high cell density in response to cell-cell contacts, indicating that PTPRK can directly sense cell contact and thereby mediate contact inhibition of cell growth and movement under normal cell conditions (59,94,95). This process is disturbed in many tumors (59,68,69,71,72). The intracellular region of PTPRK consists of phosphatase domains with dephosphorylating activity and potential transcriptional modulator function.

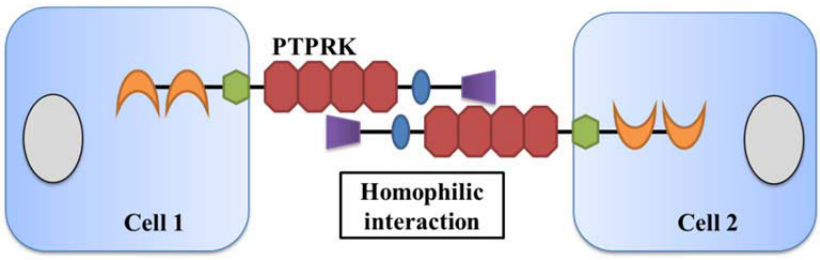

Figure 3.1: PTPRK mediates homophilic cell adhesion.

Cell surface PTPRK is expressed as a 180-kDa protein that is sequentially processed post-translationally through three proteases - furin, ADAM 10/α-secretase, and γ-secretase (Figure 2.6C) (81). The proteolytic processing is believed to be induced with increase in cell density (81). Cleavage by furin like proteases results in two non-covalently associated fragments of transmembrane PTPRK protein - E-subunit and P-subunit (81). This active membrane bound PTPRK protein is further processed by α-secretase/ADAM-10 proteases, which are induced in response to cell confluence (81). Proteolysis by α-secretase releases extracellular domain, leaving transmembrane PΔE fragment. Finally, γ-secretase regulated intramembrane cleavage of remaining transmembrane part, releases intracellular phosphatase domains from the membrane (PTPRK-ICD) (81). Moreover, all the PTPRK fragments are catalytically active and can function differently depending upon their subcellular localization (67,81). In particular, PTPRK-ICD fragment can potentially translocate to the nucleus and affect gene transcription by dephosphorylation of nuclear proteins/transcriptional regulators (81). Interesting to note is that high cell density not only induces post-translational processing of PTPRK but also results in increased PTPRK gene transcription (81). Consequently, higher PTPRK protein levels have been observed in confluent cells (81). It can be speculated that the proteolytic processing of PTPRK is compensated by increased PTPRK transcription at high cell densities. However, PTPRK expression was found to increase with cell density even when its processing was inhibited with protease inhibitors (81). This suggests that the proteolytic processing may not be causally linked to increase in PTPRK expression. An alternate notion is that relative levels of cell surface transmembrane PTPRK and proteolytically generated PTPRK-ICD isoform regulate

multiple cellular processes such as cell growth and migration. However, PTPRK-ICD fragment is often not detected in western blot analysis under normal physiological conditions. This is because the membrane free form is subjected to proteasomal degradation in the cytoplasm, prior to its nuclear translocation (81). Therefore, it is not clear how this low abundant PTPRK fragment influences signaling processes. Nevertheless, NOTCH-ICD fragment, which results from similar processing of transmembrane Notch receptor, is expressed at low levels in normal cells but is well known to play a key role in transcription of gene targets (96). Thus even low PTPRK-ICD levels might be sufficient to fulfill its function under normal conditions. Overall, functional relevance of PTPRK proteolytic processing is not yet well understood, particularly in a disease context. Our results provided the first evidence of proteolytic downregulation of full length PTPRK in high grade glioma. GBM cells selectively retain PTPRK fragments with no full length PTPRK protein. These fragments, opposite to the full length form, contribute to GBM cell migration. However, it is not clear whether PTPRK mutations can influence proteolytic processing, as the processing mainly occurs due to elevated protease levels in malignant glioma.

We have previously demonstrated tumor suppressive role of PTPRK in glioma. In this study, we explored molecular mechanisms underlying PTPRK function and effect of PTPRK expression on response to therapy in glioma. Moreover, we confirmed our LOH findings and discovered novel PTPRK gene deletion and missense mutations by sequencing of the full length PTPRK transcripts in glioma biopsies. PTPRK mutations were cloned and expressed in PTPRK-null malignant glioma cells. Effect of these mutations on PTPRK anti-oncogenic function and their association with response to anti-

glioma therapeutics, such as temozolomide and tyrosine kinase inhibitors, were subsequently analyzed using *in vitro* cell based assays. The key objectives of this study were to identify functional consequences of PTPRK genetic variants in malignant glioma and to determine the association of these variants with response to therapeutic agents. We identified several inactivating mutations, characterized their functional consequences and effect on pharmacologically relevant PTPRK-dependent molecular pathways along with their predictive significance.

3.2 Materials and methods

3.2.1 Sequencing

Six of the human glioma biopsies that were positive for LOH at the PTPRK locus were used for PTPRK sequence analysis. Briefly, RNA from these biopsies was extracted with Trizol (Life Technologies, Carlsbad, CA) and quantified using Nanodrop 2000 Spectrophotometer (ThermoScientific, Huntsville, AL). The quality of RNA was verified following a standard procedure by measuring absorbance at 230, 260 and 280 nm. Absorbance ratios, A260/A280 and A260/A230, were within the expected range of 1.8 to 2.0 and >2.0, respectively, for all the RNA samples. Five microgram of the extracted RNA from each biopsy was then reverse transcribed into cDNA using MuMLV retrotranscriptase and oligo dT (Life Technologies, Carlsbad, CA). The cDNA quality was verified by running them on 1% agarose gel. Fifty nanogram of cDNA was used for further analyses. Primers for amplification and sequencing of full length PTPRK cDNA were designed using Primer3 application (97). The primers are listed under Table 3.1. Full length amplification of the PTPRK cDNA was performed using Expand Long

Template PCR System (Roche Diagnostics, Indianapolis, IN). We selected several internal primers to sequence full length PTPRK using BigDye Terminator Cycle Sequencing 3730xl (Applied Biosystems, Foster City, CA). These Internal primers cover different regions of the PTPRK transcript and are listed under Table 3.1. PCR reactions were performed under the following conditions: 32 cycles of 95°C for 30 sec, 55°C for 30 sec, and 72°C for 3 min. Sequence alignment was done using DNA Baser v2 sequence assembly software (Heracle BioSoft, Germany). The reference PTPRK sequence NM_001135648.1 was used as a template. True variant was confirmed only if identified by both forward and reverse primers.

Table 3.1: List of primers used in this study.

Gene name	Primer	Sequence
Sequencing primers		
PTPRK-534	Forward Reverse	5- AATGGGTGCATGTTAGTGCTC -3 5- GAGCACTAACATGCACCCATT -3
PTPRK-1791	Forward Reverse	5- CTTCCCTCTGGATTGGTTAGG -3 5- CCTAACCAATCCAGAGGGAAG -3
PTPRK-2770	Forward Reverse	5- TGCATTCACCATGTGAGTCAT -3 5- ATGACTCACATGGTGAATGCA -3
PTPRK-4380	Forward Reverse	5- TGCACCATCAGATAACCTTCC -3 5- GGAAGGTTATCTGATGGTGCA -3
RT-PCR primers		
PTPRK	Forward Reverse	5- CTTTCGCCCCTGAGGTAGTTT-3 5- CTGCTGGCTCAATAGATGGAC-3
c-Myc	Forward Reverse	5- CCTACCCTCTCAACGACAGC -3 5- CTCTGACCTTTTGCCAGGAG -3
Cyclin D1	Forward Reverse	5- CTGCCGTCCATGCGGAAGATC -3 5- GTTCATGGCCAGCGGGAAGAC -3

3.2.2 Cell culture and transfection

Two different cell lines were used as recently recommended by the cancer research community. The U87-MG human glioma cell line was obtained from ATCC (Manassas, VA) and U251-MG cell line was a gift from Dr. Maltese (98). Both the cell lines were maintained in DMEM (Invitrogen, Carlsbad, CA) supplemented with 10% fetal bovine serum (Hyclone, Logan, UT), 1% penicillin/streptomycin and 1% glutamine at 37°C in 5% CO_2. Wild-type PTPRK and variants were cloned into the expression plasmid pIRES-hrGFP-II (Stratagene, La Jolla, CA) and transfected into malignant glioma cell lines using Xfect transfection reagent (Clontech, Palo Alto, CA). Mock cells were generated by transfecting the empty vector as control. All transfections were carried out according to the manufacturer's standard protocol (Clontech, Palo Alto, CA).

3.2.3 Drugs

Three drugs, temozolomide (Sigma-Aldrich, St. Louis, MO), erlotinib (gift from Dr. Andrean Burnett, University of Iowa) and gefitinib (Selleckchem, Houston, TX) were used in our studies. They were diluted in 0.25% DMSO for the highest concentrations and serial dilutions were made in the culture media.

3.2.4 Immunoblotting

Glioma cells were washed twice with ice-cold HBSS and then scrapped from the culture plates in 500 µl of lysis buffer. RIPA lysis buffer supplemented with 1x protease inhibitor cocktail, 1 mM EGTA, 5 mM EDTA, 5 mM sodium fluoride, 1 mM PMSF and 1 mM sodium orthovanadate was used for preparing the lysates. Cells were disrupted by incubating them on ice for 30 minutes, and then centrifuged at 14,000 rpm for 10 minutes

at 4^{o}C to pellet the cell debris. Supernatant was collected and the protein concentration was measured using bicinchoninic acid assay (Pierce, Rockford, IL) with bovine serum albumin as a standard. Laemmli sample buffer (2x SDS) (Bio-Rad, Hercules, CA) was added to the lysates in equal volume. The lysates were then heated at 95^{o}C for 5 minutes. 50 μg of the homogenates were loaded and separated on 7.5% polyacrylamide gel. Lysates from glioma tissue specimens that had been frozen after surgical resection were prepared similarly by adding 5 volumes of lysis buffer. Expression of PTPRK and its relevant targets (EGFR, β-catenin) was analyzed by immunoblotting with appropriate primary antibodies. To analyze PTPRK expression, PTPRK primary antibody recognizing an epitope on the intracellular domain (Ab13225, Abcam, Cambridge, MA) was used along with a PTPRK antibody, recognizing a region in the extracellular domain (gift from Dr. Fisher at the University of Michigan, Ann Arbor, MI). Specificity of the two PTPRK antibodies is shown in Figure 3.4C. Primary antibodies for total EGFR and β-catenin were purchased from Selleckchem (Houston, TX). GAPDH (6C5, Abcam, Cambridge, MA) was used as a loading control. Nitrocellulose membranes were developed with the ECL detection system (GE Healthcare, Piscataway, NJ). Band intensities were quantified with Alpha Imager software (Alpha Innotech, San Leandro, CA) using Spot-Denso application.

3.2.5 Real-time PCR

RNA from U87-MG glioma cell line transfected with empty control vector, wild-type PTPRK and its variants was extracted, tested for quality, quantified, and reverse transcribed into cDNA as described above. Real-time PCR quantification of c-Myc and cyclin D1 expression was subsequently performed. GAPDH was used as a housekeeping

gene. Primers used for c-Myc and cyclin D1 are listed under Table 3.1. The following real-time PCR protocol was used: 95 °C for 30 sec, 58 °C for 30 sec and 72 °C for 30 sec, for 40 cycles of amplification.

3.2.6 Tyrosine phosphatase assay

Tyrosine phosphatase activity was determined using an assay adapted from Xu et al. (83). In this assay, a tyrosine phosphatase catalyzes the hydrolysis of colorless substrate, p-nitrophenyl phosphate (pNPP), to yellow color p-nitrophenol. Briefly, Phosphatase assay buffer (100 µl) containing 15 mM p-nitrophenyl phosphate (NEB, Ipswich, MA), 100 µg/ml bovine serum albumin, 50 mM Tris, pH 7.6, 100 mM NaCl, and 10 mM EDTA was mixed with total cell lysate (0-50 µl) and incubated at 37°C for 40 minutes in 96-well microtiter plates. Reactions were terminated by adding 10 N NaOH. Hydrolysis of p-nitrophenyl phosphate was measured spectrophotometrically at 405 nm using a microplate reader (Spectra Max Plus, Molecular Devices, CA). Total protein concentration was same between each sample. Sodium fluoride at 5 mM final concentration was used to inhibit serine/threonine phosphatases activity that may interfere with the measurements.

3.2.7 Proliferation assays

MTT colorimetric assay (Sigma-Aldrich, St. Louis, MO), *in vitro* growth curve assay and clonogenic cell survival assay were performed to measure the proliferative potential of U87-MG and U251-MG glioma cell lines transfected with empty control vector, wild-type PTPRK or PTPRK variants. For MTT colorimetric assay, 4000 cells/well were seeded in a 96 well plate for each condition. After 72 h incubation at

37°C, 10 µl of MTT solution (final concentration 0.5 mg/ml) was added to each well and the plates were incubated for 4 h at 37°C. The resultant formazan product was dissolved in DMSO and absorbance was measured at 540 nm with background absorbance at 690 nm using a microplate spectrophotometer (Spectra Max Plus, Molecular Devices, CA). The results represent the mean ± SE values, from six independent experiments performed in triplicate, expressed as a percentage of viable cells relative to mock cells.

To analyze growth pattern of transfected cells, 4000 cells were seeded in a 24 well plate in six replicates per PTPRK variant for time points 1, 3 and 5 days. At each time point, the wells were rinsed twice in PBS, fixed for 30 minutes in 10% formalin and stained with 0.1% crystal violet solution for 10 minutes. Stained cells were washed twice with PBS. Residual PBS was allowed to drain off by inverting the plates. 300 µl of 100% methanol was then added to each well to dissolve the stain. Absorbance of the dissolved stain was measured at 540 nm. Cell growth was quantified as absorbance at 540nm of methanol-solubilized cell stain at defined time points. The results are plotted as the average growth (A540 nm) ± standard error from three independent experiments.

For clonogenic assay, single cell suspensions of 500 cells were seeded per 2 ml of culture media in 60 mm cell culture dish. After 2 weeks, cells were washed with PBS and stained with 0.05% crystal violet in 70% ethanol. Colonies were imaged with the Canon SX110 camera and quantified using ImageJ. Average values ± SE were plotted as % of colonies formed by mock cells from three independent experiments in triplicate.

3.2.8 Migration assay

Wound healing assay was performed to determine differences in cell migration rates of malignant glioma cells transfected with empty control vector, wild-type PTPRK

and PTPRK variants for 48 h. Individual wounds were made with a 10 µl pipette tip in confluent monolayers of glioma cells. Culture media was replaced with serum free DMEM to control for the effect of proliferation. Changes in wound area was monitored for period of 24 h. Cell images were taken using a Jenco microscope (Jenco, Portland, OR) equipped with a Mightex CCD camera at 0 and 24 h. Image analysis was done using TScratch software (CSElab, ETH Zurich, CH) and changes in wound areas per time were measured. Fifteen measurements were recorded per condition. The results represent the average value from three independent experiments, presented as percentage of cell migration relative to control. Error bars indicate standard error.

3.2.9 Cell invasion assay

U87-MG and U251-MG cells were plated in 6-well plates and transfected with wild-type PTPRK and its variants for 48 h. The cells were trypsinized, centrifuged and re-suspended into serum-free medium at 1 x 10^5 cells/ml. 500 µl of transfected cells were seeded into the matrigel-coated and rehydrated filter inserts of 24-well transwell chambers with 8 µm pores (BD Biosciences, Bedford, MA). Bottom chambers were filled with 750 µl of DMEM containing 10% FBS. After 24 h incubation at 37°C, filter inserts were removed, the culture medium was decanted, and the inserts were washed twice with PBS. Non-invading cells on the upper surface of the membrane were scrubbed off with a cotton swab. The invasive cells on the lower surface of the membrane were fixed with 100% cold ethanol for 5 minutes and stained with 0.1% crystal violet solution in 20% ethanol for 30 minutes. Stained cells were washed twice with PBS and counted in five random fields under a light microscope. Replicates were averaged and plotted as a percentage of invaded mock cells.

3.2.10 Cytotoxicity assay

Prior to drug treatment, U87-MG and U251-MG cells were transfected with wild-type PTPRK and its variants for 48 h in a six well plate. The mock cell lines were generated by transfecting the two malignant glioma cell lines with empty control vector. The cells were trypsinized with 0.05% trypsin and plated at a density of 4000 cells/well in a 96 well plate. After 24 h incubation at 37°C, cells were treated with temozolomide (100 μM), eroltinib (10 μM) or their combination for 72 h with each PTPRK clone having six replicates per treatment condition. Similar treatment was performed with temozolomide (100 μM), gefitinib (10 μM) or their combination. After 72 h of drug treatment, 10 μl of MTT solution (final concentration 0.5 mg/ml, Sigma-Aldrich, St. Louis, MO) was added to each well and the plates were incubated for 4 h at 37°C. The resultant formazan product was dissolved in DMSO and absorbance was measured at 540 nm with background absorbance at 690 nm using a microplate spectrophotometer (Spectra Max Plus, Molecular Devices, CA). The results represent mean ± SE values, from three independent experiments, each with six replicates per variant per treatment condition, expressed as a percentage of viable cells relative to untreated mock cells (Mock + DMSO).

3.2.11 Statistics

Statistical significance was determined using non-parametric ANOVA (SAS 9.3 software) with significance level of P-value <0.05. Multiple group comparison was done using non-parametric analog to the Tukey-Kramer method. Simple effects test was used as a follow-up test to interpret interactions between drug treatment and PTPRK variants

for demonstrating PTPRK induced chemotherapeutic response. The Bonferroni correction was used to adjust the critical alpha level and thus P-value < 0.01 was considered for statistical significance.

3.3 Results

We recently identified several copy number alterations and losses of heterozygosity (LOH) in a comprehensive population of malignant glioma tumor specimens. We discovered that alterations of the PTPRK gene were among the most significant abnormalities. Moreover, overall survival analysis identified PTPRK as a tumor suppressor candidate with prognostic, therapeutic and clinical predictive values. We subsequently established tumor suppressive role of PTPRK by overexpression and knockdown studies in malignant glioma cell lines. Despite a key role of PTPRK in glioma biology, functional data related to PTPRK alterations in glioma are lacking.

3.3.1 Sequence analysis of the PTPRK coding region revealed variants with altered functional activity

SNP arrays do not allow identification of particular coding variation because they exclusively use intronic probe sets (Mapping array SNP 6.0, Affymetrix, Santa Clara, CA). They only provide an indirect estimation of genetic alterations in the coding regions. In our recent study, loss of heterozygosity at the PTPRK locus was observed in 23% of glioma patients. However, microarray screening is often associated with false positive results and requires further confirmation. Therefore, we decided to confirm and validate our data using direct sequencing of the PTPRK coding region. Six LOH positive specimens were randomly selected for confirmation studies. The tumor cDNAs were

PCR amplified and sequenced. Sequences were compared with the known PTPRK cDNA sequence (genebank accession number NM_001135648.1). As shown in Table 3.2, sequence alignment detected two non-synonymous mutations (A3938G (T1184A) and A4064G (S1226G)) in the phosphatase domain-2 and three synonymous in the fibronectin-III domain (Table 3.2 and Figure 3.2). To predict whether these variations are likely to alter the protein function, we used the SIFT web application (http://sift.jcvi.org/). Evaluation of PTPRK mutations by SIFT showed that T1184A is a 'damaging' mutation (SIFT score = 0) whereas S1226G is 'tolerated' (SIFT score = 1). These non-synonymous mutations in the phosphatase domain-2 induce switch from polar to non-polar amino acid, and thereby may modify PTPRK function. Moreover, we found a deletion of exons 15 to 22 which encode for a region in the tyrosine phosphatase domain-1. This deletion is bound to alter PTPRK function because a part of the phosphatase domain-1 is missing (~200 amino-acids). Overall, these alterations could have strong functional implications, possibly resulting in conformational changes of the phosphatase domain or folding of the PTPRK protein. Such conformational changes in PTPRK protein can affect availability of the active site and thereby render the protein less- or non-functional. Biological consequences, functionality and predictive significance of these PTPRK variants were subsequently determined in U87-MG and U251-MG cell lines. Throughout the text, wild-type PTPRK is designated as PTPRK-wt, the variant harboring the mutation A3938G as PTPRK-mut and the variant with exons 15-22 deletion as PTPRK-del.

Table 3.2: Summary of genetic alterations in a subset of glioma specimens.

Nucleotide change	Amino acid change	Functional domain	SIFT prediction	Nomenclature
T1480C	G371G	FN_III	Tolerated	-
T2371C	Y668Y	FN_III	Tolerated	-
C2389A	L674L	FN_III	Tolerated	-
A3938G	T1184A	Phosphatase	**Damaging**	**PTPRK-mut**
A4064G	S1226G	Phosphatase	Tolerated	-
Exon 15-22 (Deletion)	-	Phosphatase	**Damaging**	**PTPRK-del**

Note: The reference PTPRK sequence NM_001135648.1 was used for annotation of the nucleotide and amino acid changes. Functional consequences of the mutations were evaluated using SIFT program.

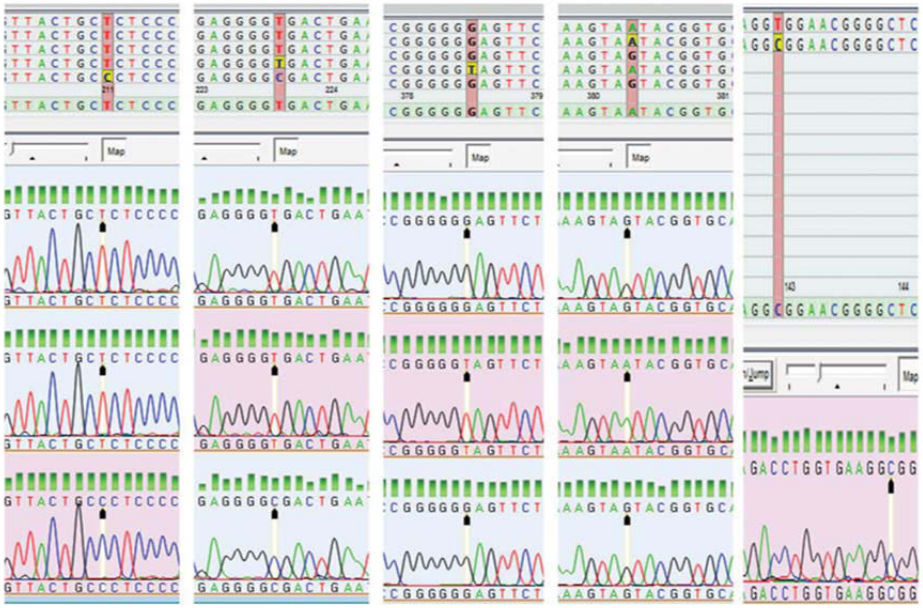

Figure 3.2: Sequence traces depicting the five mutations in coding regions of PTPRK transcripts from glioma patient samples. Sequences alignment was performed using DNA Baser sequence assembly software. The reference sequence NM_001135648.1 was used as a template.

3.3.2 PTPRK variants have lower phosphatase activity

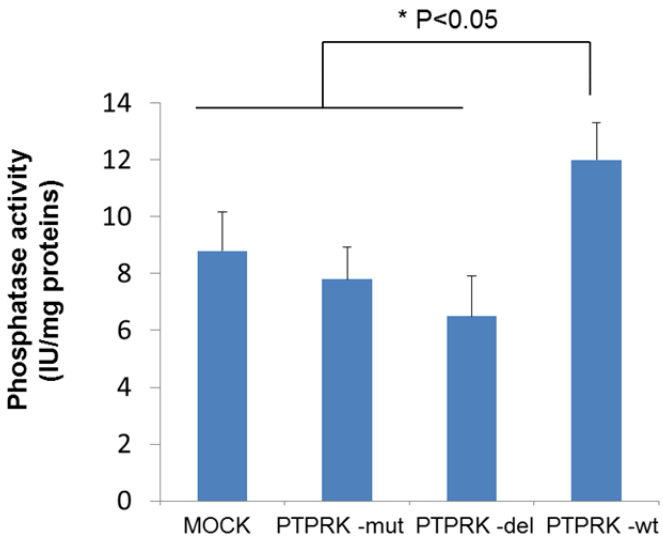

Figure 3.3: Mutation events in malignant glioma alter PTPRK phosphatase activity. Wild-type PTPRK (PTPRK-wt) and its variants were transiently re-expressed in U87-MG cells. Effect of PTPRK mutations on phosphatase activity is shown. Values are mean ± standard error of 5 assays in each group. Multiple comparisons were performed to determine activity differences between the variants. P<0.05 was considered significant for ANOVA analysis.

To study the functional impact of identified genetic variations, we cloned wild-type PTPRK and its variants into an expression vector, and performed transient re-expression studies in U87-MG cells. We selected U87-MG cell line because we have shown that it does not express functional PTPRK and therefore is an appropriate *in-vitro* model for analyzing consequences of PTPRK expression. Moreover, we opted for transient transfection because we were not able to generate stably transfected clones as cells die or lose PTPRK expression by 9-12 days after transfection. We examined the effect of PTPRK mutations on enzymatic activity by p-nitrophenyl phosphate (pNPP) assay. Difference between variants and mock cells was not significant. Both PTPRK-mut

and PTPRK-del showed significant reduction in activity compared to PTPRK-wt (Figure 3.3). PTPRK-mut and PTPRK-del are 35% and 46% less enzymatically active than PTPRK-wt (P=0.0387). These differences in PTPRK activity could possibly alter growth suppressive and anti-migratory effects among the PTPRK variants.

3.3.3 PTPRK mutations lead to differential post-translational patterns in glioma cells

Most trans-membrane receptor proteins, including receptor type PTPs, are post-translationally processed into multiple isoforms by proteases such as metalloproteases, furin, α- and γ-secretases (79,80,99,100). We previously showed that the cell surface PTPRK protein is not detectable in a majority of high grade gliomas, likely due to post-translational processing by elevated levels of proteases (Figure 2.6A). Rather, high levels of low molecular weight isoforms corresponding to intracellular PTPRK fragments (~75-kDa and ~66-kDa) were detected. In accordance with our previous findings, recent analysis of PTPRK protein levels in human glioma biopsies with positive control for full length and PTPRK-ICD form showed proteolysis of cell surface associated PTPRK protein into several fragments (Figure 3.4A). Notably, western blot analysis of total cell lysates from U87-MG cells, transfected with wild-type PTPRK or the two variants, showed differential post-translational PTPRK processing (Figure 3.4B). PTPRK-wt showed two bands; a) a 180-kDa band corresponding to the full length PTPRK protein and b) the lower band, around 120-kDa, corresponding to the extracellular region of processed PTPRK. PTPRK-mut is 100% processed as indicated by a single fragment of size 120-kDa, whereas, PTPRK-del is not processed as a single band of around 180-kDa was observed. A synonymous mutation (PTPRK-syn, C2389A) also altered processing

but was not studied further as it was too complicated to analyze but will be studied in future. Our results showed that mutation events modify PTPRK processing, possibly by changing the susceptibility to proteases such as furin, α- and γ-secretases. These modifications could alter PTPRK regulated cell proliferation and migration.

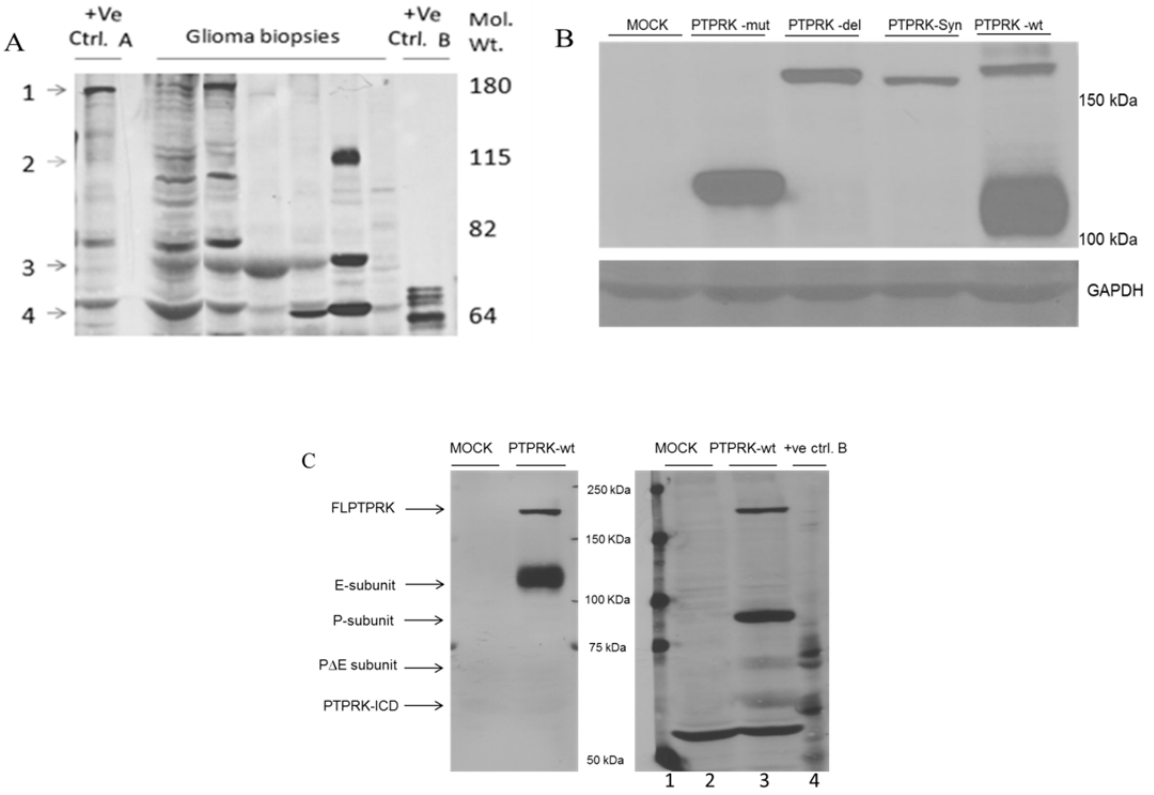

Figure 3.4: Mutation events in malignant glioma alter post-translational processing. (A) Processing of PTPRK protein was analyzed in glioma specimens by immunoblotting. Positive controls for full length PTPRK (Ctrl. A) and PTPRK-ICD fragment (Ctrl. B: GST-fusion ICD transformed bacteria) were used. 1) Full length PTPRK, 2) predicted PTPRK P-subunit, 3) predicted PΔE subunit and 4) predicted ICD domain. (B) Western blot of lysates from U87-MG mock cells and cells expressing wild-type PTPRK or indicated PTPRK mutation was performed using an antibody against the PTPRK extracellular domain, recognizing full length PTPRK (180-kDa) and processed extracellular fragment of size 120-kDa. Immunoblot was reprobed for GAPDH as a loading control. (C) Western blots of U87 mock and PTPRK-wt expressing cells with PTPRK antibody against extracellular region (Left) and PTPRK - Abcam antibody (Right) are shown. Lanes - 1) marker 2) mock cells 3) PTPRK-wt 4) +ve ctrl. B = GST-fusion PTPRK-ICD transformed bacteria.

3.3.4 Mutations alter growth suppressive, anti-migratory and anti-invasive properties of PTPRK in glioma

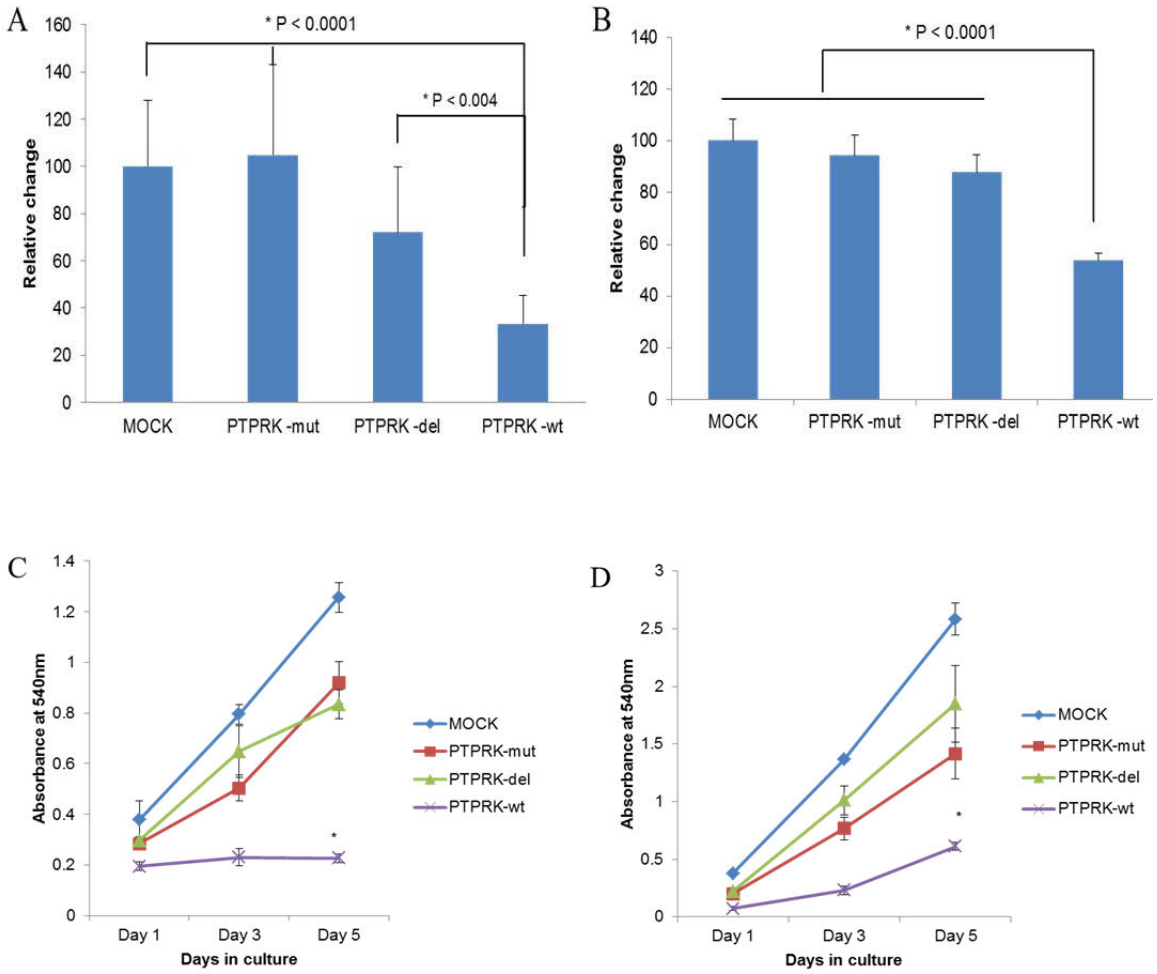

Figure 3.5: PTPRK variants alter suppressive effect of PTPRK-wt on growth of glioma cells, *in vitro*. Quantitative assessment of growth suppressive properties of PTPRK-wt and effect of variants was determined by MTT colorimetric assay in (A) U87-MG and (B) U251-MG cells. The data represent mean ± standard error of six independent experiments performed in triplicate. Growth of U87-MG and U251-MG cells, expressing PTPRK-wt or PTPRK mutants, is plotted in (C) and (D), respectively. Cell growth was assessed by crystal violet staining at indicated time points and quantified by measuring absorbance at 540 nm of methanol-solubilized cell stain. The results are plotted as the average growth ($A_{540\ nm}$) ± standard error. *, P<0.05.

We have previously shown that wild-type PTPRK inhibits the malignant phenotypes of glioma cells. Therefore, we hypothesized that alteration in PTPRK function is a critical step in the loss of contact inhibition of cell growth, facilitating proliferation and migration of tumor cells throughout the brain parenchyma. The functional consequences of discovered genetic alterations were thus assessed by examining their role in glioma cell growth, migration and invasion which are the key biological features of malignant gliomas. We performed re-expression experiments by transfecting the PTPRK variants into U87-MG and U251-MG cells. PTPRK-wt expressing cells showed significant reduction in cell number compared to PTPRK variants as well as compared to mock cells at 72 h after transfection (Figure 3.5). Quantitative analysis of PTPRK-wt growth suppressing property showed a significant (60-70%) decrease in cell proliferation compared to the PTPRK variants in U87-MG cells (Figure 3.5A; $P<0.0001$, PTPRK-wt vs. PTPRK-mut; $P<0.004$, PTPRK-wt vs. PTPRK-del). Similar level of differences in proliferation among the PTPRK isoforms were also observed in U251-MG cells (Figure 3.5B; $P<0.0001$, PTPRK-wt vs. variants). Further, consistent with our previous finding, PTPRK-wt expressing cells had significantly lower growth than mock cells (Figure 3.5A and 3.5B; $P<0.0001$, PTPRK-wt vs. mock). However, PTPRK-mut and PTPRK-del had no influence on proliferation compared with the mock cells ($P=0.215$). These findings were further validated by comparing growth curves of cells expressing either the PTPRK-wt or its variant forms (Figure 3.5C and 3.5D). As expected, malignant glioma cells expressing PTPRK-wt proliferated at a significantly reduced rate, resulting in 80% difference in growth compared to mock cells (Figure 3.5C and 3.5D, $P=0.0002$). Moreover, PTPRK-wt expressing U87-MG and

U251-MG cells had growth rates 60-70% less than that of PTPRK variant expressing cells (Figure 3.5C and 3.5D, P<0.001).

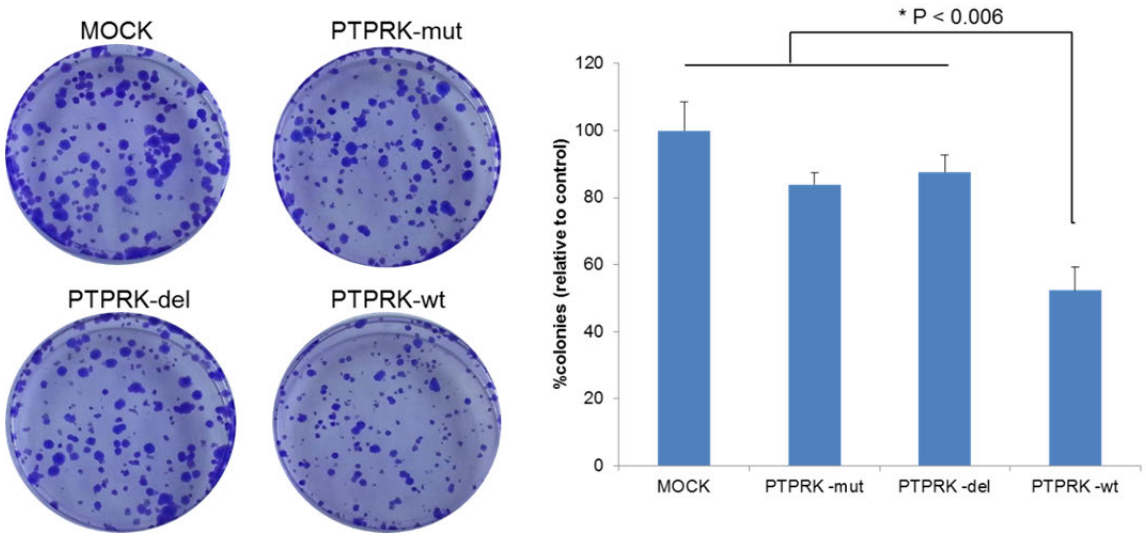

Figure 3.6: Effect of PTPRK-wt and its variants on colony formation in U251-MG cells. Clonogenic assay was performed to assess colony forming ability of U251-MG cell line transfected with wild-type PTPRK and its variants. Bar graph representing average differences in number of colonies between the PTPRK forms relative to mock cells, from three independent experiments in triplicate. *, P<0.006.

Effect of PTPRK mutants on survival and proliferation of glioma cells was further validated by clonogenic assay. Reconstitution of full length, wild-type PTPRK in U251-MG cell line resulted in smaller colonies along with about two fold reduction in number of colonies compared to mock and PTPRK variants (Figure 3.6, P<0.006). In contrast, mock cells and PTPRK mutant isoforms formed abundant colonies (P=0.08). These data suggest that the growth suppressive effect of wild-type PTPRK is compromised due to two mutations in the PTPRK gene.

Further, we determined consequences of PTPRK variants on diffusive characteristic of glioma cells with *in vitro* wound healing assay. As shown previously, reconstitution of wild-type PTPRK significantly (P=0.003) reduced cell migration of PTPRK-null U87-MG cells compared to mock cells by 60% (Figure 3.7A and 3.7B). Parallel to the proliferation assay results, anti-migratory effect of PTPRK was abrogated for PTPRK-mut and PTPRK-del (Figure 3.7B; P=0.006, PTPRK-wt vs. variants). The effect of PTPRK variants on migratory nature of U87-MG cells was not statistically significant (P=0.076 and P=0.052, respectively). Moreover, rate of cell migration was not different between the PTPRK variants (P=0.4). This effect of PTPRK mutations on PTPRK mediated inhibition of glioma migration was further confirmed in U251-MG cell line (Figure 3.8).

We next evaluated role of PTPRK and its variants in glioma invasion using matrigel invasion chambers. Cell invasion is one of the most important hallmarks of malignant gliomas. PTPRK role in glioma cell invasion was not analyzed in our previous study. As shown in Figure 3.9, PTPRK-wt expression significantly suppressed invasion ability of glioma cell by 40% (P<0.001). On the contrary, compared to wild-type PTPRK, expression of PTPRK variants failed to suppress invasive characteristics of U87-MG cells (Figure 3.9A and 3.9B). These findings were further confirmed in U251-MG cells. PTPRK-wt expressing cells showed 45% less invasion (P<0.003) and the mutations abrogated this anti-invasive effect of PTPRK (Figure 3.9A and 3.9C). There was no difference in percentage of invaded cells between the PTPRK variants and mock cells. Overall, the data indicate that mutations and deletions of the PTPRK gene alter its suppressive effect on the invasive phenotype of malignant glioma.

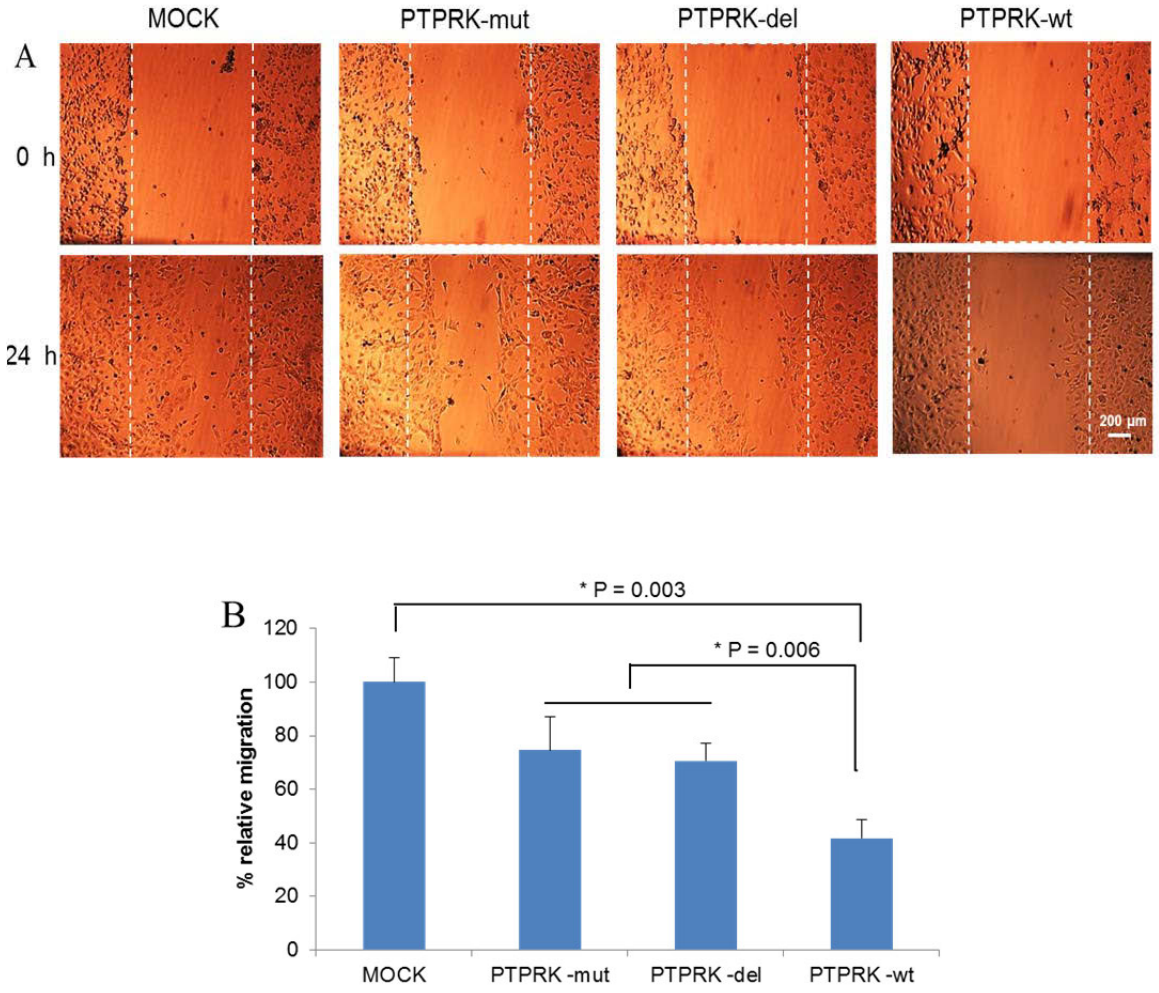

Figure 3.7: PTPRK variants alter anti-migratory effect of PTPRK-wt on glioma cells. (A) Confluent U87 cells transfected with empty, wild-type or mutants PTPRK were scratched and imaged at 0 and 24 h. Changes in wound area per time were evaluated using TScratch software. Dotted white lines indicate approximate wound edge at 0 h. Scale bar = 200 µm. (B) Bar graph shows changes in wound area per time in glioma cells transfected with empty (n=15), mutants (n=15) or PTPRK-wt (n=15). $P<0.05$ (*) was considered significant for ANOVA analysis.

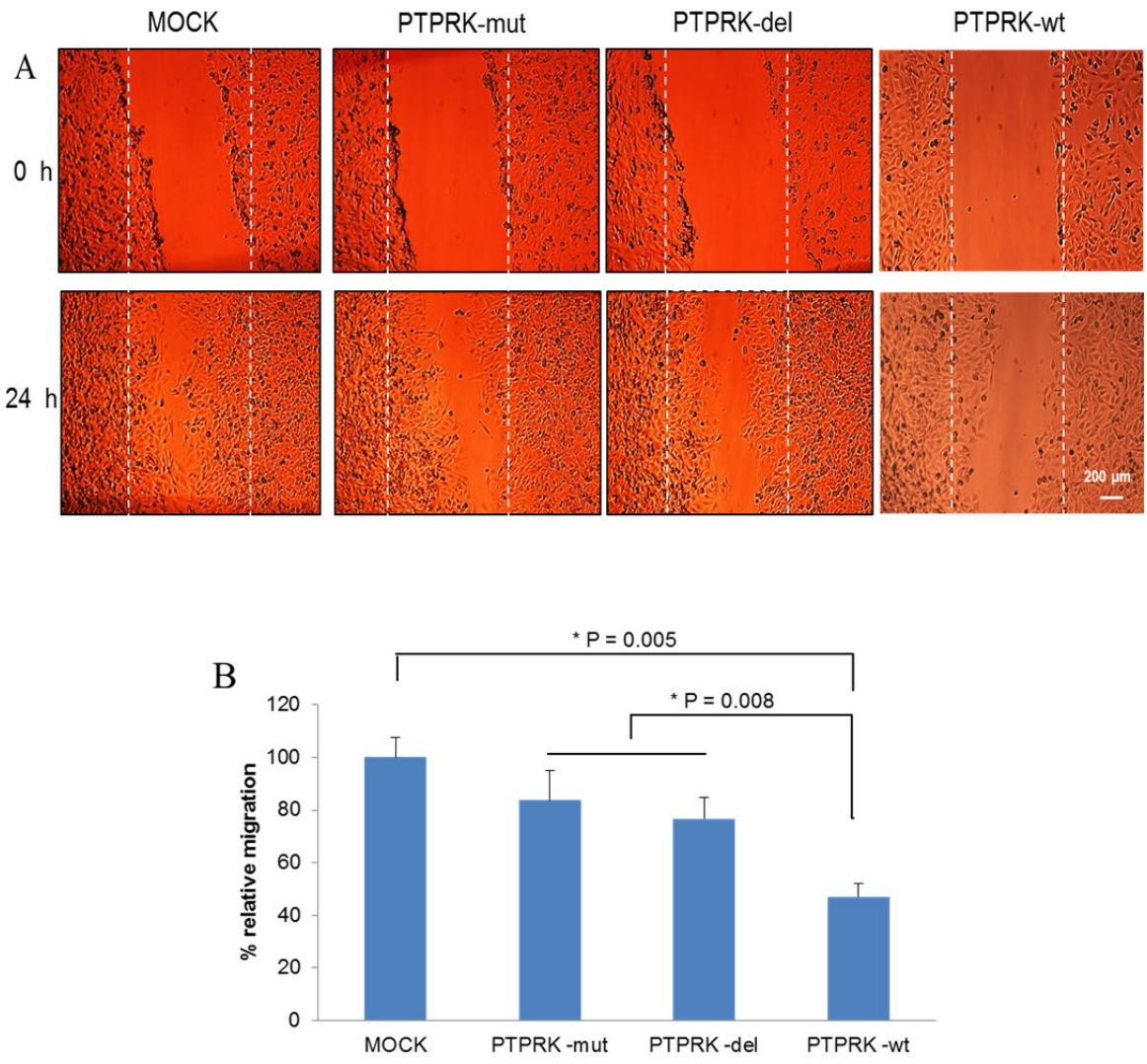

Figure 3.8: PTPRK variants alter suppressive effect of wild-type PTPRK on migration of U251-MG cells. (A) Confluent monolayers of U251-MG cells transfected with empty, wild-type or mutants PTPRK were scratched and imaged at 0 and 24 h. Dotted white lines indicate approximate wound edge at 0 h. Scale bar = 200 µm. (B) Bar graph shows changes in wound area per time, n=15, $P<0.05$ was considered significant for ANOVA analysis.

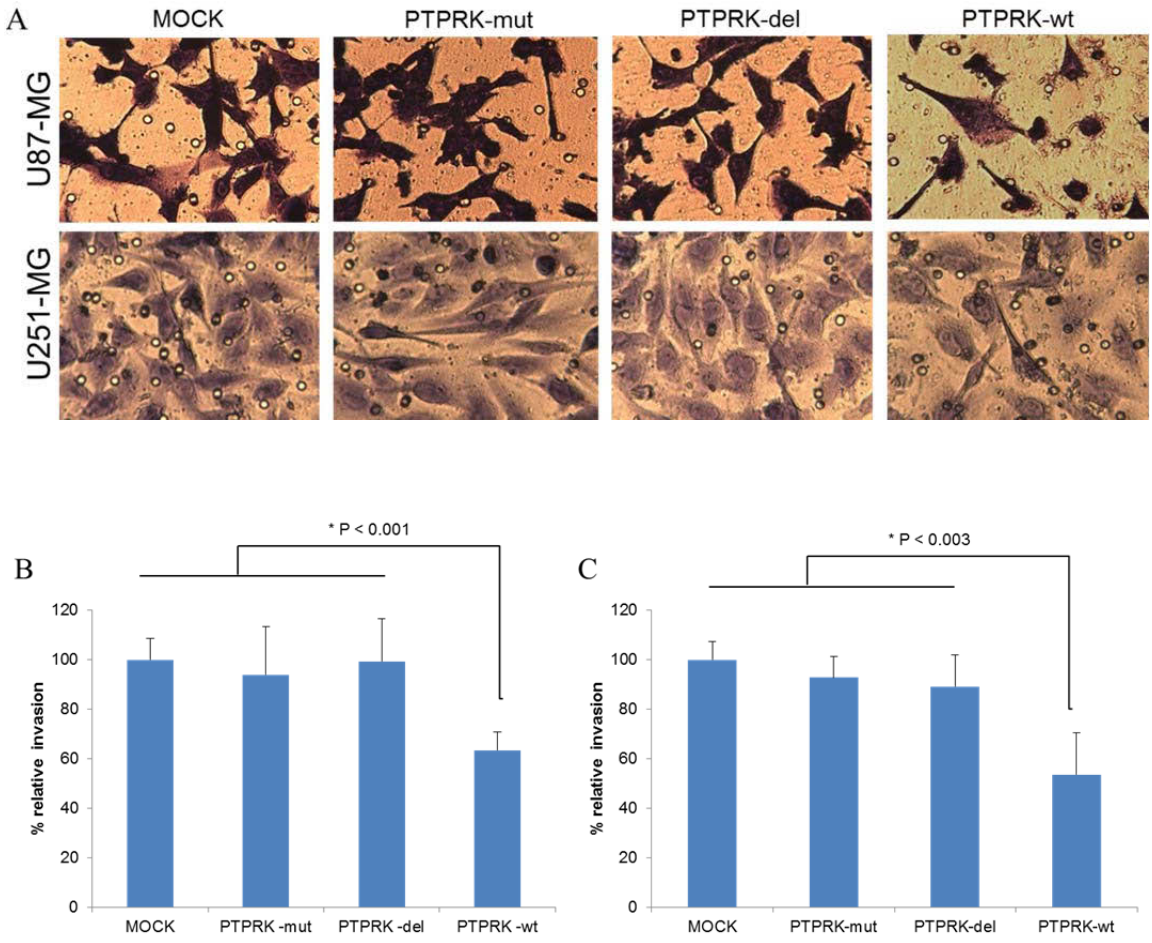

Figure 3.9: PTPRK variants alter suppressive effect of PTPRK-wt on glioma cell invasion. A) Images showing invasive behavior of U87 (top) and U251 (bottom) malignant glioma cells transfected with PTPRK clones. Invaded cells were stained with crystal violet, photographed under an inverted light microscope using 25 x objectives, and quantified by manual counting and using ImageJ software in five randomly selected areas. Invasion of (B) U87-MG and (C) U251-MG cells, expressing PTPRK or its mutant forms, was assessed by matrigel invasion assay. Histograms show average count of invaded cells for each PTPRK clone as a percentage of invading mock cells.

3.3.5 PTPRK expression sensitizes glioma cells to anti-glioma therapeutics

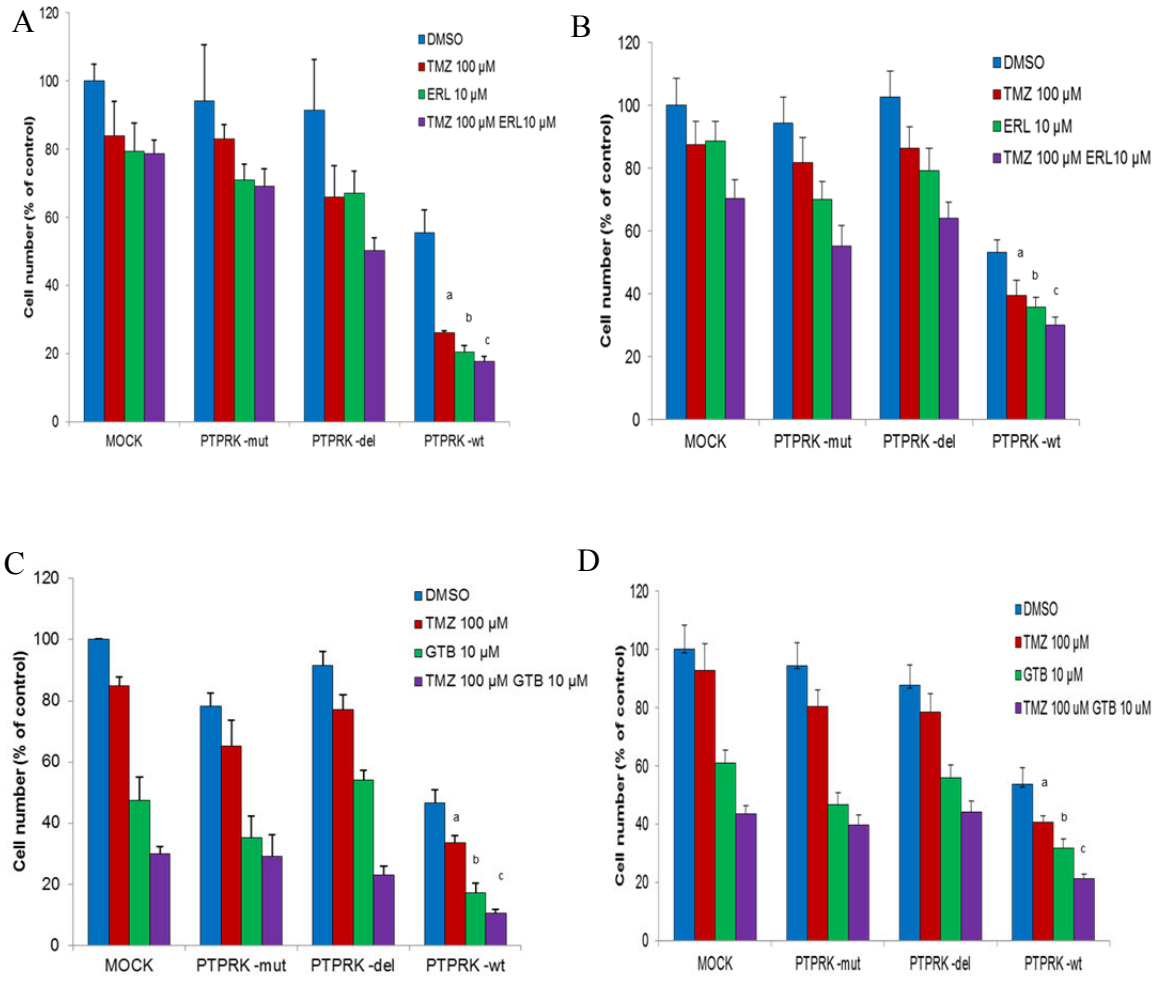

Figure 3.10: PTPRK variants alter response to anti-glioma agents. (A) U87-MG and (B) U251-MG cells expressing PTPRK-wt or variants were treated with temozolomide (100 µM), erlotinib (10 µM) or their combination. Additionally, (C) U87-MG and (D) U251-MG were treated with temozolomide (100 µM), gefitinib (10 µM) or in combination. MTT assay was performed to assess viability. Data are represented as means ± standard error of six determinants per condition from three independent experiments. Significant differences between PTPRK-wt vs. mock and PTPRK-wt vs. variants is indicated by 'a' for temozolomide (TMZ) treatment; 'b' for treatment with either erlotinib (ERL) or gefitinib (GTB), and 'c' for combination treatment (TMZ + ERL, TMZ + GTB). $P<0.01$ was considered significant.

Since we observed a major role of PTPRK in checking glioma aggressiveness (proliferation, diffusion and invasion), and as malignant gliomas are characterized by a remarkably high chemo-resistance, we analyzed whether PTPRK status modulates chemosensitivity of malignant glioma cells. We selected temozolomide (current standard of care) and two tyrosine kinase inhibitors (TKis), erlotinib and gefitinib. These TKis are currently being used in several glioma clinical trials as agents for reducing excessive tyrosine phosphorylation that is frequently observed in glioma (91,92,101,102). Our hypothesis is that tumors with normal PTPRK will respond better to TKi-based therapies whereas tumors with altered PTPRK will be refractory. The synergistic effect of TK inhibition and reduction of tyrosine phosphorylation levels by active PTPRK could increase responsiveness to the TK inhibitors.

As expected, using MTT cytotoxicity assay, we observed increased sensitivity of malignant glioma cells to anticancer drugs following expression of functionally active wild-type PTPRK and little or no significant change in sensitivity with abnormal PTPRK, compared to mock cells. Specifically, re-introduction of PTPRK-wt in U87-MG cells resulted in about 71% decrease in cell number upon treatment with temozolomide relative to treated mock cells (Figure 3.10A and 3.10C, $P<0.001$). Whereas, PTPRK-mut and PTPRK-del expression reduced cellular growth only by 15-20% indicating moderate improvement (PTPRK-mut, $P=0.1$; PTPRK-del, $P=0.08$). Similarly, treatment with erlotinib or gefitinib showed better response in PTPRK-wt expressing cells than PTPRK-null or PTPRK mutant-expressors. PTPRK-wt enhanced cytotoxic effects of erlotinib and gefitinib by 75% (erlotinib, $P<0.001$) and 65% (gefitinib, $P<0.0001$), respectively, compared to treated mock cells (Figure 3.10A and 3.10C). Furthermore, we evaluated

benefits of combination therapy of temozolomide with erlotinib or gefitinib. The combination therapy increased cell death even in PTPRK-null mock cells (Figure 3.10B). In comparison to PTPRK-null mock cells, reconstitution of PTPRK further increased sensitivity by 54% to treatment with combination of temozolomide and gefitinib/erlotinib (Figure 3.10A and 3.10C, $P<0.005$). However, the two variants altered the singular and combined effects of these drugs. Differences between mock and wild-type PTPRK-expressing cells in their response to each drug treatment condition (temozolomide/erlotinib/gefitinib alone or indicated combinations) were statistically significant (simple effect tests; $P<0.01$). PTPRK induced chemosensitivity of glioma cells was further confirmed in U251-MG cell line and was consistent with findings in U87-MG cells (Figure 3.10B and 3.10D). Since, the observed drug effects could merely be secondary to the anti-proliferative effects of PTPRK; we analyzed our data after controlling for effect on cell growth due to ectopic expression of PTPRK and variants. These results clearly indicate that PTPRK-wt significantly improves existing clinical response to conventionally used anti-cancer agents and tyrosine kinase inhibitors.

3.3.6 PTPRK alterations modify expression of the PTPRK targets EGFR and β-catenin

PTPRK is involved in cell-cell contact-mediated signaling pathways both directly through intercellular homophilic binding and indirectly through its dephosphorylating activity (66). Based on previous studies, we hypothesized that PTPRK negatively regulate aggressive phenotype of glioma cells through tyrosine dephosphorylation of β-catenin and receptor tyrosine kinases such as EGFR. Interestingly, our results indicated that the reconstitution of PTPRK-wt in U87 cells negatively regulates β-catenin and

EGFR expression (Figure 3.11). PTPRK-wt expression significantly reduced total EGFR and β-catenin protein levels (Figure 3.11, 45% and 63% vs. mock, respectively, P<0.001).

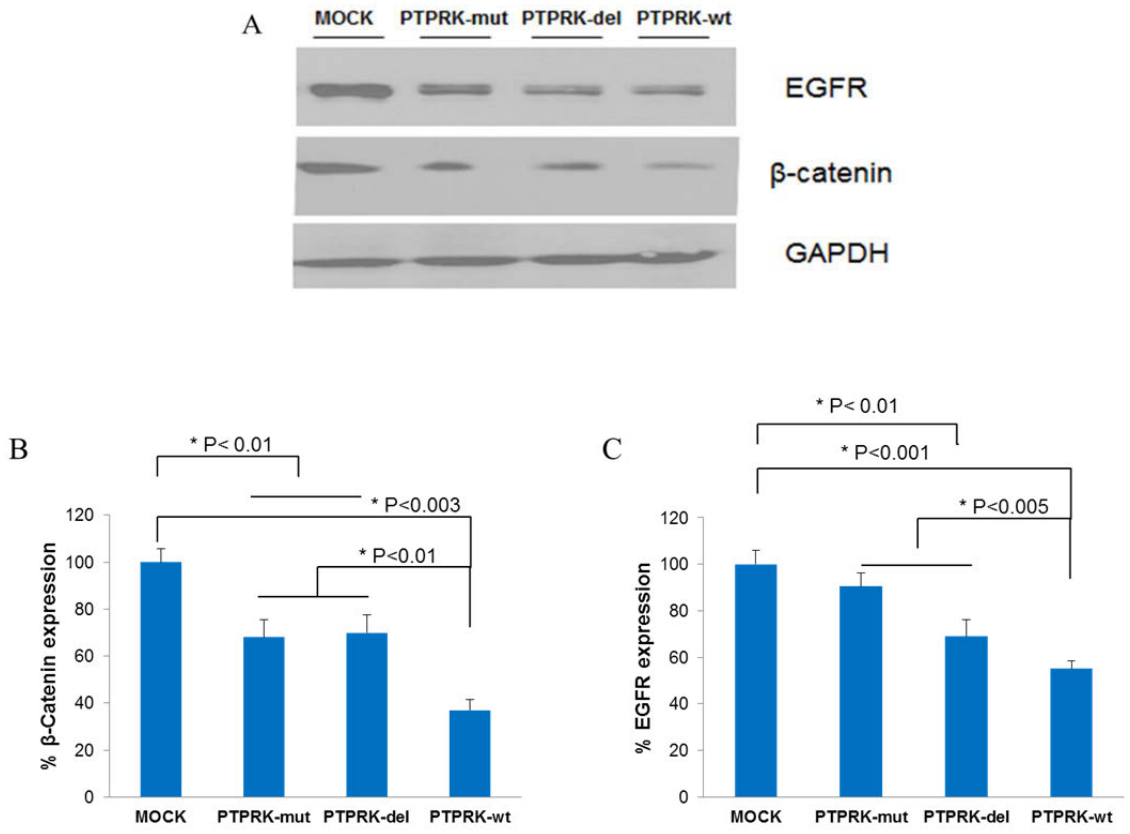

Figure 3.11: Reconstitution of PTPRK in U87-MG cells altered expression of β-catenin and EGFR. (A) U87-MG cells transfected with PTPRK-wt, PTPRK-mut and PTPRK-del were assessed for the levels of β-catenin and EGFR by immunoblot. (B) β-catenin and (C) EGFR protein levels quantified by densitometry are shown as a percentage relative to the mock cells.

PTPRK mutants, compared to the mock cells, though reduced EGFR and β-catenin levels (PTPRK-mut: 10% (P=0.1) and 32% (P<0.01), PTPRK-del: 30% (P<0.01) and 30% (P<0.01), respectively), but not to the same extent as PTPRK-wt (P<0.05).

Moreover, levels of β-catenin transcriptional targets, cyclin D1 and c-Myc, were reduced in wild-type PTPRK expressing malignant glioma cells (Figure 3.12A and 3.12B, P=0.001). Real-time PCR analysis showed decrease in c-Myc and cyclin D1 transcript levels. Mutant forms of PTPRK though showed decrease in cyclin D1 and c-Myc expression compared to mock cells (P= 0.08, mock vs. variants), but the effect was not to the same extent as observed with wild-type PTPRK (P=0.002, PTPRK-wt vs. variants). Differential regulation of PTPRK targets as a consequence of deletions/non-synonymous mutations and altered proteolytic processing correlate with observed effects of these variants on glioma cell proliferation and migration as shown in Figures 3.5 to 3.9. These results suggest that PTPRK expression negatively regulate EGFR and β-catenin expression in malignant glioma likely resulting from a decrease in tyrosine phosphorylation of EGFR and β-catenin (40,83,103,104).

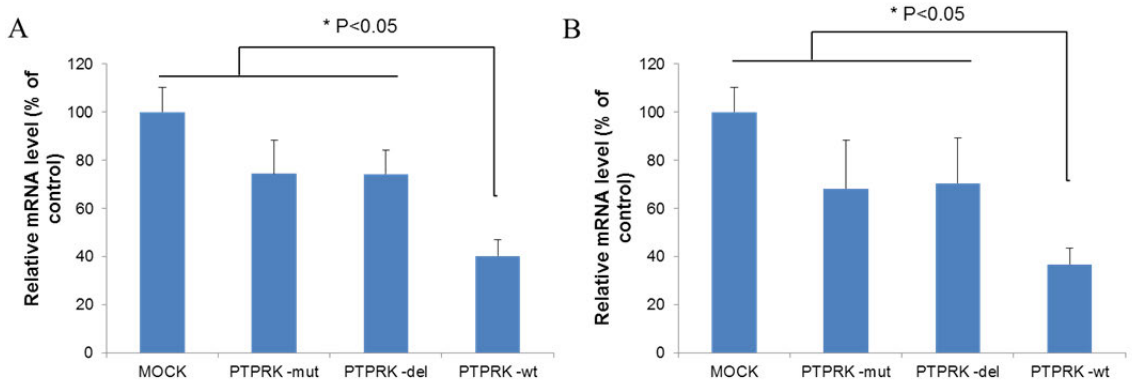

Figure 3.12: PTPRK reconstitution in U87-MG cells reduces c-Myc and cyclin D1 expression. Expression levels of β-catenin transcriptional targets, (A) cyclin D1 and (B) c-Myc, were analyzed by real-time PCR after transfection with empty vector, wild-type and mutant PTPRK forms. Histograms represent mRNA levels as a percentage relative to mock cells *, P<0.05 for significance.

3.4 Discussion

Our recent SNP array screening of glioma biopsies implicated PTPRK as an independent prognostic factor in malignant glioma. We observed that the PTPRK locus undergoes allelic loss in glioma which may contribute to the cancer phenotype. Glioma patients with deleted or inactivated PTPRK have poor overall survival compared to those with normal PTPRK locus. Further, inactivation of PTPRK has been recently observed in other tumors (68,69), indicating and independently confirming its tumor suppressive role. Our previous findings in relation to function of PTPRK in malignant glioma demonstrated its biological relevance as a negative regulator of glioma proliferation and migration. This current extension of our investigations into the role of PTPRK in malignant glioma illustrates effect of mutations on PTPRK function, PTPRK-regulated signaling pathways and response to therapy.

We identified several synonymous, non-synonymous mutations and deletions in the PTPRK gene, and focused on the most 'damaging' phenotype. These genetic alterations influenced PTPRK dephosphorylation properties and were responsible for major alterations in PTPRK mediated suppression of glioma cell migration, diffusion and invasion. Moreover, we discovered that the PTPRK genetic status can predict response to anti-glioma therapies such as temozolomide and several tyrosine kinase inhibitors*, in vitro*.

Few *in vitro* studies in other cell models indicate β-catenin as a substrate of PTPRK (82,105). β-catenin signaling plays an important function in cell migration and contributes to tumor development (40,103,104,106). It plays dual role as a major binding partner of cadherins in cell-adhesion processes and as nuclear transcriptional regulator (85). Cadherin based cell-cell adhesion is highly influenced by tyrosine phosphorylation

events (37,103). Tyrosine kinases induced phosphorylation of β-catenin at tyrosine residues (pY-654) results in its disruption from cadherin-catenin complexes and subsequent increase in the cytoplasmic and nuclear pool of free phospho β-catenin (40,85,103). The free β-catenin together with other transcription factors drives gene expression of key cell cycle regulator gene cyclin D1 and c-Myc, ultimately contributing to tumor migration and invasion (85,103,107,108). PTPRK mediated dephosphorylation of β-catenin can prevent this disassembly of cadherin-catenin complexes and simultaneously inhibit transcriptional activation of β-catenin downstream targets by preventing cytoplasmic accumulation of β-catenin phosphorylated form. Thus PTPRK can promote stability of cadherin-catenin dependent adhesion complexes and inhibit β-catenin transcriptional activity. Few previous PTPRK investigations have in fact shown PTPRK mediated β-catenin dephosphorylation (82). However, the results were indirect and not conclusive. Further, PTPRK plays a critical role in regulating EGFR signaling via tyrosine dephosphorylation of EGFR (83). Activation of EGFR and its variants via constitutive tyrosine phosphorylation is a frequent phenomenon in multiple cancers (109). Phosphotyrosine residues of kinase domain function as binding sites for signaling molecules which thereby initiate downstream signaling pathway (109). PTPRK has been shown to directly dephosphorylate EGFR in human keratinocytes and thus can suppress its downstream signal transduction (83). Based on the facts that 1) PTPs are believed to have tissue-specific functions, 2) EGFR and β-catenin signaling are among the most frequently deregulated oncogenic pathways in glioma and 3) PTPRK is highly expressed in brain, we hypothesized that PTPRK exerts anti-glioma effect by inhibiting EGFR and β-catenin oncogenic signaling.

Interestingly, PTPRK-wt expression reduced EGFR and β-catenin protein levels in glioma (Figure 3.11). This possibly suggests that apart from catalyzing dephosphorylation of EGFR and β-catenin, PTPRK also regulates their protein expression in malignant glioma by interacting directly with transcription or by negative feedback-loop after dephosphorylation of EGFR and β-catenin. Alternatively, PTPRK can possibly sense cell-cell contact by trans- homophilic interactions and mediate contact inhibition in cells dependent on EGFR and β-catenin activity for proliferation and migration. Thus, re-expression of PTPRK and consequent intercellular homophilic interactions in glioma cells induces contact inhibition of growth and perhaps sends downstream signals to reduce EGFR and β-catenin cellular levels. Moreover, reduced expression of key cell cycle regulator genes, c-Myc and cyclin D1, in PTPRK expressing U87-MG cells reflects PTPRK mediated cell cycle arrest of these cells in G1 phase, as observed previously. Further investigations are required to clearly delineate whether PTPRK plays dual role as a negative transcriptional regulator and a tyrosine dephosphorylase of EGFR and β-catenin signaling. Nonetheless, PTPRK mutations altered the inhibitory effect of wild-type PTPRK on EGFR and β-catenin signaling pathways which correlate with observed alterations in PTPRK mediated suppressive effects on growth and migration of glioma cells. Apart from regulation of EGFR and β-catenin function, other not as yet known signaling processes could be negatively regulated by PTPRK, leading to inhibition of the phenotypic hallmarks of malignant glioma. Screening of PTPRK substrates using commercially available “tyrosine phosphatase substrate sets” and subsequent validation of identified substrates in relation

to their relevance in glioma biology is required for better understanding of PTPRK regulated molecular events in gliomas.

Ectopic expression of PTPRK-wt in glioma cells showed significant reduction in the proliferation, migration and invasion rates compared to PTPRK variants, and reduced EGFR and β-catenin expression. Our results suggest that tumor derived mutations of the PTPRK gene significantly alter PTPRK functionality, and thereby the PTPRK regulated signaling cascade by two ways: 1) altering its phosphatase activity; and, 2) altering post-translational processing of PTPRK. Genetic alterations (PTPRK-mut and PTPRK-del) resulted in significantly lower phosphatase activity compared to PTPRK-wt. PTPRK-mut alteration is exclusively in the phosphatase domain-2 which is catalytically inactive but regulates enzymatic activity of the phosphatase domain-1. The deletion in PTPRK-del encompasses a region in phosphatase domain-1 prior to the conserved catalytic motif critical for phosphatase activity. Furthermore, PTPRK mutation (PTPRK-mut) results in 100% post-translational processing of full length PTPRK protein potentially leading to several PTPRK isoforms (PΔE and intracellular domain) whereas PTPRK-del showed no post-translational processing. The large deletion might have resulted in conformational changes in the PTPRK protein leading to resistance to proteases. As hypothesized, these alterations in PTPRK phosphatase activity and post-translational modification altered the suppressive effects of PTPRK on glioma growth, migration and invasive phenotypes. Interestingly, though not statistically significant, PTPRK-mut and PTPRK-del showed decrease in relative migratory activity which could be explained based on alteration in phosphatase activity and post-translational processing of these variants. Specifically, PTPRK-del showed no proteolytic processing thus could be localized exclusively on the

cell membrane. Therefore, PTPRK-del can induce contact mediated inhibition of glial cell migration via homophilic interactions. In fact, expression of catalytically inactive RPTP-μ (PTPRK homolog) in a prostate cancer cell line was shown to stabilize adherens junctions (110). This indicates that cell surface associated RPTPs can indeed function independently of phosphatase activity. However, weak homophilic interactions due to mutations, together with reduced phosphatase activity can subsequently result in weak or altered transduction of downstream signals in response to migrating glial cells. Moreover, both PTPRK-mut and PTPRK-del showed decrease in levels of EGFR and β-catenin which are among major players in cell migration.

Furthermore, our results showed that limiting glioma infiltration and migration by expression of functional PTPRK results in improved response to several anti-glioma agents. The rationale is that infiltrative behavior of malignant glioma cells into surrounding brain parenchyma which makes current treatments less effective is highly dependent on PTPRK genetic status. Moreover, decreased EGFR and β-catenin levels in PTPRK expressing malignant glioma cells can potentially translate into better response to chemotherapeutic drugs. After all, overactivated β-catenin and receptor tyrosine kinases signaling such as EGFR contributes to drug resistance (23,84,86,111). Indeed, U87-MG and U251-MG cells ectopically expressing PTPRK-wt showed significantly higher response to temozolomide and/or tyrosine kinase inhibitor treatment. Thus PTPRK-wt expression significantly increases the drug efficacy. However, non-synonymous mutations or deletions abrogated this observed improvement. This variation in clinical response to chemotherapy could be explained by differences in phosphatase activity, post-translational modifications, and consequent differences in regulation of EGFR and

β-catenin signaling. Moreover, one of the major mechanisms of resistance to gefitinib and erlotinib is overexpression of ATP binding cassettes efflux carriers (ABCTs). ABCt transporters are activated by phosphorylation (112) and inactivation of certain ABCTs by PTPRK might explain improvement in clinical response to these drugs. However, the exact molecular mechanism is as yet unclear and requires further investigation.

Another interesting aspect to note was that although erlotinib and gefitinib are structurally related and have a similar mechanism of action, glioma cells showed better response to treatment with gefitinib than erlotinib, either alone or in combination with temozolomide. This difference in response was enhanced by PTPRK-wt expression. Poor response to erlotinib monotherapy has been previously attributed to PTEN and EGFR mutations (EGFRvIII) in malignant glioma cells (101). However, response to gefitinib treatment was contrary to recent glioma study results (113). Another study has recently shown cooperative effect of erlotinib and temozolomide combination therapy at lower doses (1 μM and 25 μM, respectively) in glioma cells (38). This synergistic effect at sub-optimal doses of erlotinib (2.5 μM) and temozolomide (25 μM) was not observed in our experimental conditions. We observed only 10-20% decrease in viable cells with combination of erlotinib (2.5 μM) and varying range of temozolomide concentrations (25 μM, 100 μM and 200 μM) relative to untreated U87-MG cells (data not shown). Moreover, the relationship between PTPRK status (cell-cell contact) and temozolomide (targets DNA repair) is currently unclear. A recent study in glioma showed a possible cooperation between EGFR inhibition and temozolomide related reduction in tumor growth (38). Based on this study, it can be speculated that PTPRK-mediated check on EGFR signaling improves response of PTPRK expressing cells to temozolomide treatment. Overall, our

results clearly indicate that PTPRK expression in glioma cells improves clinical response to these anti-cancer drugs, *in vitro*.

CHAPTER IV

CONCLUSION, FUTURE WORK AND CHALLENGES

4.1 Conclusion

Gliomas are the most frequent primary brain tumors with poor prognosis and response to treatment largely due to extensive migration of tumor cells into surrounding normal brain tissues. Survival in patients with malignant glioma has not improved over the years. Therefore, it is critical to develop alternate therapeutic strategies, which requires better understanding of glioma migration-related molecular processes. Genome-wide studies hold great potential in discovery of novel signaling molecules relevant to glioma migration, with prognostic and predictive significance.

Genomic explorations in the representative population of glioma patients led to discovery of an important regulator of cell migration, PTPRK, that function both as a cell adhesion molecule and a regulator of cellular tyrosine phosphorylation levels. Loss of cell adhesion molecules and aberrant tyrosine phosphorylation signaling are key events in glioma cell migration. Frequent alterations of PTPRK in glioma indicate its important function as a tumor suppressor that limits tumor cell migration. PTPRK was thus selected as a candidate gene for further validation.

PTPRK genomic and transcriptomic status was found to predict survival of patients with glioma. PTPRK expression was shown to be lower in malignant glioma than normal brain tissues at both mRNA and protein levels. Further, high grade gliomas do not express cell surface associated PTPRK protein. Rather, several small fragments due to proteolysis were observed. Full length PTPRK overexpression in three high grade glioma cell lines significantly reduced growth and migration. This supports the hypothesis that

PTPRK is a potential prognostic marker and a functional tumor suppressor gene downregulated in gliomas. Moreover, novel PTPRK mutations were discovered in malignant gliomas that altered functionality of PTPRK protein. These mutations abrogated anti-oncogenic function of PTPRK in malignant glioma by influencing its phosphatase activity and post-translational processing. Further, PTPRK expression improved response to treatment in glioma, which was otherwise nullified by the PTPRK variants.

In summary, our findings provide compelling evidence in support of tumor-suppressive properties of PTPRK in glioma. It is a novel regulator of glioma cell proliferation, migration and invasion that predicts prognosis and response to treatment. The results demonstrate biological relevance of PTPRK loss in glioma pathogenesis and progression. However, it is not yet clear if the maintenance of required PTPRK expression levels could serve as a sufficient "checkpoint" in the molecular events leading to glioma development and progression. Future studies require further analysis of PTPRK variants in a larger group of glioma patients. Mutational screening in an alternative glioma population will validate the significance of identified mutations. Although PTPRK interacts with β-catenin and EGFR, *in vitro*, it is likely that other cellular substrates of its phosphatase activity contribute to anti-glioma effect of PTPRK. In future, with data herein being confirmed using *in vitro* and *in vivo* models, PTPRK may be used as a therapeutic predictive marker for tyrosine kinase inhibitors and other anti-glioma agents.

4.2 Future work

4.2.1 Validate *in vitro* data in mice studies

PTPRK role in glioma was studied primarily in malignant glioma cell lines, *in vitro*. Multiple cell lines were used for the cell-based functional assays to corroborate the observed functional relationships. These findings now need to be validated *in vivo* using orthotopic xenograft mouse models to closely mimic tumor microenvironment. Tumor phenotypes and their infiltrative capacities should be analyzed after orthotopic injection of malignant glioma cell lines expressing PTPRK and its variants into the mice. Additionally, orthotopic mice models of primary GBM cells transduced with scrambled or PTPRK specific shRNA will confirm effect of PTPRK fragments on glioma infiltration. Further, PTPRK induced chemotherapeutic response and effect of variants observed in cell-based studies, should be validated *in vivo*, using anticancer cytotoxicity screening assay of xenografted glioma cell lines expressing appropriate PTPRK forms. Time to disease progression, relative growth compared to controls and rate of regression should be subsequently determined.

4.2.2 Screen for PTPRK targets

EGFR and β-catenin are the only known PTPRK substrates. It is likely that PTPRK interacts with other cellular proteins. Therefore, screening of PTPRK dephosphorylation targets using commercially available “tyrosine phosphatase substrate sets” is required. However, stand-alone *in vitro* screen has often resulted in artifacts as purified phosphatase protein can potentially dephosphorylate any substrate partly because of less strained protein structure in cell free conditions (93). Therefore, identified

physiological substrates of PTPRK from initial screen should be further verified by other techniques such as "substrate-trapping mutant" approach and by analyzing effect of PTPRK modulation on potential substrates, *in vitro*. Identification of novel PTPRK substrates will provide better understanding of PTPRK regulated molecular events in glioma.

Moreover, PTPRK fragments from post-translational processing can have differential accessibility to the substrates depending upon their subcellular localization. Even PΔE might have its own microenvironment and interact with substrates differently compared to full length PTPRK protein. This necessitates determination of substrate specificity of the PTPRK fragments. PTPRK role in nucleus is not yet clear. Microarray experiments can provide better understanding of PTPRK role in gene transcription.

4.2.3 Large scale validation of PTPRK variants

Clinical relevance of identified PTPRK mutations needs to be determined and validated in a larger population set of glioma patients such as in biopsies from NCI repository bank. Frequency of discovered mutations should be evaluated by sequencing glioma tumor specimens. Sequencing of PTPRK transcript would also identify the presence of other exonic mutations. Subsequent functional studies will establish effect of these mutations on PTPRK function. Prognostic and predictive significance of the identified mutations should be evaluated to determine if PTPRK variant(s) increase prognostic and predictive accuracy.

4.3 Challenges in PTP research

Our understanding of tyrosine phosphorylation signaling pathways has improved immensely over the past decades. Several investigations have broadened the spectrum of tyrosine phosphorylation regulators and highlighted the complex network of regulatory interactions among various signaling pathways. Many receptor type PTPs have been implicated in process of tumor development and progression, and possess tumor specific role (94,114). Although progress has been made in defining functional role of RPTPs in cancer, several important concerns are yet to be addressed.

The expression of RPTPs in cancer can be regulated by many mechanisms from transcriptional to post-translational levels including mutations, deletions, alternate splicing, receptor dimerization, post-translational changes and oxidation of the catalytic site (59,60,67). More often or not, these mechanisms have been studied in singularity. Multiple mechanisms can simultaneously regulate RPTP activity. For example, oxidative stress in tumor microenvironment generally results in burst of reactive oxygen species which can easily render RPTPs catalytically inactive (67). Alongside, high levels of proteases in cancer can alter functional properties of RPTPs by post-translational processing (67). Exact regulatory mechanism(s) that leads to biologically relevant changes in RPTP expression, in a tumor setting, are not as yet clear. Interestingly, phosphorylation of RPTPs by kinases itself can modulate RPTP mediated cellular responses (Figure 4.1). Phosphorylated RPTPs have been shown to activate tyrosine kinases leading to activation of oncogenic signals (67,115,116). However, the molecular events leading to phosphorylation of RPTPs in cancer are not yet understood.

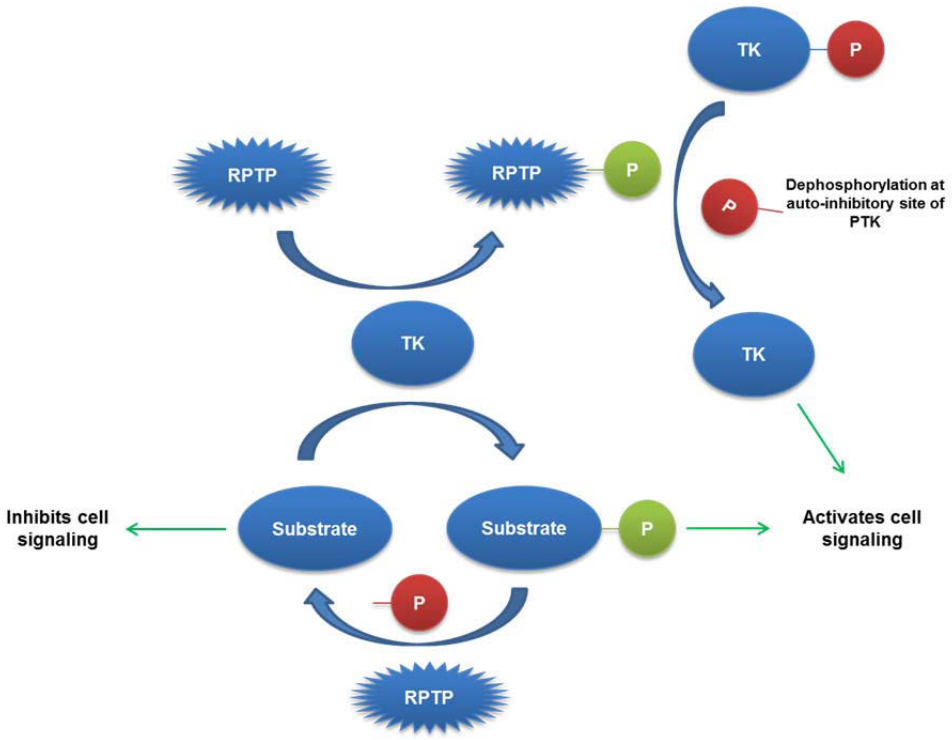

Figure 4.1: Protein tyrosine phosphorylation signaling network. Tyrosine phosphorylation of proteins, including tyrosine kinases (TK) is vital for activation of many cellular processes. Receptor protein tyrosine phosphatase (RPTP) mediated dephosphorylation of tyrosine kinases and their substrates inhibit activation of signaling processes. However, tyrosine phosphorylation of RPTPs by tyrosine kinases can alter RPTP function. Phosphorylated RPTPs can induce dephosphorylation at autoinhibitory tyrosine residues of TKs leading to their activation.

Our understanding of functional relevance of RPTPs in cancer is also limited by the fact that interaction with particular ligand or substrate can vary with cell type (59,93). In addition, as several RPTPs are together expressed in normal tissue, choice of RPTP(s) for execution of particular function in signaling pathway could be rather dependent on selective expression and localization of their specific substrates and/or ligands, instead of selective RPTP expression. However, it is not clear how the specificity is achieved *in vivo*. Structural resolution of full length RPTPs in absence or presence of binding partners will greatly facilitate RPTP research in the future.

Since RPTPs play important role in multiple cancer-related signaling pathways (59,65), they can well be considered as potential therapeutic targets. However, for several RPTPs as the objective is to activate rather than inhibit them, targeting with drugs is difficult. Further, targeting activity of specific RPTP is a challenge due to highly conserved catalytic site of RPTPs. Nonetheless, PTP-based therapeutics has increasingly gained interest over the years. Selective inhibitors for oncogenic PTPs and activators of tumor suppressive PTPs are being designed by targeting unique regions surrounding the catalytic site of each PTPs (117,118). Moreover, the extracellular regions of RPTPs are structurally diverse and could be targeted using small molecules and monoclonal antibodies to activate function of certain RPTPs by blocking their inactive dimer forms (65,119). Use of activating ligands or small-peptide agonists to trigger the tyrosine phosphatase activity of PTPs holds potential to balance aberrant tyrosine phosphorylation levels (118-120). Small molecule agonists of T-cell PTP (TCPTP) have in fact been shown to activate TCPTP *in vitro* and thereby inhibit RTK signaling (118,121). Since, tumor suppressive PTPs are generally mutated or absent in cancer cells, using agonists may not present any potential advantage. Small molecules mimicking PTPs could function as RTK antagonists (121-123). Additionally, PTPs with oncogenic function represent potential drug targets (120,123). In fact, inhibitors of PTP1B are in clinical trials for treatment of type II diabetes and obesity (124).

Apart from several challenges in the development of clinically useful PTP modulators, another challenge in relation to gliomas is the blood brain barrier, which is a major hurdle for drug delivery. Nevertheless, a better understanding of physiological

ligands and molecular mechanisms of RPTP function will ultimately allow improved therapeutic modalities for diseases with unbalanced protein tyrosine phosphorylation.

APPENDIX A

LOSS OF HETEROZYGOSITY

Loss of heterozygosity (LOH) analysis is useful in identifying chromosomal regions that harbor putative tumor suppressor genes (TSGs). TSGs are like the brake pedal of cell cycle that prevents inappropriate cell growth and survival. However mutations or deletions in these genes result in brake failure leading to unchecked cell proliferation and cancer development. LOH analysis is based on Knudson's two-hit hypothesis (Figure A1). A normal somatic cell has two functional copies (wild-type allele) of a TSG. Thus, two independent hits are required in a somatic cell to make a TSG non-functional. The first acquired hit in form of mutations inactivates one copy of a TSG. This makes the cell heterozygous for the non-functional mutant allele. Moreover, individuals can inherit first hit in every cell due to germline mutation and thus are heterozygous for the mutant allele of a TSG. A subsequent hit in the second copy of the TSG causes LOH, leading to initiation of cancer.

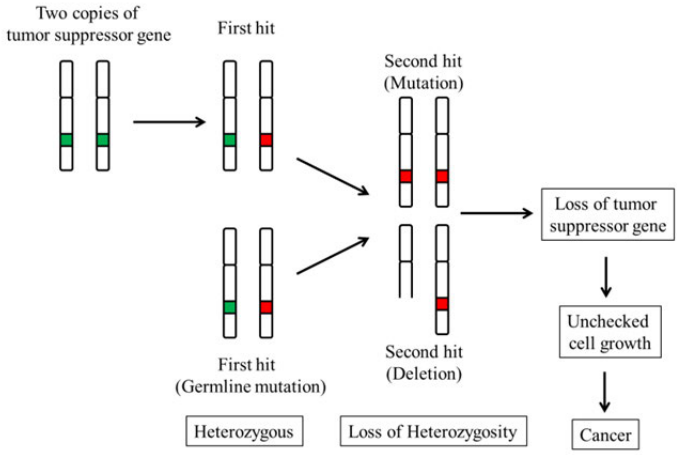

Figure A1: Knudson's two-hit hypothesis. Inactivation of a TSG requires two independent mutation events. Only one mutation event is required in individuals with germline mutations. A functional tumor suppressor is indicated in green. Inactivated allele due to mutations is indicated in red.

APPENDIX B

PUBLICATIONS AND ABSTRACTS

PUBLICATIONS

Agarwal S, Al-Keilani MS, Alqudah MA, Sibenaller Z, Ryken TC**,** Assem M. Tumor derived mutations of Protein Tyrosine Phosphatase Receptor Type K affect its function and alter sensitivity to chemotherapeutics in glioma. PlosOne, 2013, In Press.

Assem M*,* Sibenaller Z, **Agarwal S**, Al-Keilani MS, Alqudah MA, Ryken TC. Enhancing diagnosis, prognosis and therapeutic outcome prediction of gliomas using genomics. OMICS, March 2012, 16(3): 113-122

ABSTRACTS

Agarwal S, Al-Keilani MS, Alqudah MA, Sibenaller Z, Ryken TC**,** Assem M. Receptor protein tyrosine phosphatase type kappa is a prognostic marker, essential for regulating malignant behavior of glioma cells. American Association of Cancer Research annual meeting, 2012

Agarwal S, Al-Keilani MS, Alqudah MA, Sibenaller Z, Ryken TC**,** Assem M. Receptor protein tyrosine phosphatase type kappa (PTPRK) as a potential tumor suppressor and a predictive marker in gliomas. American Association of Pharmaceutical Scientists annual meeting, 2011

S. Agarwal, M. Al-Keilani, M. Alqudah, Z. Sibenaller, T. Ryken, M. Assem. PTPRK as a potential tumor suppressor and a predictive marker in gliomas. Health Sciences Research Week–translational genomics, University of Iowa, IA, 2011

REFERENCES

(1) Riemenschneider MJ, Jeuken JW, Wesseling P, Reifenberger G. Molecular diagnostics of gliomas: state of the art. Acta Neuropathol 2010 Nov;120(5):567-584.

(2) Gilbertson RJ, Rich JN. Making a tumour's bed: glioblastoma stem cells and the vascular niche. Nat Rev Cancer 2007 Oct;7(10):733-736.

(3) Holland EC, Celestino J, Dai C, Schaefer L, Sawaya RE, Fuller GN. Combined activation of Ras and Akt in neural progenitors induces glioblastoma formation in mice. Nat Genet 2000 May;25(1):55-57.

(4) Dolecek TA, Propp JM, Stroup NE, Kruchko C. CBTRUS statistical report: primary brain and central nervous system tumors diagnosed in the United States in 2005-2009. Neuro Oncol 2012 Nov;14 Suppl 5:v1-49.

(5) Louis DN, Ohgaki H, Wiestler OD, Cavenee WK, Burger PC, Jouvet A, et al. The 2007 WHO classification of tumours of the central nervous system. Acta Neuropathol 2007 Aug;114(2):97-109.

(6) Ichimura K, Ohgaki H, Kleihues P, Collins VP. Molecular pathogenesis of astrocytic tumours. J Neurooncol 2004 Nov;70(2):137-160.

(7) Assem M, Sibenaller Z, Agarwal S, Al-Keilani MS, Alqudah MA, Ryken TC. Enhancing diagnosis, prognosis, and therapeutic outcome prediction of gliomas using genomics. OMICS 2012 Mar;16(3):113-122.

(8) Cancer Genome Atlas Research Network. Comprehensive genomic characterization defines human glioblastoma genes and core pathways. Nature 2008 Oct 23;455(7216):1061-1068.

(9) Furnari FB, Fenton T, Bachoo RM, Mukasa A, Stommel JM, Stegh A, et al. Malignant astrocytic glioma: genetics, biology, and paths to treatment. Genes Dev 2007 Nov 1;21(21):2683-2710.

(10) Maher EA, Furnari FB, Bachoo RM, Rowitch DH, Louis DN, Cavenee WK, et al. Malignant glioma: genetics and biology of a grave matter. Genes Dev 2001 Jun 1;15(11):1311-1333.

(11) Norden AD, Wen PY. Glioma therapy in adults. Neurologist 2006 Nov;12(6):279-292.

(12) Gupta M, Djalilvand A, Brat DJ. Clarifying the diffuse gliomas: an update on the morphologic features and markers that discriminate oligodendroglioma from astrocytoma. Am J Clin Pathol 2005 Nov;124(5):755-768.

(13) See SJ, Gilbert MR. Anaplastic astrocytoma: diagnosis, prognosis, and management. Semin Oncol 2004 Oct;31(5):618-634.

(14) Smith JS, Perry A, Borell TJ, Lee HK, O'Fallon J, Hosek SM, et al. Alterations of chromosome arms 1p and 19q as predictors of survival in oligodendrogliomas, astrocytomas, and mixed oligoastrocytomas. J Clin Oncol 2000 Feb;18(3):636-645.

(15) Sanson M, Thillet J, Hoang-Xuan K. Molecular changes in gliomas. Curr Opin Oncol 2004 Nov;16(6):607-613.

(16) Nord H, Hartmann C, Andersson R, Menzel U, Pfeifer S, Piotrowski A, et al. Characterization of novel and complex genomic aberrations in glioblastoma using a 32K BAC array. Neuro Oncol 2009 Dec;11(6):803-818.

(17) Freije WA, Castro-Vargas FE, Fang Z, Horvath S, Cloughesy T, Liau LM, et al. Gene expression profiling of gliomas strongly predicts survival. Cancer Res 2004 Sep 15;64(18):6503-6510.

(18) Schwartzbaum JA, Fisher JL, Aldape KD, Wrensch M. Epidemiology and molecular pathology of glioma. Nat Clin Pract Neurol 2006 Sep;2(9):494-503; quiz 1 p following 516.

(19) Kaur B, Khwaja FW, Severson EA, Matheny SL, Brat DJ, Van Meir EG. Hypoxia and the hypoxia-inducible-factor pathway in glioma growth and angiogenesis. Neuro Oncol 2005 Apr;7(2):134-153.

(20) Ravi R, Mookerjee B, Bhujwalla ZM, Sutter CH, Artemov D, Zeng Q, et al. Regulation of tumor angiogenesis by p53-induced degradation of hypoxia-inducible factor 1alpha. Genes Dev 2000 Jan 1;14(1):34-44.

(21) Chamberlain MC. Radiographic patterns of relapse in glioblastoma. J Neurooncol 2011 Jan;101(2):319-323.

(22) Dunn GP, Rinne ML, Wykosky J, Genovese G, Quayle SN, Dunn IF, et al. Emerging insights into the molecular and cellular basis of glioblastoma. Genes Dev 2012 Apr 15;26(8):756-784.

(23) Drappatz J, Norden AD, Wen PY. Therapeutic strategies for inhibiting invasion in glioblastoma. Expert Rev Neurother 2009 Apr;9(4):519-534.

(24) Demuth T, Berens ME. Molecular mechanisms of glioma cell migration and invasion. J Neurooncol 2004 Nov;70(2):217-228.

(25) Lefranc F, Brotchi J, Kiss R. Possible future issues in the treatment of glioblastomas: special emphasis on cell migration and the resistance of migrating glioblastoma cells to apoptosis. J Clin Oncol 2005 Apr 1;23(10):2411-2422.

(26) Sofroniew MV, Vinters HV. Astrocytes: biology and pathology. Acta Neuropathol 2010 Jan;119(1):7-35.

(27) Nakada M, Nakada S, Demuth T, Tran NL, Hoelzinger DB, Berens ME. Molecular targets of glioma invasion. Cell Mol Life Sci 2007 Feb;64(4):458-478.

(28) Teodorczyk M, Martin-Villalba A. Sensing invasion: cell surface receptors driving spreading of glioblastoma. J Cell Physiol 2010 Jan;222(1):1-10.

(29) Utsuki S, Sato Y, Oka H, Tsuchiya B, Suzuki S, Fujii K. Relationship between the expression of E-, N-cadherins and beta-catenin and tumor grade in astrocytomas. J Neurooncol 2002 May;57(3):187-192.

(30) D'Abaco GM, Kaye AH. Integrins: molecular determinants of glioma invasion. J Clin Neurosci 2007 Nov;14(11):1041-1048.

(31) Mahesparan R, Read TA, Lund-Johansen M, Skaftnesmo KO, Bjerkvig R, Engebraaten O. Expression of extracellular matrix components in a highly infiltrative in vivo glioma model. Acta Neuropathol 2003 Jan;105(1):49-57.

(32) Nakada M, Okada Y, Yamashita J. The role of matrix metalloproteinases in glioma invasion. Front Biosci 2003 Jan 1;8:e261-9.

(33) Rao JS. Molecular mechanisms of glioma invasiveness: the role of proteases. Nat Rev Cancer 2003 Jul;3(7):489-501.

(34) Binder DK, Berger MS. Proteases and the biology of glioma invasion. J Neurooncol 2002 Jan;56(2):149-158.

(35) Raftopoulou M, Hall A. Cell migration: Rho GTPases lead the way. Dev Biol 2004 Jan 1;265(1):23-32.

(36) Muller PA, Caswell PT, Doyle B, Iwanicki MP, Tan EH, Karim S, et al. Mutant p53 drives invasion by promoting integrin recycling. Cell 2009 Dec 24;139(7):1327-1341.

(37) Nakada M, Kita D, Teng L, Pyko IV, Watanabe T, Hayashi Y, et al. Receptor tyrosine kinases: principles and functions in glioma invasion. Adv Exp Med Biol 2013;986:143-170.

(38) Ramis G, Thomas-Moya E, Fernandez de Mattos S, Rodriguez J, Villalonga P. EGFR inhibition in glioma cells modulates Rho signaling to inhibit cell motility and invasion and cooperates with temozolomide to reduce cell growth. PLoS One 2012;7(6):e38770.

(39) Lilien J, Balsamo J. The regulation of cadherin-mediated adhesion by tyrosine phosphorylation/dephosphorylation of β-catenin. Curr Opin Cell Biol 2005 10;17(5):459-465.

(40) Piedra J, Martínez D, Castaño J, Miravet S, Duñach M, de Herreros AG. Regulation of β-Catenin Structure and Activity by Tyrosine Phosphorylation. Journal of Biological Chemistry 2001 June 08;276(23):20436-20443.

(41) Giannini C, Burger PC, Berkey BA, Cairncross JG, Jenkins RB, Mehta M, et al. Anaplastic oligodendroglial tumors: refining the correlation among histopathology, 1p 19q deletion and clinical outcome in Intergroup Radiation Therapy Oncology Group Trial 9402. Brain Pathol 2008 Jul;18(3):360-369.

(42) Parsons DW, Jones S, Zhang X, Lin JC, Leary RJ, Angenendt P, et al. An integrated genomic analysis of human glioblastoma multiforme. Science 2008 Sep 26;321(5897):1807-1812.

(43) Rich JN, Hans C, Jones B, Iversen ES, McLendon RE, Rasheed BK, et al. Gene expression profiling and genetic markers in glioblastoma survival. Cancer Res 2005 May 15;65(10):4051-4058.

(44) Norden AD, Lesser GJ, Drappatz J, Ligon KL, Hammond SN, Lee EQ, et al. Phase 2 study of dose-intense temozolomide in recurrent glioblastoma. Neuro Oncol 2013 Apr 3.

(45) Brada M, Hoang-Xuan K, Rampling R, Dietrich PY, Dirix LY, Macdonald D, et al. Multicenter phase II trial of temozolomide in patients with glioblastoma multiforme at first relapse. Ann Oncol 2001 Feb;12(2):259-266.

(46) Yung WK, Albright RE, Olson J, Fredericks R, Fink K, Prados MD, et al. A phase II study of temozolomide vs. procarbazine in patients with glioblastoma multiforme at first relapse. Br J Cancer 2000 Sep;83(5):588-593.

(47) Perry J, Chambers A, Spithoff K, Laperriere N. Gliadel wafers in the treatment of malignant glioma: a systematic review. Curr Oncol 2007 Oct;14(5):189-194.

(48) Westphal M, Hilt DC, Bortey E, Delavault P, Olivares R, Warnke PC, et al. A phase 3 trial of local chemotherapy with biodegradable carmustine (BCNU) wafers (Gliadel wafers) in patients with primary malignant glioma. Neuro Oncol 2003 Apr;5(2):79-88.

(49) Fenstermaker RA, Ciesielski MJ. Immunotherapeutic strategies for malignant glioma. Cancer Control 2004 May-Jun;11(3):181-191.

(50) De Witt Hamer PC. Small molecule kinase inhibitors in glioblastoma: a systematic review of clinical studies. Neuro Oncol 2010 Mar;12(3):304-316.

(51) Raymond E, Brandes AA, Dittrich C, Fumoleau P, Coudert B, Clement PM, et al. Phase II study of imatinib in patients with recurrent gliomas of various histologies: a European Organisation for Research and Treatment of Cancer Brain Tumor Group Study. J Clin Oncol 2008 Oct 1;26(28):4659-4665.

(52) Wen PY, Yung WK, Lamborn KR, Dahia PL, Wang Y, Peng B, et al. Phase I/II study of imatinib mesylate for recurrent malignant gliomas: North American Brain Tumor Consortium Study 99-08. Clin Cancer Res 2006 Aug 15;12(16):4899-4907.

(53) Seystahl K, Wiestler B, Hundsberger T, Happold C, Wick W, Weller M, et al. Bevacizumab alone or in combination with irinotecan in recurrent WHO grade II and grade III gliomas. Eur Neurol 2013;69(2):95-101.

(54) Friedman HS, Prados MD, Wen PY, Mikkelsen T, Schiff D, Abrey LE, et al. Bevacizumab alone and in combination with irinotecan in recurrent glioblastoma. J Clin Oncol 2009 Oct 1;27(28):4733-4740.

(55) Zhang G, Huang S, Wang Z. A meta-analysis of bevacizumab alone and in combination with irinotecan in the treatment of patients with recurrent glioblastoma multiforme. J Clin Neurosci 2012 Dec;19(12):1636-1640.

(56) Camp ER, Summy J, Bauer TW, Liu W, Gallick GE, Ellis LM. Molecular mechanisms of resistance to therapies targeting the epidermal growth factor receptor. Clin Cancer Res 2005 Jan 1;11(1):397-405.

(57) Fenton TR, Nathanson D, Ponte de Albuquerque C, Kuga D, Iwanami A, Dang J, et al. Resistance to EGF receptor inhibitors in glioblastoma mediated by phosphorylation of the PTEN tumor suppressor at tyrosine 240. Proc Natl Acad Sci U S A 2012 Aug 28;109(35):14164-14169.

(58) Wiltshire RN, Herndon JE,2nd, Lloyd A, Friedman HS, Bigner DD, Bigner SH, et al. Comparative genomic hybridization analysis of astrocytomas: prognostic and diagnostic implications. J Mol Diagn 2004 Aug;6(3):166-179.

(59) Ostman A, Hellberg C, Bohmer FD. Protein-tyrosine phosphatases and cancer. Nat Rev Cancer 2006 Apr;6(4):307-320.

(60) Ostman A, Bohmer FD. Regulation of receptor tyrosine kinase signaling by protein tyrosine phosphatases. Trends Cell Biol 2001 Jun;11(6):258-266.

(61) Cox C, Bignell G, Greenman C, Stabenau A, Warren W, Stephens P, et al. A survey of homozygous deletions in human cancer genomes. Proc Natl Acad Sci U S A 2005 Mar 22;102(12):4542-4547.

(62) Andersen JN, Jansen PG, Echwald SM, Mortensen OH, Fukada T, Del Vecchio R, et al. A genomic perspective on protein tyrosine phosphatases: gene structure, pseudogenes, and genetic disease linkage. FASEB J 2004 Jan;18(1):8-30.

(63) Wood LD, Parsons DW, Jones S, Lin J, Sjoblom T, Leary RJ, et al. The genomic landscapes of human breast and colorectal cancers. Science 2007 Nov 16;318(5853):1108-1113.

(64) Wang Z, Shen D, Parsons DW, Bardelli A, Sager J, Szabo S, et al. Mutational analysis of the tyrosine phosphatome in colorectal cancers. Science 2004 May 21;304(5674):1164-1166.

(65) Julien SG, Dube N, Hardy S, Tremblay ML. Inside the human cancer tyrosine phosphatome. Nat Rev Cancer 2011 Jan;11(1):35-49.

(66) Brady-Kalnay SM, Tonks NK. Protein tyrosine phosphatases as adhesion receptors. Curr Opin Cell Biol 1995;7(5):650-657.

(67) Tonks NK. Protein tyrosine phosphatases: from genes, to function, to disease. Nat Rev Mol Cell Biol 2006 Nov;7(11):833-846.

(68) Barghorn A, Speel EJM, Farspour B, Saremaslani P, Schmid S, Perren A, et al. Putative Tumor Suppressor Loci at 6q22 and 6q23-q24 Are Involved in the Malignant Progression of Sporadic Endocrine Pancreatic Tumors. Am J Pathol 2001 June 1;158(6):1903-1911.

(69) Nakamura M, Kishi M, Sakaki T, Hashimoto H, Nakase H, Shimada K, et al. Novel Tumor Suppressor Loci on 6q22-23 in Primary Central Nervous System Lymphomas. Cancer Res 2003 February 15;63(4):737-741.

(70) Chuaqui R, Silva M, Emmert-Buck M. Allelic Deletion Mapping on Chromosome 6q and X Chromosome Inactivation Clonality Patterns in Cervical Intraepithelial Neoplasia and Invasive Carcinoma, Gynecol Oncol 2001 3;80(3):364-371.

(71) Flavell JR, Baumforth KR, Wood VH, Davies GL, Wei W, Reynolds GM, et al. Down-regulation of the TGF-beta target gene, PTPRK, by the Epstein-Barr virus encoded EBNA1 contributes to the growth and survival of Hodgkin lymphoma cells. Blood 2008 Jan 1;111(1):292-301.

(72) Schnekenburger J, Mayerle J, Krüger B, Buchwalow I, Weiss FU, Albrecht E, et al. Protein tyrosine phosphatase κ and SHP-1 are involved in the regulation of cell-cell contacts at adherens junctions in the exocrine pancreas. Gut 2005 October 01;54(10):1445-1455.

(73) Starr TK, Allaei R, Silverstein KA, Staggs RA, Sarver AL, Bergemann TL, et al. A transposon-based genetic screen in mice identifies genes altered in colorectal cancer. Science 2009 Mar 27;323(5922):1747-1750.

(74) Assem M, Schuetz EG, Leggas M, Sun D, Yasuda K, Reid G, et al. Interactions between hepatic Mrp4 and Sult2a as revealed by the constitutive androstane receptor and Mrp4 knockout mice. J Biol Chem 2004 May 21;279(21):22250-22257.

(75) Kakuguchi W, Kitamura T, Kuroshima T, Ishikawa M, Kitagawa Y, Totsuka Y, et al. HuR knockdown changes the oncogenic potential of oral cancer cells. Mol Cancer Res 2010 Apr;8(4):520-528.

(76) Lal M, Caplan M. Regulated intramembrane proteolysis: signaling pathways and biological functions. Physiology (Bethesda) 2011 Feb;26(1):34-44.

(77) VanMeter TE, Rooprai HK, Kibble MM, Fillmore HL, Broaddus WC, Pilkington GJ. The role of matrix metalloproteinase genes in glioma invasion: co-dependent and interactive proteolysis. J Neurooncol 2001 Jun;53(2):213-235.

(78) Beroukhim R, Lin M, Park Y, Hao K, Zhao X, Garraway LA, et al. Inferring loss-of-heterozygosity from unpaired tumors using high-density oligonucleotide SNP arrays. PLoS Comput Biol 2006 May;2(5):e41.

(79) Burgoyne AM, Phillips-Mason PJ, Burden-Gulley SM, Robinson S, Sloan AE, Miller RH, et al. Proteolytic cleavage of protein tyrosine phosphatase mu regulates glioblastoma cell migration. Cancer Res 2009 Sep 1;69(17):6960-6968.

(80) Chow JP, Fujikawa A, Shimizu H, Suzuki R, Noda M. Metalloproteinase- and gamma-secretase-mediated cleavage of protein-tyrosine phosphatase receptor type Z. J Biol Chem 2008 Nov 7;283(45):30879-30889.

(81) Anders L, Mertins P, Lammich S, Murgia M, Hartmann D, Saftig P, et al. Furin-, ADAM 10-, and gamma-secretase-mediated cleavage of a receptor tyrosine phosphatase and regulation of beta-catenin's transcriptional activity. Mol Cell Biol 2006 May;26(10):3917-3934.

(82) Novellino L, De Filippo A, Deho P, Perrone F, Pilotti S, Parmiani G, et al. PTPRK negatively regulates transcriptional activity of wild type and mutated oncogenic β-catenin and affects membrane distribution of β-catenin/E-cadherin complexes in cancer cells. Cell Signal 2008 5;20(5):872-883.

(83) Xu Y, Tan L, Grachtchouk V, Voorhees JJ, Fisher GJ. Receptor-type Protein-tyrosine Phosphatase-κ Regulates Epidermal Growth Factor Receptor Function. Journal of Biological Chemistry 2005 December 30;280(52):42694-42700.

(84) Nager M, Bhardwaj D, Canti C, Medina L, Nogues P, Herreros J. beta-Catenin Signalling in Glioblastoma Multiforme and Glioma-Initiating Cells. Chemother Res Pract 2012;2012:192362.

(85) Valenta T, Hausmann G, Basler K. The many faces and functions of beta-catenin. EMBO J 2012 May 22;31(12):2714-2736.

(86) Shi Z, Qian X, Li L, Zhang J, Zhu S, Zhu J, et al. Nuclear translocation of beta-catenin is essential for glioma cell survival. J Neuroimmune Pharmacol 2012 Dec;7(4):892-903.

(87) Zhu H, Acquaviva J, Ramachandran P, Boskovitz A, Woolfenden S, Pfannl R, et al. Oncogenic EGFR signaling cooperates with loss of tumor suppressor gene functions in gliomagenesis. Proc Natl Acad Sci U S A 2009 Feb 24;106(8):2712-2716.

(88) Gan HK, Kaye AH, Luwor RB. The EGFRvIII variant in glioblastoma multiforme. J Clin Neurosci 2009 Jun;16(6):748-754.

(89) Burgoyne AM, Palomo JM, Phillips-Mason PJ, Burden-Gulley SM, Major DL, Zaremba A, et al. PTPmu suppresses glioma cell migration and dispersal. Neuro Oncol 2009 Dec;11(6):767-778.

(90) Ulbricht U, Eckerich C, Fillbrandt R, Westphal M, Lamszus K. RNA interference targeting protein tyrosine phosphatase zeta/receptor-type protein tyrosine phosphatase beta suppresses glioblastoma growth in vitro and in vivo. J Neurochem 2006 Sep;98(5):1497-1506.

(91) Hunter T. Tyrosine phosphorylation: thirty years and counting. Curr Opin Cell Biol 2009 Apr;21(2):140-146.

(92) Sathornsumetee S, Reardon DA. Targeting multiple kinases in glioblastoma multiforme. Expert Opin Investig Drugs 2009 03/01;18(3):277-292.

(93) Tiganis T, Bennett AM. Protein tyrosine phosphatase function: the substrate perspective. Biochem J 2007 Feb 15;402(1):1-15.

(94) Xu Y, Fisher GJ. Receptor type protein tyrosine phosphatases (RPTPs) - roles in signal transduction and human disease. J Cell Commun Signal 2012 Aug;6(3):125-138.

(95) Zondag GC, Koningstein GM, Jiang YP, Sap J, Moolenaar WH, Gebbink MF. Homophilic interactions mediated by receptor tyrosine phosphatases mu and kappa. A critical role for the novel extracellular MAM domain. J Biol Chem 1995 Jun 16;270(24):14247-14250.

(96) Stockhausen MT, Kristoffersen K, Poulsen HS. The functional role of Notch signaling in human gliomas. Neuro Oncol 2010 Feb;12(2):199-211.

(97) Rozen S, Skaletsky H. Primer3 on the WWW for general users and for biologist programmers. Methods Mol Biol 2000;132:365-386.

(98) Overmeyer JH, Young AM, Bhanot H, Maltese WA. A chalcone-related small molecule that induces methuosis, a novel form of non-apoptotic cell death, in glioblastoma cells. Mol Cancer 2011 Jun 6;10:69-4598-10-69.

(99) Cauwe B, Van den Steen PE, Opdenakker G. The biochemical, biological, and pathological kaleidoscope of cell surface substrates processed by matrix metalloproteinases. Crit Rev Biochem Mol Biol 2007 May-Jun;42(3):113-185.

(100) Kopan R, Ilagan MX. Gamma-secretase: proteasome of the membrane? Nat Rev Mol Cell Biol 2004 Jun;5(6):499-504.

(101) Fan Q, Cheng CK, Nicolaides TP, Hackett CS, Knight ZA, Shokat KM, et al. A Dual Phosphoinositide-3-Kinase α/mTOR Inhibitor Cooperates with Blockade of Epidermal Growth Factor Receptor in PTEN-Mutant Glioma. Cancer Research 2007 September 01;67(17):7960-7965.

(102) Chang C, Shen C, Su H, Chen C. Gefitinib induces apoptosis in human glioma cells by targeting Bad phosphorylation. Journal of Neuro-Oncology 2011;105(3):507-522.

(103) Sallee JL, Wittchen ES, Burridge K. Regulation of Cell Adhesion by Protein-tyrosine Phosphatases. Journal of Biological Chemistry 2006 June 16;281(24):16189-16192.

(104) Reiss K, Maretzky T, Ludwig A, Tousseyn T, de Strooper B, Hartmann D, et al. ADAM10 cleavage of N-cadherin and regulation of cell-cell adhesion and beta-catenin nuclear signalling. EMBO J 2005 Feb 23;24(4):742-752.

(105) Fuchs M, Müller T, Lerch MM, Ullrich A. Association of Human Protein-tyrosine Phosphatase κ with Members of the Armadillo Family. Journal of Biological Chemistry 1996 July 12;271(28):16712-16719.

(106) Perez-Moreno M, Jamora C, Fuchs E. Sticky Business: Orchestrating Cellular Signals at Adherens Junctions. Cell 2003 2/21;112(4):535-548.

(107) Stockinger A, Eger A, Wolf J, Beug H, Foisner R. E-cadherin regulates cell growth by modulating proliferation-dependent β-catenin transcriptional activity. The Journal of Cell Biology 2001 September 17;154(6):1185-1196.

(108) Utsunomiya T, Doki Y, Takemoto H, Shiozaki H, Yano M, Sekimoto M, et al. Correlation of beta-catenin and cyclin D1 expression in colon cancers. Oncology 2001;61(3):226-233.

(109) Blume-Jensen P, Hunter T. Oncogenic kinase signalling. Nature 2001 May 17;411(6835):355-365.

(110) Hellberg CB, Burden-Gulley SM, Pietz GE, Brady-Kalnay SM. Expression of the receptor protein-tyrosine phosphatase, PTPmu, restores E-cadherin-dependent adhesion in human prostate carcinoma cells. J Biol Chem 2002 Mar 29;277(13):11165-11173.

(111) Yeung J, Esposito MT, Gandillet A, Zeisig BB, Griessinger E, Bonnet D, et al. beta-Catenin mediates the establishment and drug resistance of MLL leukemic stem cells. Cancer Cell 2010 Dec 14;18(6):606-618.

(112) Chambers TC, Pohl J, Raynor RL, Kuo JF. Identification of specific sites in human P-glycoprotein phosphorylated by protein kinase C. J Biol Chem 1993 Mar 5;268(7):4592-4595.

(113) Chang CY, Shen CC, Su HL, Chen CJ. Gefitinib induces apoptosis in human glioma cells by targeting Bad phosphorylation. J Neurooncol 2011 Dec;105(3):507-522.

(114) Mohebiany AN, Nikolaienko RM, Bouyain S, Harroch S. Receptor-type tyrosine phosphatase ligands: looking for the needle in the haystack. FEBS J 2012 Jun 11.

(115) Gil-Henn H, Elson A. Tyrosine phosphatase-epsilon activates Src and supports the transformed phenotype of Neu-induced mammary tumor cells. J Biol Chem 2003 May 2;278(18):15579-15586.

(116) Zheng XM, Resnick RJ, Shalloway D. A phosphotyrosine displacement mechanism for activation of Src by PTPalpha. EMBO J 2000 Mar 1;19(5):964-978.

(117) Xie J, Seto CT. A two stage click-based library of protein tyrosine phosphatase inhibitors. Bioorg Med Chem 2007 Jan 1;15(1):458-473.

(118) Mattila E, Ivaska J. High-throughput methods in identification of protein tyrosine phosphatase inhibitors and activators. Anticancer Agents Med Chem 2011 Jan;11(1):141-150.

(119) Bohmer F, Szedlacsek S, Tabernero L, Ostman A, den Hertog J. Protein tyrosine phosphatase structure-function relationships in regulation and pathogenesis. FEBS J 2013 Jan;280(2):413-431.

(120) Jiang ZX, Zhang ZY. Targeting PTPs with small molecule inhibitors in cancer treatment. Cancer Metastasis Rev 2008 Jun;27(2):263-272.

(121) Mattila E, Pellinen T, Nevo J, Vuoriluoto K, Arjonen A, Ivaska J. Negative regulation of EGFR signalling through integrin-alpha1beta1-mediated activation of protein tyrosine phosphatase TCPTP. Nat Cell Biol 2005 Jan;7(1):78-85.

(122) Mattila E, Auvinen K, Salmi M, Ivaska J. The protein tyrosine phosphatase TCPTP controls VEGFR2 signalling. J Cell Sci 2008 Nov 1;121(Pt 21):3570-3580.

(123) Zhang ZY, Zhou B, Xie L. Modulation of protein kinase signaling by protein phosphatases and inhibitors. Pharmacol Ther 2002 Feb-Mar;93(2-3):307-317.

(124) Zhang S, Zhang ZY. PTP1B as a drug target: recent developments in PTP1B inhibitor discovery. Drug Discov Today 2007 May;12(9-10):373-381.